



5-2011

Developing A Remote Sensing Algorithm For Deriving Soil Moisture From Spectral Reflectance

Santosh Rijal

Follow this and additional works at: <https://commons.und.edu/theses>

 Part of the [Earth Sciences Commons](#)

Recommended Citation

Rijal, Santosh, "Developing A Remote Sensing Algorithm For Deriving Soil Moisture From Spectral Reflectance" (2011). *Theses and Dissertations*. 2516.

<https://commons.und.edu/theses/2516>

This Thesis is brought to you for free and open access by the Theses, Dissertations, and Senior Projects at UND Scholarly Commons. It has been accepted for inclusion in Theses and Dissertations by an authorized administrator of UND Scholarly Commons. For more information, please contact zeinebyousif@library.und.edu.

DEVELOPING A REMOTE SENSING ALGORITHM FOR DERIVING SOIL
MOISTURE FROM SPECTRAL REFLECTANCE

by

Santosh Rijal

Bachelor of Science, Tribhuvan University, 2007

A Thesis

Submitted to the Graduate Faculty

of the

University of North Dakota

in partial fulfillment of the requirements

for the degree of

Master of Science

Grand Forks, North Dakota

May


2011

Copyright 2011 Santosh Rijal

This thesis, submitted by Santosh Rijal in partial fulfillment of the requirements for the degree of Master of Science from the University of North Dakota, has been read by the Faculty Advisory Committee under whom the work has been done and is hereby approved.

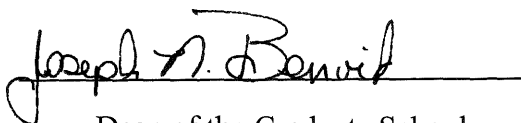

Chairperson







This thesis meets the standards for appearance, conforms to the style and format requirements of the Graduate School of the University of North Dakota, and is hereby approved.


Dean of the Graduate School

March 22, 2011
Date

PERMISSION

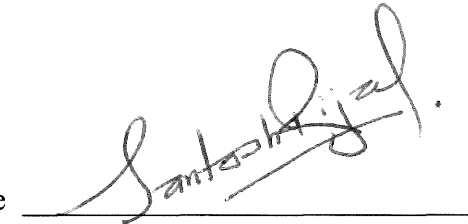
Title Developing a Remote Sensing Algorithm for Deriving Soil
Moisture from Spectral Reflectance

Department Earth System Science and Policy

Degree Master of Science

In presenting this thesis in partial fulfillment of the requirements for a graduate degree from the University of North Dakota, I agree that the library of this University shall make it freely available for inspection. I further agree that permission for extensive copying for scholarly purposes may be granted by the professor who supervised my thesis work or, in his absence, by the chairperson of the department or the dean of the Graduate School. It is understood that any copying or publication or other use of this thesis or part thereof for financial gain shall not be allowed without my written permission. It is also understood that due recognition shall be given to me and to the University of North Dakota in any scholarly use which may be made of any material in my thesis.

Signature



Date

02 / 22 / 2011

TABLE OF CONTENTS

LIST OF FIGURES	viii
LIST OF TABLES.....	xii
ACKNOWLEDGEMENTS	xiii
ABSTRACT	xv
CHAPTER	
I INTRODUCTION.....	1
Objectives.....	3
Description of the Study Area.....	4
Landsat 5 TM	7
AEROCam	9
II LITERATURE REVIEW.....	11
Remote Sensing of Soil.....	11
Soil Texture.....	11
Organic Matter.....	12
Soil Structure, Roughness and Agricultural Practices	12
Remote Sensing of Surface Soil Moisture.....	14
Microwave Sensing of Surface Soil Moisture	15
Passive Microwave Sensing of Surface Soil Moisture	16
Active Microwave Sensing of Surface Soil Moisture	18

	Optical Sensing of Surface Soil Moisture.....	21
III	METHODOLOGY.....	28
	Laboratory and Outdoor Experiment.....	28
	Soil Used	28
	Preparation of Soil Sample and Soil Sample Box	28
	Calibration of Watermark 200 Soil Matric Potential Sensor	28
	Volumetric Soil Moisture Measurement.....	31
	Laboratory Experimental Set-up.....	31
	Measuring Spectral Reflectance of Soil at Varying Moisture Condition.....	32
	First Laboratory Experiment.....	33
	Second Laboratory Experiment.....	33
	Measuring Spectral Reflectance under Natural Light.....	34
	Field Measurement of Soil Moisture in the RRV of the North Basin	35
	A flowchart for Data Collection	36
	A flowchart of Methodology Used for Landsat 5 TM.....	37
	Variation of Spectral Reflectance with Moisture in the Experiments.....	38
	Problems Encountered with the Reflectance Spectra while Continuously Using ASD	39
	Model Preparation	42
IV	RESULTS AND DISCUSSION	43
	Landsat and AEROCam	43
	Regression Analysis for Landsat 5 TM	50
	Regression Analysis for AEROCam	52

Observations in the Red River Valley59

Observation in the Fairmount Experimental Field61

V CONCLUSION, LIMITATION AND FUTURE
WORK OF THE STUDY.....71

 Conclusion.....71

 Limitation of the Study.....72

 Future Work73

APPENDICES75

REFERENCES90

LIST OF FIGURES

Figure	Page
1. Locations of the study areas (a) the RRV and the Fairmount experimental field; (b) counties in North Dakota where field experiments of soil moisture were carried out	5
2. Experimental field at Fairmount, Richland County, North Dakota.....	6
3. Images of the Fairmount experimental field (a) in the beginning of growing season of 2010 (b) corn midway through the growing season of 2010.....	6
4. Laboratory spectra of four different soils at different volumetric water contents (Lobell and Asner, 2002).....	13
5. Part of the electromagnetic spectrum showing Visible with Infrared and Microwave wavelengths where studies on soil moisture has been carried out, provided by Rossel and McBratney (1998), and modified for the purpose of the study	14
6. Instruments used for calculating gravimetric soil moisture content: (a) soil sample box, (b) porcelain plate and auger, (c), soil oven and (d) a scale of precision + 0.001g.....	29
7. The relationship between gravimetric soil water content and the logarithmic soil moisture potential at 15 cm depth.....	30
8. Laboratory experimental set up to collect the spectral reflectance of soil in a naturally drying moisture condition	32
9. The soil sample box with different instruments that were used in the outside measurement	34
10. A Flowchart showing data collection in lab and field experiment.....	36

11.	A Flowchart showing detailed methodology for developing the model for Landsat 5 TM	37
12.	Measured reflectance spectrum (left y-axis) and its 1 st derivative (right y-axis) with respect to wavelength (nm). (a) First observed jump at 25 hours of continuous operation, (b) after 35 hours of continuous operation, (c) after 40 hours of continuous operation, (d) after 55 hours of continuous operation, (e) after 65 hours of continuous operation, and (f) after 70 hours of continuous operation.....	40
13.	The temporal variation of the jump (a) at 975 nm and (b) at 1760 nm where they increased in a linear fashion at the beginning and remained relatively constant after about 100 hours of operation.....	41
14.	Simulated reflectance of soil collected in various moisture levels: (a) first lab experiment (b) second lab experiment (c) outdoor experiment with respect to the center wavelength for Landsat 5 TM	44
15.	Simulated reflectance of soil collected at various moisture levels: (a) first lab experiment (b) second lab experiment (c) outdoor experiment with respect to the center wavelength for AEROCam.....	45
16.	Different band and band combinations for the simulated reflectance value of Landsat 5 TM plotted with respect to soil moisture from all three experiments.....	46
17.	Different band and band combination for the simulated reflectance value of AEROCam plotted with respect to soil moisture from all three experiments	47
18.	Relationship between volumetric soil moisture and simulated reflectance of Landsat band (B5-B1) collected during all three experiments.....	48
19.	Relationship between volumetric soil moisture and simulated reflectance of AEROCam band (NIR) collected during all three experiments.....	49
20.	Graphical relationships between soil moisture and simulated reflectance of selected band combination (B5-B1) for Landsat 5 TM.....	51
21.	Graphical relationship between soil moisture and simulated reflectance of selected band (NIR) for AEROCam.....	53
22.	Variation of surface soil reflectance with changing soil moisture (a) for Newtonia silt loam (Bowers and Hanks, 1965) and (b) from first laboratory experiment (Roliss-Lindas Hamerly Doran).....	55

23.	Absorption coefficient of water (Segelstein, 1981) with the ASD measured Spectra obtained in first lab experiment.....	57
24.	Absorption coefficient of water (Segelstein, 1981) with the simulated reflectance of Landsat in first lab experiment.....	58
25.	Absorption coefficient of water (Segelstein, 1981) with the simulated reflectance of AEROCam in first lab experiment.....	59
26.	A comparison of surface soil moisture content measured in different experimental fields in RRV with respect to the soil moisture content acquired from Landsat 5 TM based model	60
27.	Location of soil moisture sensors (SMS) overlaid in a false color AEROCam image of the Fairmount experimental field.....	62
28.	The difference in estimated soil moisture on drained and undrained portion of the Fairmount experimental field (a) on May 11, 2008 and (b) May 18, 2008...	64
29.	The difference in estimated soil moisture on drained and undrained portion of the Fairmount experimental field (a) on May 21, 2009 and (b) May 30, 2009...	65
30.	The difference in estimated soil moisture on drained and undrained portion of the Fairmount experimental field (a) on April 15, 2010 and (b) April 22, 2010...	67
31.	The difference in estimated soil moisture on drained and undrained portion of the Fairmount experimental field (a) on May 7, 2010 and (b) May 17, 2010.....	68
32.	Comparison of reflectance spectra of soil on drained/undrained portion of Fairmount experimental field collected (a) on June 5, 2009 (b) on September 10, 2009	69
33.	Soil map of North Dakota with the location of field measurement indicated by the triangles	78
34.	The spectral response function for Landsat 5 TM, Band 1 (CEOS, 2010)	79
35.	The spectral response function for Landsat 5 TM, Band 5 (CEOS, 2010).....	80
36.	The spectral response function for NIR Band of AEROCam	81
37.	Fairmount experimental field, Richland County, where field moisture measurements were carried out in the locations indicated by triangles	82

38. Experimental field in Fairmount 'A', Richland County, where field moisture measurements were carried out in the locations indicated by triangles.....83
39. Experimental field in Fairmount 'B', Richland County, where field moisture measurements were carried out in the locations indicated by triangles84
40. Experimental field in Fairmount 'C', Richland County, where field moisture measurements were carried out in the locations indicated by triangles85
41. Experimental field in Mayville, Trail County, where field moisture measurements were carried out in the locations indicated by triangles86
42. Experimental field in Wahpeton, Richland County where field moisture measurements were carried out in the locations indicated by triangles87
43. Experimental field in Walcott, Richland County, where field moisture measurements were carried out in the locations indicated by triangles88
44. Experimental field in Devils Lake, Ramsey County, where field moisture measurements were carried out in the locations indicated by triangles89

LIST OF TABLES

Table	Page
1. Location of experimental fields and a brief introduction of the soils found in those areas (Web Soil Survey, 2010).....	8
2. Summary of physics, advantages and limitation of some remote sensing techniques used for surface soil moisture estimation (Moran et al., 2004).....	27
3. Regression analysis for selected band combination (Band 5-Band1) for Landsat 5 TM	50
4. Regression analysis for selected band (NIR) for AEROCam.....	52
5. Band designation of Landsat 5 TM and the use of these bands	54
6. Correlation analysis between estimated soil moisture and soil moisture measured in field.....	61

ACKNOWLEDGEMENTS

I would like to thank the Department of Earth System Science and Policy, University of North Dakota, for providing me this golden opportunity to further my academic carrier, hone my knowledge and skill in the field of remote sensing, and for providing important resources and facilities throughout my Masters study. I would like to express my deep and sincere gratitude to my advisor Dr. Xiaodong Zhang for his continuous guidance, support and encouragement for conducting this research. His academic visions and instructions build firmness in my educational career. His ideals and concepts have has a remarkable influence on my entire career too.

I would like to thank my committee members for being the foundation of my research. I wish to express my warm and sincere thanks to Dr. Xinhua Jia of North Dakota State University for providing me with the research field to conduct my experiments and several other resources. I owe my sincere gratitude to Dr. Soizik Laguette, Department Chair and my committee member. Her constructive criticism and excellent advice for preparing the final thesis helped to make the paper excellent.

I would also like thank Dr. Michael J. Hill and Dr. Rebecca J. Romsdahl for the research ideas they provided me on the class. I would like to thank my classmates Junyu Yang, Navin Thapa, Anduin K. Mckelroy and Shawn O'Neil for sharing every moment during my study. I warmly thank Dr. Hojin Kim for providing me great knowledge about ASD which I used in my experiment. Furthermore, I was able to gain remarkable knowledge on GIS, digital imagery, image interpretation, processing and analyzing

satellite images, in the Geospatial Lab under his guidance. I wish to thank Mr. Steve Finlay for revising the english of my manuscript. During this work, I have collaborated with many colleagues for whom I have great regard, and I wish to extend my warmest thanks to all those who have helped me in my work.

I would like to thank the two most beautiful ladies of our department, Kathy Ebertowski and Karen Katrinak for being so pleasant, cheerful and rushing everytime to help students in the best possible way. Thanks for creating a family in ESSP. I would like to thank Ms. Anu Mishra, for her encouragement and moral support. I would also like to thank Ishara Rijal, Qiang Zhou and Hom Jyoti Adhikari for their suggestions in my thesis. I missed my loving nephew Pragyana, whole a lot, while my study here in US.

I owe my loving thanks to my family. My hardworking father, mother and my two sisters are in every cell of my body, sacrificing their entire life to me, and expecting nothing in return.

To My Family

ABSTRACT

Wet weather cycle since 1993 has brought ground water level closer to the surface of the soil in many areas in the Red River Valley (RRV) of the North basin. Many farmers have to delay spring plantation or autumn harvest due to excessive moisture in their farmland. In such case, it becomes increasingly important to have timely and accurate information on the soil moisture conditions. Conventional soil moisture measurement techniques are point-based that results in poor spatial representation of soil moisture. Remote sensing techniques offer many potential advantages over traditional means such as repetitive coverage and areal representation. The objective of this study was to develop a remote sensing algorithm to be used by Landsat 5 TM and Aerocam to map surface soil moisture during the early stage of growing season in the RRV of the North basin.

Soil samples were collected and hyperspectral reflectances of the soil at various moisture levels were recorded under laboratory conditions. The first two experiments were carried out with Halogen lamps as the source of light whereas the third experiment was performed outdoor. Landsat 5 TM and Aerocam spectral response function were applied to the measured hyperspectral values to simulate the multispectral reflectance for each sensor. The results from these three experiments were consistent to each other and therefore were binned together. By using simple mathematical computations, band or band combinations that best estimates the surface soil moisture was found out. For validation, soil moisture was measured in different agricultural fields in the RRV during

the time of Landsat overpass, and soil moisture was continuously monitored in a farm field in Fairmount, Richland County, North Dakota.

The difference of bands 5 and 1 was shown to correlate best with soil moisture concentration while the NIR band itself is the best for Aerocam. The estimated soil moisture using Landsat 5 TM agreed with the measurements with an $R^2 = 0.90$. The model performed well in dry or moderately wet conditions, but slightly underestimated by 3-4% for excessively wet conditions of more than 40% soil moisture in the field. The evaluation at the Fairmount experimental field also showed that the model performed well. Field verification for Aerocam imagery remained incomplete due to lack of irradiance value.

CHAPTER 1

INTRODUCTION

Soil moisture is an important factor influencing a range of environmental processes that include the growth of plants, soil biogeochemistry, and land-atmosphere exchange of heat and water (Lobell and Asner, 2002). It controls the partitioning of water and energy fluxes at the earth's surface and plays a significant role in continental water distribution through the land-surface-atmosphere mechanism (de Rosnay et al., 2006). Soil moisture also affects land-use and agricultural planning (de Rosnay et al., 2006) and has significant impacts on the development of regional as well as global weather patterns (Nemani et al., 1993).

Surface soil moisture contributes to the hydrological processes of evapotranspiration and runoff generation both affecting the exchange of water and energy fluxes at the land surface and atmosphere interface (Wang and Qu, 2009). Moisture on the surface of the soil has special significance and has many implications on studies related to biological and biogeochemical processes. The role of soil moisture in the top 1 to 2 m of the Earth's surface has been widely recognized as a key variable in many environmental studies including meteorology, hydrology, agriculture and climate change (Wang and Qu, 2009). Hence, timely and accurate estimates of spatial and temporal variations of soil moisture are important (Lobell and Asner, 2002).

Conventional measurement techniques such as gravimetric and time domain reflectrometry (TDR) are point-based and require on-site operations and tedious post-

processing (Moran et al., 2000). These point based measurements usually result in poor spatial representation of soil moisture because of the variability of soil moisture over a land surface with the soil type, land structure, landuse and other ecological features. Surface moisture fluctuates at high spatial and temporal frequencies which make precise characterization of its variability difficult over large areas (Famiglietti, 1999). To adequately represent temporal and spatial distributions of soil moisture, a large number of data are required, and the cost of acquiring these data by manual measurements is often prohibitive (Lindsey et al., 1992). Furthermore, management requirements for operational use of such data may be such that the time taken between collection, delivery, and processing of data, before using them in a model, can make the data obsolete (Lindsey et al., 1992). Therefore, techniques for determination of soil moisture, without the necessity for extensive and costly manual measurements, would be beneficial in characterizing soil moisture within a given region or field (Kaleita et al., 2005).

A variety of techniques for measuring soil moisture across a wide range of area in a continuous manner has been offered by technological advances in remote sensing (Wang and Qu, 2009). Compared to other methods for measuring surface soil moisture, remote sensing is synoptic, provides for timely coverage with repeat passes, and offers efficiencies of scale that cannot be matched by traditional means. Remote sensing technology has capabilities for rapid acquisition of spatial-temporal information on soil moisture that is vital to agricultural, hydrological and geographical studies (Huan-Jun, 2009). Therefore, there is growing interest in developing remote sensing techniques for monitoring surface soil moisture over large areas (Bryant et al., 2003). As remote sensors do not measure soil moisture content directly, it becomes important to derive

mathematical models that can describe the connection between the measured signal and soil moisture content (de Troch et al., 1996). There are many remote sensing approaches and methods developed using microwave remote sensing for estimating soil moisture while a limited number of methods have been developed using multispectral sensors. Considering all the advantages of remote sensing and the lack of sufficient study and methods for detecting surface soil moisture using multispectral sensors like Landsat 5 Thematic Mapper (TM), the present study is carried out.

The wet weather cycle since 1993 has brought ground water level closer to the soil surface in many areas in the Red River Valley (RRV) of the North Basin. Many farmers have to delay the spring planting or autumn harvest due to excessive moisture in soil. It becomes important to have timely information on soil moisture conditions to help farmers make decisions regarding their farming schedule or management plan such as whether to install sub-surface drainage. Hence, the purpose of this study is to develop an algorithm for estimating surface soil moisture from Landsat 5 TM and AEROCam imagery for the RRV.

Objectives

The overall objective of the study was to develop a remote sensing algorithm using Landsat 5 TM and AEROCam data to map surface soil moisture during the early growing season in the RRV. To achieve this objective, the following studies have been conducted:

1. hyperspectral reflectance of the surface soil sample was measured at various soil moisture content levels under both indoor and outdoor illumination

2. a remote sensing algorithm was developed for deriving soil moisture from Landsat 5 TM and AEROCam images
3. the developed algorithm was validated using field observations

Description of the Study Area

The RRV of the North Basin has been selected as the study area for this research (Fig. 1). Soil moisture data has been collected from several fields in the RRV (Fig. 1b, Table 1) and a farm field in Fairmount, Richland County (Figs. 2 and 3). The soil used for indoor and outdoor experiments was collected from the Fairmount farm field situated over the Fairmount aquifer, 15 km west of the Bois de Sioux River and about 3 km south of the town of Fairmount. The Fairmount field has a total area of 44 ha, of which 20 ha have sub-surface drainage installed (Jia et al., 2008). In a Landsat 5 TM scene with a spatial resolution of 30m, the total number of pixels from east to west is 27 and 19 from north to south. In the drained section of the field, drainage pipes are installed at 0.9-1.5 m depth of the field with a spacing of 18m from west to east toward a pumping station. The drainage water is pumped to a county ditch located near the northeast corner of the field.

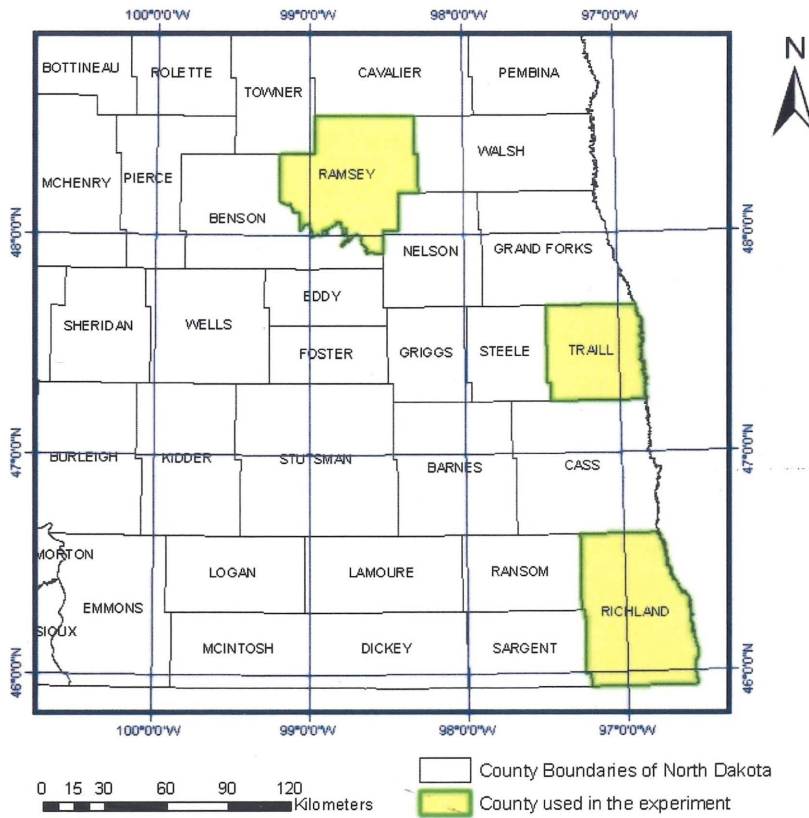
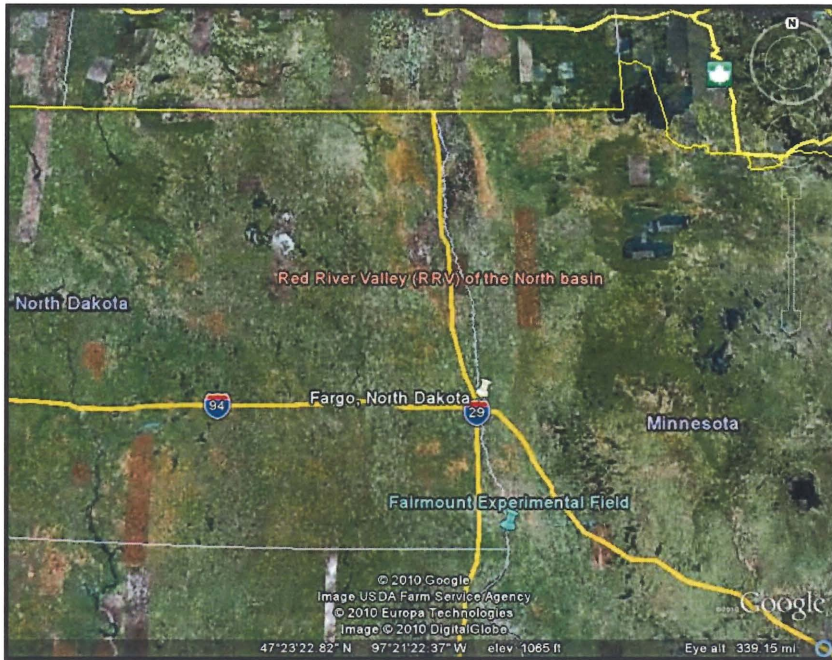


Figure 1. Locations of the study areas (a) the RRV and the Fairmount experimental field; (b) counties in North Dakota where field experiments of soil moisture were carried out

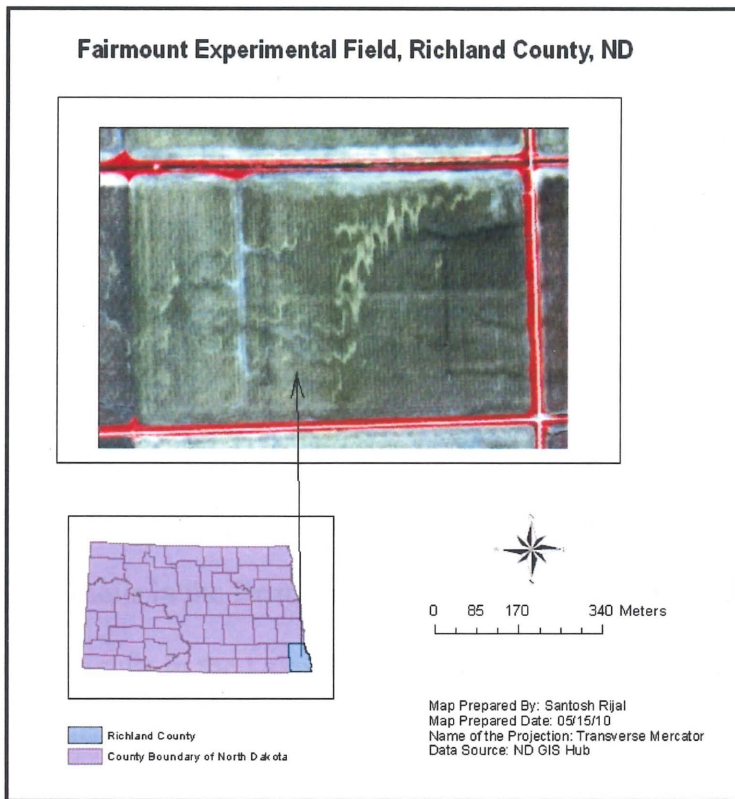


Figure 2. Experimental field at Fairmount, Richland County, North Dakota



(a)



(b)

Figure 3. Images of the Fairmount experimental field (a) in the beginning of the growing season of 2010 and (b) corn midway through the growing season of 2010

According to Stoner et al. (1993), there are eight major soil associations that occur in the RRV: black, limy, clayey soils in the Drift Prairie, RRV Lake Plain, and Lake-Washed Till Plain areas; black, loamy soils in the Drift Prairie in North and South Dakota and in the southern Moraine area of Minnesota; rolling, wooded soils in the Turtle Mountains and Pembina Escarpment in North Dakota and in the moraine area in Minnesota; sandy soils along the western and eastern edge of the RRV Lake Plain and in the Lake-Washed Till Plain area in Minnesota; loamy soils in the RRV Lake Plain and the moraine areas of Minnesota; clayey soils in the RRV Lake Plain area; black, limy, clayey soils in the Drift Prairie, RRV Lake Plain, and Lake-Washed Till Plain areas; organic soils in the Lake-Washed Till Plain area in Minnesota (Stoner et al., 1993). However, brief information of the soil used in the experiment is shown in Table 1.

Landsat 5 TM

Landsat TM sensors have been orbiting the globe since 1982, providing near-continuous multispectral coverage of the United States every 16 days. The Landsat 5 TM satellite was developed and launched on March, 1984 by the National Aeronautics and Space Administration (NASA) and continues to acquire quality TM images (Chander et al., 2004). Landsat 5 TM has 6 spectral bands in the visible, near-infrared and short-wave infrared with 30 m spatial resolution and one thermal band with 120 m resolution. The U.S. Geological Survey (USGS) Center for Earth Resources Observation and Science (EROS) took the lead in operating it since 2001 as well as archiving and processing all of the data acquired by the sensor (Barsi et al., 2007). Landsat data record has proved to be very important for terrestrial remote sensing and global change research because of its relatively fine spatial

Table 1: Location of experimental fields and a brief introduction of the soils found in those areas (Web Soil Survey, 2010)

Experimental field	Geographic Location	Name of the soil	Sub-Category	% slope	Elevation (ft)	Mean annual precipitation(inch)	Landforms	Drainage class	Parent material
Fairmount experimental field; Fairmount Field 'C'; Wahpeton field	46.0089°N, 96.6036°W; 46.327°N, 96.3228°W; 46.1508°N, 96.6512°W	Roliss-Lindas-Hamerly-Doran	Roliss	0-1	750-1250	19-24	Swales	Poorly drained	Fine loamy till
			Lindas	0-2	750-1250	19-24	Flats	Poorly drained	Fine loamy till
			Hamerly	0-3	750-2000	19-24	Flats	Somewhat poorly drained	Fine loamy till
			Doran	0-2	1000-2050	16-20	Flats	Somewhat poorly drained	Glaciolacustrine deposit
Fairmount Field 'A', 'B'	46.0533°N, 96.7256°W; 46.0493°N, 96.6952°W	Glyndon		0-1	750-1250	19-24	Flats	Somewhat poorly drained	Coarse silty glaciolacustrine
Mayville Field	47.4933°N, 97.089°W	Perella-Colvin-Bearden	Perella	0-1	750-1250	19-24	Flats	Poorly drained	Fine silty glaciofluvial
			Colvin	0-1	750-1250	19-24	Depressions	Poorly drained	Fine silty glaciolacustrine
			Bearden	0-2	750-1250	19-24	Flats	Somewhat poorly drained	Fine silty glaciolacustrine
Walcott Field	46.5171°N, 96.8385°W	Fargo		0-3	750-1250	19-24	Flats	Poorly drained	Clayey glaciolacustrine
Devil's Lake Field	48.0485°N, 98.6228°W	Vallers-Svea-Hamerly-Buse-Barnes	Vallers	0-1	1000-2490	16-20	Flats	Poorly drained	Fine loamy till
			Svea	0-3	750-1250	19-24	Moraines	Moderately well drained	Fine loamy till
			Hamerly	0-3	750-2490	19-24	Flats	Somewhat poorly drained	Fine loamy till
			Buse	3-9	750-1250	19-24	Knolls	Well drained	Fine loamy till
			Barnes	3-6	750-1250	19-24	Rises	Well drained	Fine loamy till

resolution, extensive terrestrial coverage and temporal baseline over a period when significant anthropogenic terrestrial change has occurred. Landsat 5 TM has the ability to detect and quantify changes in the earth's environment and its global energy balance by providing calibrated and consistent measurement of earth's surface features (Chander and Markham, 2003). After launching, Landsat 5 TM marked a significant advance in remote sensing through the addition of a more sophisticated sensor system and an increased data acquisition and transmission capability (Chander et al., 2004).

AEROCam

Airborne images acquired from aircraft-based sensors, as compared to satellite-based sensors, have a unique role in seasonal monitoring of variable soil conditions, and in time-specific and time-critical crop management (Moran et al., 1997). They are, therefore, useful in a variety of agricultural purposes such as monitoring crop condition and delineating management zones (Zhang et al., 2010a). They have the advantage of offering a finer spatial resolution (~ 1-5 m) than many other satellite observations (15 - 60 m for e.g. SPOT, Landsat or ASTER). Nevertheless, they also have some disadvantages, such as higher cost due to the use of aircraft and crew time. Therefore, despite its potential in precision agriculture, airborne imagery is seldom routinely used by farmers or ranchers (Zhang et al., 2010b). The University of North Dakota's Airborne Environmental Research Observational Camera (AEROCam) serves a major solution by freely distributing AEROCam images for research purposes within the Northern Great Plain (NGP) region of the USA. Upper Midwest Aerospace Consortium (UMAC) developed and has been flying the AEROCam, providing high resolution aerial images for research and non-commercial applications in the NGP region of the USA. AEROCam

images are typically acquired during the growing season of the UMAC area and are distributed to the users through the Digital Northern Great Plains system (Zhang et al., 2010b).

AEROCam is an airborne multispectral digital imaging system capable of acquiring data in visible (400-720nm) and near infrared bands (720-840nm) (UMAC, 2010). AEROCam was developed by the department of Earth System Science and Policy in partnership with several UND departments, the School of Engineering & Mines, and the flight operations at the John D. Odegard School of Aerospace Sciences (UMAC, 2010). The imaging system comprises of a Red lake MS4100 area-scan multi-spectral digital camera that features a 1920 x 1080 CCD array (7.4-micron pixels), with 8-bit quantization. With four spectral bands at blue, green, red and near-infrared, the camera can record images in true color and in standard false color format (Zhang et al., 2010a). When operated at 1828.8 m above ground level, images have a pixel size of one meter with a horizontal field of just over one mile. Pixel size of 0.25 to 2 meters can also be accommodated dependent on the users' requirements and mean elevation of the site (UMAC, 2010).

CHAPTER II
LITERATURE REVIEW
Remote Sensing of Soil

Soil is the upper weathered organic and mineral debris of the Earth's solid surface modified over time by weather and climate. It is a complex material extremely variable in its physical and chemical composition due to the mixture of primary and secondary minerals along with organic matter, water, air, and living organisms (Ben-Dor et al., 2009). The upper soil surface is characterized by factors, such as, soil moisture, soil degradation processes, salinity, organic matter, surface runoff, and infiltration capacity of the soil and is, therefore, very important in study related to soil. Preparation of accurate maps of soil distribution and monitoring of temporal variation of soil status, for effective monitoring and management of soil, is crucial (Campbell, 2009). Remote sensing technology is an essential tool for acquiring data providing information on soil distribution and recording both spatial and temporal variation of soil properties. Soil specific properties that play important role, while remotely sensing soil, needs to be identified. Soil properties of significance to remote sensing are:

Soil Texture

Soil texture characterizes the particle size distribution of the mineral component of the soil with less than 2 mm diameter. Huge variation of soil texture in nature gives distinctive spectral characteristics. According to Naz and Bowling (2008), the amount of

moisture retained by the soil surface layer is primarily a function of soil texture. A finer soil texture tends to retain more moisture, resulting in less incident energy reflectance from the soil surface, thus appearing darker than coarse-textured soils in imagery. Optical characteristics of varied soil textures is so closely interrelated to so many other soil properties that it is difficult to isolate its role from other influences (Campbell, 2009).

Organic Matter

The debris, remains of plants, animals and insects decompose to form organic component of soil. Soil organic matter forms an important dimension of soil fertility, moisture holding capacity, soil color and is, therefore, an important variable for many application of remote sensing of soil (Campbell, 2009). Like most other soil properties, its spectral characteristics are closely connected to other properties. Proportion of organic matter in the soil affects the soil's brightness giving distinctive spectral characteristics.

Soil Structure, Roughness and Agricultural Practices

The clumps or the binding of soil are significant in remote sensing as they have impact on the soil spectral characteristics. The thin upper layer of soil that is eventually sensed by remote sensors is affected by many factors such as plowing, particle size distribution, vegetation coverage and physical crusts. Roughness has special impact in decreasing the spectral reflectance of soil because of an increase of multiple scattering and shadowing (Rondeaux, 1996). According to Engman and Chauhan (1995), soil roughness may not be a serious limitation for passive sensors for most natural surfaces but are major factors for radar due to their impact on backscattering. Long term use of the land for intensive agriculture practices changes the properties of soil. Such change in

surface soil properties can be studied through temporal observation using remote sensing technology.

Over the past few decades, it has been shown that soil spectra across the visible (VIS) (400 nm-700 nm), near infra-red (NIR) (700 nm- 1100 nm) and short wave infra-red (SWIR) (1100 nm-2500 nm) spectral region are characterized by significant spectral signals that enable recognizing soils qualitatively and quantitatively (Rossel et al., 2006). Fig. 4 shows laboratory spectra of four different soils from 350 nm to 2500 nm at various moisture contents (Lobell and Asner, 2002). We can notice distinctive spectral characteristics of all the soils. Water absorption bands around 1400 nm and 1900 nm can be clearly seen in the curve.

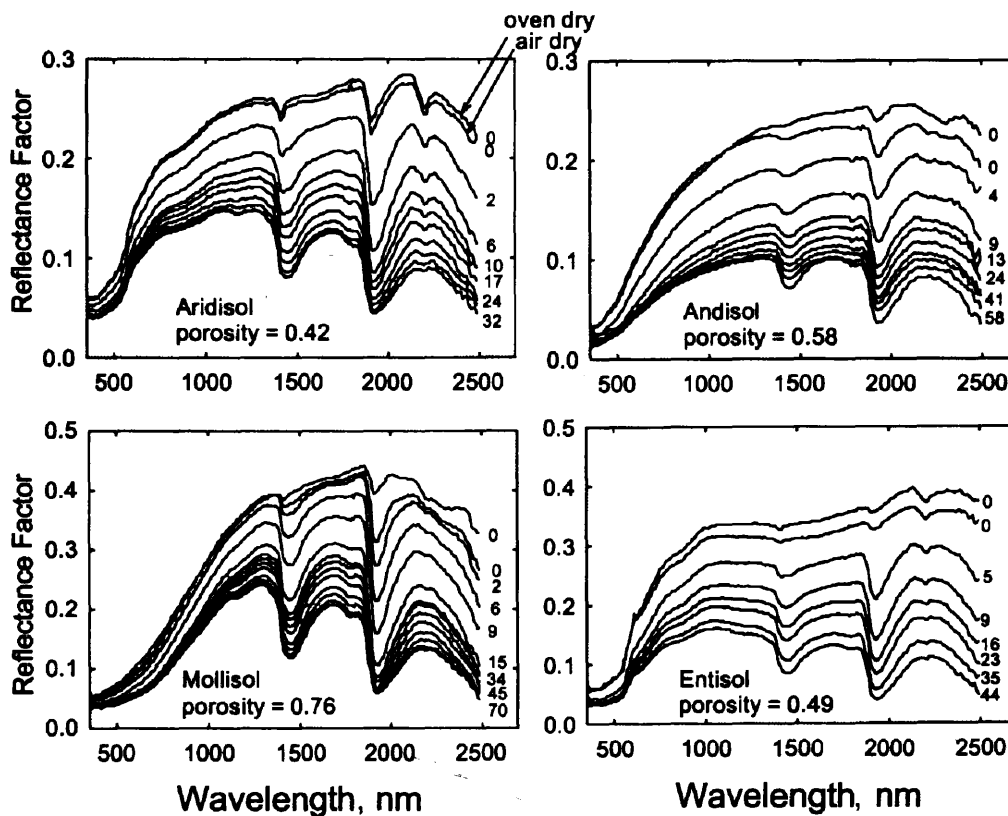


Figure 4. Laboratory spectra of four different soils at different volumetric water contents (Lobell and Asner, 2002)

Remote Sensing of Surface Soil Moisture

Soil moisture can be measured by a variety of techniques using all regions of the electromagnetic spectrum (Engman and Chauhan, 1995). Many different regions of the spectrum have been used to estimate soil moisture (Fig. 5), including thermal infrared (Price, 1982), passive and active microwave and visible (VIS) and near-infrared (NIR) (Kaleita et al., 2005).

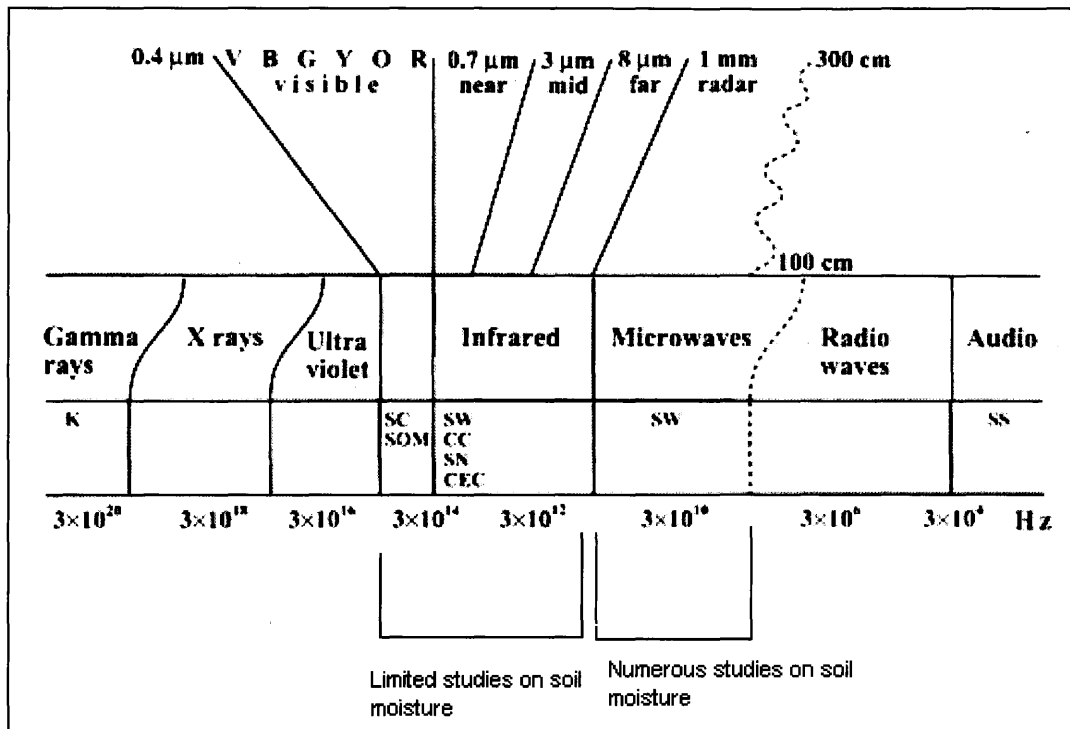


Figure 5: Part of electromagnetic spectrum showing Visible with Infrared and Microwave wavelengths where studies on soil moisture has been carried out, provided by Rossel and McBratney (1998), and modified for the purpose of the study

Many studies have shown that near surface soil moisture can be measured by optical and thermal infrared remote sensing, as well as passive and active microwave remote sensing techniques in which the basic difference are the wavelength region of the electromagnetic spectrum used, the source of the electromagnetic energy, the response measured by the sensor, and the physical relation between the response and the soil

moisture content (Wang and Qu, 2009). We will briefly discuss the techniques used, advantages and drawbacks, and sensors in orbit under each of these techniques.

Microwave Sensing of Surface Soil Moisture

Microwave remote sensing can provide a direct measurement of the surface soil moisture in a wide range of cover conditions and within a limited error bound (Jackson et al., 1996). They have the benefit of being largely unaffected by solar illumination and cloud cover. The ability of the microwave sensors to penetrate non raining clouds makes them very attractive for use as soil moisture sensors (Schmugge, 1978). Furthermore, they have the advantage of being able to penetrate into the soil to a wavelength dependent depth and through vegetation cover (Kaleita et al., 2005). They can maintain their sensitivity to soil moisture variation in the presence of canopy as well (Schmugge, 1978). Hence numerous researches have been conducted for estimating surface soil in the microwave region of the electromagnetic spectrum (Fig. 5). However, accurate soil moisture estimates are limited to the regions that have either bare soil or low to moderate vegetation cover (Njoku and Entekhabi, 1996).

The microwave region of the electromagnetic spectrum consists of wavelengths between 1 and 100 cm which is further subdivided into bands which are often referred to by a lettering system. Some of the relevant bands that are used are: X (~0.8 cm), K (~3 cm), C (~5 cm), S (~10 cm), L (~20 cm), and P (~50 cm). Moreover, within these bands, there are small ranges that are protected for applications such as radioastronomy (Jackson et al., 1996).

A number of scientific experiments using microwave sensors on aircraft and satellites have shown that for bare soil surface, the moisture within a thin layer, of the

order of 0-5 cm, can be correctly determined using microwave (Haider et al., 2004).

Hence, many research projects for estimating surface soil moisture have been focused on the microwave part of the spectrum, based on the facts that moisture strongly affects soil dielectric properties, and longer wavelengths can make a relatively deep penetration into the ground (Bryant et al., 2003).

The amount of water present in a soil affects its dielectric properties, the theoretical basis of which is based on the large contrast between the dielectric properties of liquid water and of dry soil (Engman and Chauhan, 1995). The dielectric properties, along with several other physical characteristics, determine the microwave measurement (Jackson et al., 1996). In addition, the significance of the dielectric properties depends upon the sensor design, especially the wavelength. Instruments operating at longer wavelengths (> 5 cm) have fewer problems with the atmosphere and vegetation, penetrate a deeper soil layer and maximize soil moisture sensitivity. Another instrument concern is whether to use an active or passive microwave approach. Active approaches, especially Synthetic Aperture Radar (SAR), can provide extremely good ground resolution (<100m) from space. Passive methods currently provide much coarser resolution data (>10 km). (Jackson et al., 1996)

Passive Microwave Sensing of Surface Soil Moisture

Passive microwave remote sensing measures the intensity of microwave emissions from the soil at wavelength 1-30cm which is related to its moisture content due to significant differences in the dielectric constant of dry soil (-3.5) and water (-80) (Moran et al., 2004). The intensity of emission from the soil surface is proportional to the product of the surface temperature and surface emissivity (Schmugge, 1978). This

temperature is commonly referred to as the microwave brightness temperature (T_b) (Engman and Chauhan, 1995) and can be expressed as:

$$T_b = t(H) \times [T_{sky} + (1 - r)T_{soil}] + T_{atm} \quad \text{Eq. 1}$$

where $t(H)$ is the atmospheric transmissivity for a radiometer at height H above the soil, r is the smooth surface reflectivity, T_{soil} is the soil temperature, T_{atm} is the average atmospheric temperature and T_{sky} is the contribution from the reflected sky brightness.

According to Schmugge (1978), qualitative observations of the passive microwave sensitivity have been made from satellite platforms at wavelength 21cm and 1.55 cm and found the possibility to monitor the moisture status of the surface soil measuring the thermal emissivity. The spatial resolutions of passive microwave sensors currently conceived for space operation are in the range of 10-20 km in which the most useful frequency range for soil moisture sensing is from 1-5 GHz (Njoku and Entekhabi, 1996).

A particular advantage of passive microwave sensors is the dominant effect of soil moisture on the received signal in the absence of significant vegetation cover (Schmugge, 1978). However, a problem with passive microwave methods is the spatial resolution. For a given antenna size, the footprint size increases as wavelength and altitude increase. For realistic satellite designs at L band, this might result in a footprint as large as 100 km. Recent research has focused on the use of synthetic aperture thinned array radiometers which could decrease the footprint size to 10 km (Jackson et al., 1996).

Examples of passive microwave system for aircraft platform includes the L band (~21cm) radiometers called the pushbroom microwave radiometer (PMBR) operated since 1983 and the electronically scanned thinned array radiometer (ESTAR) which is

supported by NASA. Both of these radiometers have supported soil moisture research significantly for a large area by collecting footprints simultaneously along a flightline utilizing conventional antenna technology (Jackson et al., 1996). For the satellite platform system, all passive microwave sensors operate at very short wavelengths (< 1.5 cm). It includes the SSM/I package on the defense meteorological satellites. The advanced microwave scanning radiometer (AMSR-E) is developed by the National Space Development Agency of Japan (NASDA) and was launched in 2002 which provides a potentially improved soil moisture sensing capability over previous spaceborne radiometers due to its combination of low frequency and higher spatial resolution of approximately 60 km at 6.9 GHz (Njoku et al., 2003).

Active Microwave Sensing of Surface Soil Moisture

An active microwave sensor sends and receives a microwave pulse. The power of the received signal is compared to that which is sent back to determine the backscattering coefficient and finally the coefficient is related to the characteristics of the target (Jackson et al., 1996). Active radar transmits an electromagnetic pulse that is directionally scattered and reflected off rough surfaces. Multiple frequency and polarization observations are required to simultaneously obtain small-scale roughness and dielectric properties which clearly manifest soil moisture (Scott et al., 2003).

Currently, satellites that can meet the spatial resolution and coverage required for watershed management are active microwave sensors among which SAR is the most common imaging active microwave configuration. SAR transmits a series of pulses as the radar antenna traverses the scene. The pulses are then processed together to simulate a very long aperture capable of high surface resolution (Moran et al., 2004). The

backscatter coefficient, σ° , obtained from SAR sensors, is related to the topographic conditions of the locality, surface roughness and dielectric constant of the soil. The difference in dielectric constant between water and dry soil and its variation is an indicator of the concentration of soil moisture (Haider et al., 2004). The coefficient σ° is composed of backscatter from vegetation, σ_v , and from soil, σ_s , and the attenuation caused by the vegetation canopy, L which can be expressed as:

$$\sigma^\circ = \sigma_v + \sigma_s/L \quad \text{Eq. 2}$$

The parameter σ_s has a direct association with volumetric soil moisture, M_v , given by

$$\sigma_s = R_s S M_v \quad \text{Eq. 3}$$

where R_s and S are surface roughness and soil moisture sensitivity terms, respectively (Haider et al., 2004)

Some of the SAR satellite systems with frequencies suitable for soil moisture are ESA ERS-1/2 C-band SAR, ESA ENVISAT C-band ASAR, the Canadian C-band RADARSAT-1/2, the Japanese L-band ALOS-PALSAR (Advanced Land Observing Satellite-Phased Array type L-band SAR (JERS-2) and the German X-band Terra SAT (Wang and Qu, 2009). These SAR systems can provide resolutions from 10 to 100 m over a swath width of 50–500 km, thus meeting most spatial requirements for the application at watershed scale (Moran et al., 2004). It is possible to make use of the coherent nature of the signal in active microwave systems such as SAR to obtain better resolutions but the strong effects of the incidence angle and surface roughness makes the unambiguous determination of soil moisture difficult with this type of sensor (Schmugge, 1978). A major difficulty in the development of soil moisture retrieval algorithms from active microwave sensors like SAR is due to the confounding influences of surface

roughness conditions, which significantly affect the relationships between radar backscatter and soil moisture (Davidson et al., 2000). Past studies have resulted in a multitude of methods, algorithms and models that relate satellite-based images of SAR backscatter to surface soil moisture, but no operational algorithm exists using SAR data acquired by the existing spaceborne sensors (Moran et al., 2004).

Examples of active microwave system for aircraft platform includes the AIRSAR which is operated by NASA's Jet Propulsion Lab (Dubois et al., 1995) and another, a multipolarization X and C band SAR developed by the Canadian Center for remote sensing (Jackson et al., 1996). For the satellite platform system, there are four radar satellites that include the ERS-1 and ERS-2, launched by European Space Agency, JERS-1 launched by the Japanese and the Canadian RADARSAT. Yet every of these satellite systems have some limitations such as a single polarization and temporal resolution of 35 days for the ERS-1 and JERS-1, whereas the RADARSAT have only potential of more frequent coverage only in some of its operating modes (Jackson et al., 1996). The 20–30 m spatial resolution of active microwave sensors in the form of radars aboard the European remote sensing (ERS) satellite, Japan Earth resources (JERS) satellite, RadarSat, and EnviSat is very good to retrieve the information about soil moisture but this solution requires expensive aircraft operation and at the same time the ERS and JERS satellites are no longer operational (Scott et al., 2003).

Active microwave sensors have the capability to provide high spatial resolution data but their sensitivity to soil moisture may be confused more by the surface roughness, topographic features and vegetation than the passive systems (Engman and Chauhan, 1995). In contrast, passive microwave systems are less sensitive to target features but can

only provide spatial resolutions on the order of tens of kilometers. Therefore, many considerations should be made on how the data will be used and these sensors have the limited use if one is interested in more detailed hydrological process and partial area hydrology (Engman and Chauhan, 1995). Practically achievable resolution with microwave sensors is not as fine as that with comparable optical sensors because as wavelength increases, the footprint size also increases (Kaleita et al., 2005). Thermal remote sensing systems are uncommon and generally provide very low spatial resolution for soil moisture monitoring (Bryant et al., 2003). Due to the limited applications of microwave imagery for soil related studies such as infrequent repeat coverage (Moran et al., 2004), and the currently relatively high cost of acquiring microwave data, microwave sensors are not as practical for the use in estimating soil moisture and agricultural related activities from an economic standpoint as sensors in VIS (0.4 μm -0.7 μm) to NIR wavelengths (Kaleita et al., 2005).

Optical Sensing of Surface Soil Moisture

Despite the multitude of optical sensors that are currently in orbit, only a limited body of literatures exists on the use of VIS (0.4 μm -0.7 μm), NIR (0.7 μm -1.1 μm) and shortwave infrared (SWIR) (1.1 μm -2.5 μm) and hyperspectral sensors for the estimation of soil moisture (Muller and Decamps, 2000). Optical remote sensing has the limitation of measuring the reflectance or emittance from the top few millimeters of the surface and, unlike the longer microwave wavelengths, it has limited ability to penetrate clouds and vegetation canopy, and is highly attenuated by the earth's atmosphere (Moran et al., 2004).

Most approaches to estimating surface soil moisture from spectral reflectance are based on the fact that increasing soil moisture up to a certain level leads to a decrease in reflectance values over the VIS-NIR to SWIR part of the spectrum (Haubrock et al., 2008). Weidong et al. (2002) conducted a study to investigate the change in spectral reflectance with soil surface moisture varying from very low to very high moisture contents for different wavelengths for a range of soil types. Their results show that for low soil moisture levels, reflectance decreases when soil moisture increases whereas for the higher soil moisture levels, reflectance increases when soil moisture increases. This particular point of higher soil moisture when reflectance begins to increase varies with soil properties and field condition. In a fully saturated condition when water film covers all the soil particles, or the water moisture is at the field holding capacity, reflectance of soil increases as compared to the reflectance at its minimum in a wet condition (Weidong et al., 2002). Spectral reflectance measured by Bowers and Hanks (1965), over a range of soils confirmed a decrease in reflectance with increasing moisture content.

Moisture has great influence on the reflection of shortwave radiation from soil surfaces in the VIS-NIR and SWIR regions of the electromagnetic spectrum (Bowers and Hanks, 1965). Therefore these regions of the electromagnetic spectrum can be used to estimate surface soil moisture. Ben-Dor et al. (2002) conducted a field study in which they mapped multiple soil properties including soil moisture using DAIS-7915 hyperspectral scanner data. They concluded that visible, NIR and SWIR spectral regions allow soil moisture estimation based on their well-known spectral absorption features of water. Similarly, Lobell and Asner (2002) conducted a study to establish quantitative relationships between soil moisture and reflectance that minimized the differences

between soil types for use in operational soil moisture retrieval algorithms and canopy radiative transfer models. Their modeling results indicated that the SWIR region offers significant potential for relating moisture and reflectance. Hence all these studies showed the potential of NIR and SWIR region of the electromagnetic spectrum to estimate surface soil moisture.

The rate of decrease in reflectance as soil moisture increases holds for the range from 350 to 2500 nm, although some part of the spectrum show significant differences in absorption quantities than other part (Haubrock et al., 2008). According to Profeti and Macintosh (1997), in the visible and infrared spectrum, soil water absorption causes a decrease of soil reflectivity in several wavelength intervals, the main two being located in the mid-infrared and centered at 1.45 and 1.95 μm . The review of the physical processes linking soil moisture to its reflectance clearly shows that the spectral variation due to water absorption at different region of the electromagnetic spectrum could be used to get an estimation of soil water content (Weidong et al., 2003). Further research has shown that the shape of the reflectance spectra was modified because of the occurrence of the well-defined water absorption bands in the short wave infrared domain (Weidong et al., 2002).

According to Weidong et al. (2003), the overtone and combination absorption bands of molecular water around 900 nm, 1400 nm, 1900 nm and the fundamental absorption band around 2800 nm are sensitive regions that show increased variability. Bowers and Smith (1972) observed a linear relationship between the absorption in a water absorption band (970-980 nm, 1200 nm, 1450 nm) and soil water content (Wang and Qu, 2009). To estimate surface soil moisture, Weidong et al. (2002), conducted a

laboratory experiment to study a single band reflectance approach in which they analyzed 18 different soil types to determine the relativity, i.e., the ratio between measured reflectance and the reflectance of the corresponding reference sample under dry conditions and found that best results can be achieved in the major absorption band around 1944 nm.

Although soil texture and soil composition have a great influence on the reflectance, it is expected that by using selective wave bands, the dependence of moisture detection on soil composition can be reduced. By using the spectral reflectance signature of a surface, one can estimate moisture content of the soil surface (Heusinkveld et al., 2008). Bowers and Hanks (1965), demonstrated this by measuring the light reflection from a soil sample in the 0.5–2.6 mm range of an equilibrated moist soil sample placed under a spectrometer. The water absorption bands in the reflected spectra were evident around 1.45 μm and 1.93 μm , however in satellite remote sensing these wavebands cannot be used since the solar radiant energy at these wave bands is absorbed in the atmosphere.

Weidong et al. (2003) conducted an experiment in which the first derivative is calculated as the difference in reflectance between two consecutive bands. As a generalization of this, they also created the reflectance difference between two arbitrary bands for all wavelength combinations and established a linear regression between these differences and the soil moisture values. This relationship finally generated better correlations as compared to the relative reflectance and reflectance derivatives applied in their studies. Bogrekci and Lee (2004) used a combination of the wavelengths 340nm, 1450nm, and 1940nm to estimate soil moisture. The main advantage of multi-band

spectral features in studying soil moisture is that their best results are not necessarily limited in the water absorption bands and hence in the context of developing an outdoor methodology that may be applied from airborne and space-borne sensors, this advantage is crucial (Haubrock et al., 2008).

Normalized multiband drought index (NMDI) for remotely sensing soil and vegetation water content has been designed, which is based on the soil and vegetation spectral signatures (Wang and Qu, 2009). Similar to the Normalized Difference Water Index (NDWI), NMDI uses the 860 nm channel as the reference; instead of using a single liquid water absorption channel centered at 1240 nm in NDWI, it uses the difference between two liquid water absorption channels centered at 1640 nm and 2130 nm as the soil and vegetation moisture sensitive band. Strong differences between these two water absorption bands in response to soil and leaf water content change gives this combination potential to estimate the water content for both soil and vegetations (Wang and Qu, 2009). Analysis revealed that by combining information from multiple near infrared, and short wave infrared channels, NMDI has enhanced the sensitivity to drought severity, and is well suited to estimate both soil and vegetation moisture.

Several indirect approaches have also been used for the estimation of soil surface moisture. According to Moran et al. (2004), surface soil moisture estimation using remotely sensed thermal wavebands is related to the use of radiative temperature (T_R) measurements, either singularly or in combination with vegetation indexes derived from visible and NIR wavelengths. Friedl and Davis (1994) found that variation in T_R is highly correlated with the variations in surface soil moisture. They derived these results with the study of the relationship between T_R and Normalized Difference Vegetation Index

(NDVI) over a tall grass prairie in northeastern Kansas. Chebouni et al. (2001) with their study on semi arid grassland site with static vegetation conditions found that multidirectional T_R data from field infrared thermometers could be used to estimate surface soil moisture. According to Kustas et al. (2003), the advanced application of the dual use of thermal imagery and spectral vegetation indices has been used in the estimation of surface soil moisture through the estimation of surface evapotranspiration rates. Many approaches such as temperature-vegetation contextual approach (TVX), surface temperature-vegetation index ($T_s/NDVI$) and temperature-vegetation dryness index (TVDI) have the potential to estimate soil moisture indirectly through the study of transpiration from vegetation (Moran et al., 2004). Hence approaches based on the directional TR or the complimentary TR vegetation indexes are powerful to estimate soil moisture but have the common limitation as like the optical techniques.

Table 2 shows physics applied for estimating surface soil moisture in three different remote sensing techniques, some major advantages associated with them and their limitations (Moran et al., 2004).

Table 2. Summary of physics, advantages and limitation of some remote sensing techniques used for surface soil moisture estimation (Moran et al., 2004)

Physics	Advantages	Limitations
Passive Microwave Sensing (Radiometer)		
Measures emission of thermal microwave radiation from soil Difference in dielectric constant of water (80) and soil (3.5) provides the main basis	Wide spatial coverage Insensitive to clouds and earth's atmosphere	Coarse resolution Influenced by surface roughness and vegetation biomass
Emissivity of soil varies from 0.6 (wet) to 0.9 (dry)	Satellite and aircraft sensors available	Costly
For a soil at temperature 300K, the variation in emissivity corresponds to the microwave brightness temperature of 90 K (40%-5% moisture) Microwave brightness temperatures are influenced by vegetation cover and atmospheric attenuation Increase in surface soil moisture generally increase in microwave brightness temperature	In the absence of significant vegetation cover soil moisture is the dominant effect on the received signal Good surface penetration	
Active Microwave Sensing (RADAR)		
Sends and receives a microwave pulse, radar antenna traverses the scene The backscatter coefficient is related to the topographic conditions of the locality, surface roughness and dielectric constant of the soil	High spatial resolution Many satellite sensors are operational	Infrequent repeat coverage Influenced by surface roughness and vegetation biomass
Magnitude of backscatter coefficient is related to surface soil moisture through the contrast of dielectric constant of soil and water	Insensitive to clouds and earth's atmosphere	Costly
Increase in surface soil moisture generally increase in backscatter coefficient	High surface penetration	
Optical remote Sensing		
Spectral information in VIS, NIR and SWIR regions can be helpful to study soil properties and moisture characteristics	Wide spatial coverage	Low surface penetration
Decrease in soil moisture leads to increase in soil reflectance Water absorption bands that are present in the spectrum are helpful for studying soil moisture content	High spatial resolution Multispectral sensors available	Influenced by vegetation Low ability to penetrate clouds, attenuated by earth's atmosphere
Numerous Indirect approach available- (NMDI), Directional TR, Complementary TR Vegetation Index	Numerous satellite sensors operational	Infrequent repeat coverage

CHAPTER III

METHODOLOGY

Laboratory and Outdoor Experiment

Soil Used

Laboratory and outdoor experiments were carried out with the soils from the Fairmount experimental field. In the Fairmount experimental field, there are four different soil series present. The eastern half consists of Antler silty clay loam (1396A) and Antler-Mustinka silty clay loam (1397A) which are both fine loamy soils and typic calciaquolls. The western half of the field consists of Doran clay loam (typic argiborolls, 1243A) and Clearwater-Reis silty clays (vertic haplaquolls, 1236A) (Jia et al., 2008).

Preparation of Soil Sample and Soil Sample Box

After collecting the soil from the Fairmount experimental field, soil was air dried for about a week and passed through a 6 mm sieve. It was kept in a soil sample box (47 cm × 47 cm × 20 cm (l×w×h) which was lined with thin black polythene to prevent water being absorbed by the wood. Three Watermark 200 Soil Matric Potential Sensors (Campbell Sci, Logan UT) that measures the soil Matric potential (Kpa) were placed in the soil at the depths of 5 cm, 10 cm and 15 cm respectively (Figure 6a).

Calibration of Watermark 200 Soil Matric Potential Sensor

Water was slowly poured in along the edge of the soil box (Fig. 6a) until the soil was fully saturated. After free water on the soil surface evaporated, the readings by the Soil Matric Potential Sensors at three different depths were recorded every 5 minutes. In

the mean time, samples of the soil were collected using an auger (Fig. 6b) in different interval of time to calibrate the Watermark 200 Soil Matric Potential Sensor.

The weight of wet soil was measured first (Fig. 6d) with approximately same volume for all the samples. Then the wet soil was placed in the soil oven for 24 hours at a temperature of 105 degree Celsius (Fig. 6c). This oven-dried soil was again weighed and the difference between the wet and dry weights was calculated to estimate gravimetric soil moisture content.

$$\text{Gravimetric Moisture Content} = (\text{Weight of wet soil} - \text{Weight of dry soil}) / \text{Weight of dry soil} \quad \text{Eq. 4}$$

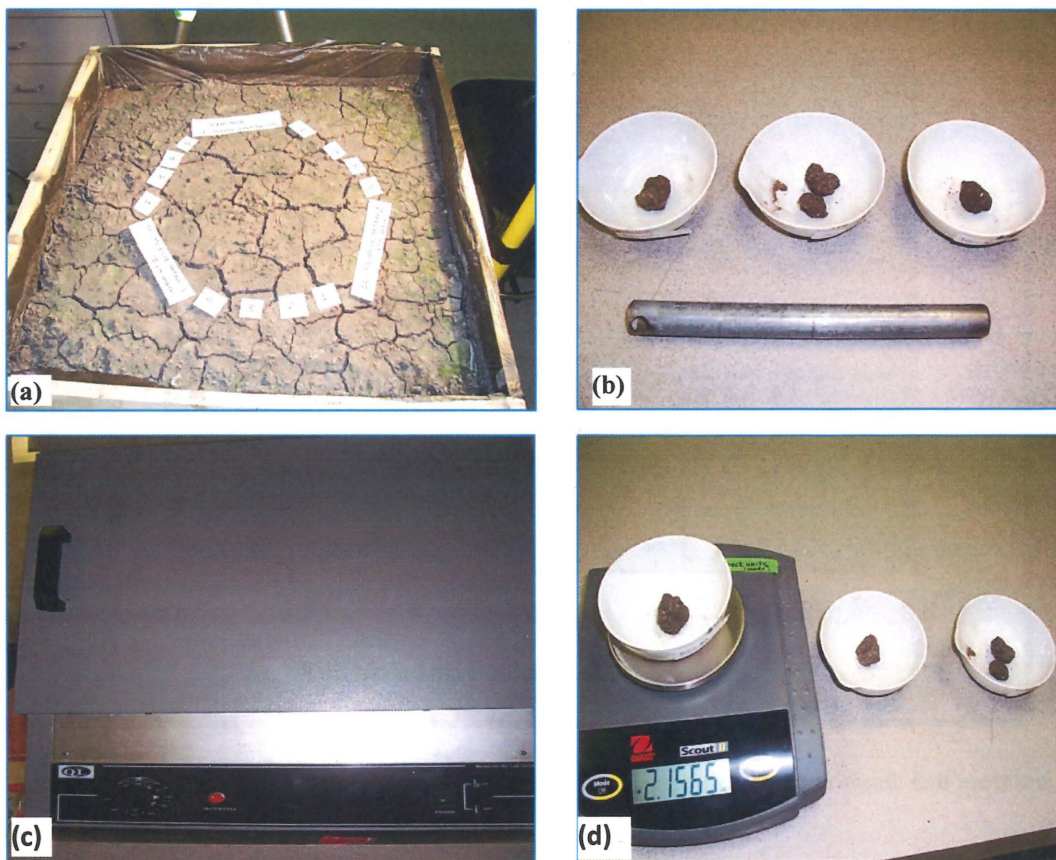


Figure 6. Instruments used for calculating gravimetric soil moisture content: (a) soil sample box, (b) porcelain plate and auger, (c) soil oven and (d) a scale of precision $\pm 0.001g$

A total of 12 soil samples were collected. The correlation between calculated gravimetric soil moisture concentrations with the readings by the Watermark 200 Soil Matric Potential Sensors can be seen in Fig. 7. The relationship was fitted with a 3rd order polynomial regression:

$$y = -1.4469(x^3) + 0.4361(x^2) - 0.0216(x) + 0.3254 \quad \text{Eq. 5}$$

where y is the gravimetric soil moisture, x is the logarithmic of soil water potential (Kpa) readings measured by the sensor.

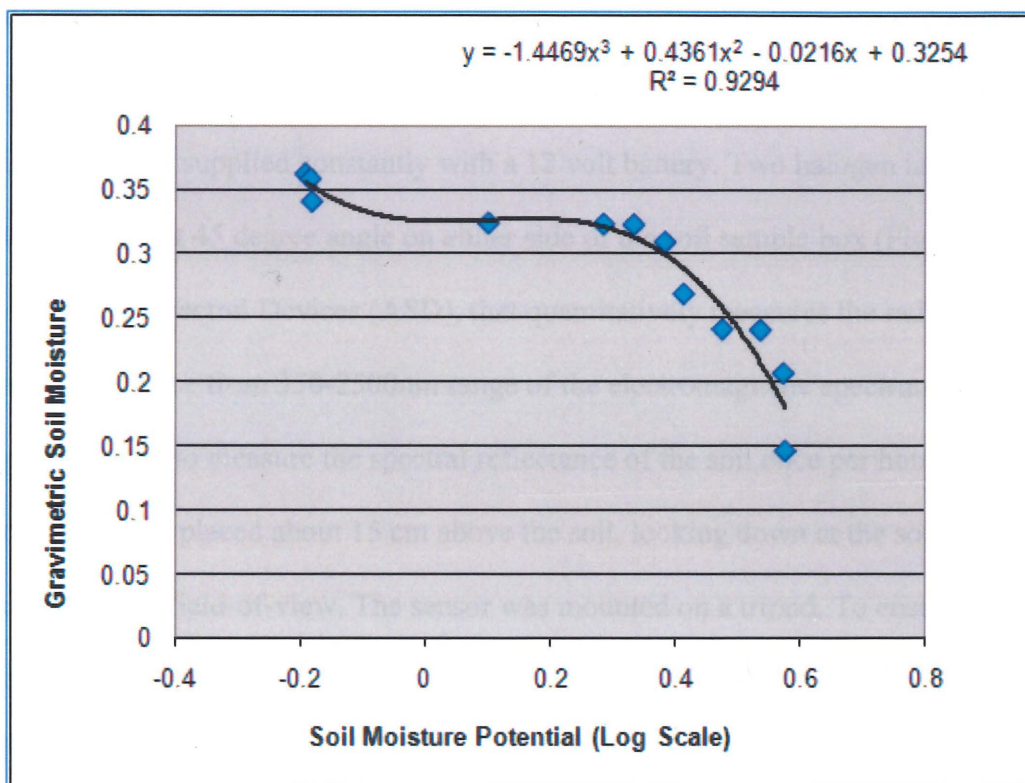


Figure 7. The relationship between gravimetric soil water content and the logarithmic soil moisture potential at 15 cm depth

The gravimetric soil moisture was later converted to volumetric soil moisture by factoring in soil bulk density (1.2 grams per cubic cm).

Volumetric Soil Moisture Measurement

With the arrival of ProCheck PC-1 soil moisture sensors (Decagon Devices, Inc.), the volumetric soil moisture concentration can be read directly. The ProCheck is a hand-held readout device used to interface with analog and digital soil moisture sensors and obtain instantaneous results. It can take digital reading of soil moisture in less than a minute.

Laboratory Experimental Set-up

The laboratory experiments were carried out in the wet lab of the ESSP department. Wires of the soil moisture sensors were routed from one end of the box to the soil moisture interface. Power for the Watermark 200 Soil Matric Potential Sensors interface was supplied constantly with a 12 volt battery. Two halogen lamps illuminated the soil box at 45 degree angle on either side of the soil sample box (Fig. 8). The Analytical Spectral Devices (ASD), that quantitatively measures the radiance, irradiance and reflectance from 350-2500nm range of the electromagnetic spectrum, was programmed to measure the spectral reflectance of the soil once per hour. The sensor of the ASD was placed about 15 cm above the soil, looking down at the soil surface with an eight degree field-of-view. The sensor was mounted on a tripod. To ensure the accuracy of the measurements, the ambient light that could interfere with the experiment was blocked. All equipment was carefully configured to avoid casting shadows into the field view of the ASD sensor. To minimize the effect due to variations in output from the halogen lights, gain and offset settings for the ASD were fixed during the measurements.

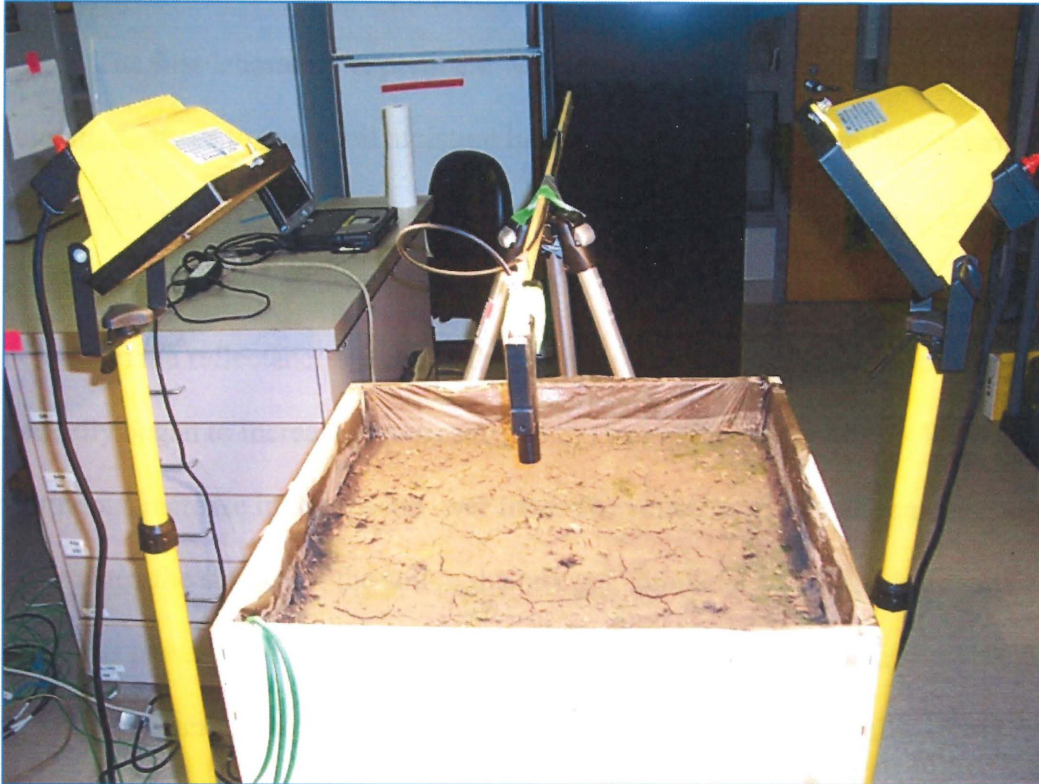


Figure 8. Laboratory experimental set up to collect the spectral reflectance of soil in a naturally drying moisture condition.

Measuring Spectral Reflectance of Soil at Varying Moisture Condition

Spectral measurements were performed in the laboratory to control irradiance conditions and isolate them from other interfering external conditions. Spectral reflectance data was acquired over the 350-2500 nm wavelength range using an ASD. The lamps were connected to a voltage regulation device to avoid possible variation of electrical power supply. A calibrated white spectralon panel (12 cm×12 cm) was used to get an absolute reflectance reference. During the natural drying process, spectral reflectance was measured hourly and the corresponding soil moisture was concurrently measured. At times during the experiment, an electric fan was used to expedite evaporation.

First Laboratory Experiment

The first laboratory experiment was carried out using Watermark 200 Soil Matrix Potential Sensors to track soil moisture in the soil sample box. Two 500 W lamps illuminated the soil sample box at 45 degree angle from either side of the soil sample box. With ASD continuously taking the reflectance spectra, we observed only subtle increase in the reflectance spectra in the beginning of the experiment. However, it gradually began to increase significantly as the soil in the box got drier. We observed a continuous increase in the spectra over time. The reflectance spectra remained almost stable when the surface of the soil in the box got completely dry, which was indicated by the cracks present in the soil. We observed that the soil moisture reading at the end of the experiment when the soil was dry was about 20 percent. A large number of reflectance spectra were collected over the course of the experiment. However, for the final calculation, only 14 different spectra were selected ignoring spectra that indicate only very subtle soil moisture differences. Some spectra were averaged when soil moisture readings were almost the same. Finally, the spectra obtained from the experiment were used in the calculation of simulated band reflectance using Eq. 6, the objective of which was to examine the correct band combination for detecting soil moisture.

Second Laboratory Experiment

The second laboratory experiment was carried out using a ProCheck soil moisture sensor. Two 300 W lamps illuminated the soil sample box at 45 degree angle from either side of the soil sample box. Because soil moisture readings could be made in real time, the ProCheck soil moisture sensor helped to collect the spectra in a more organized and systematic way. Soil from the first laboratory experiment was dumped and fresh soil was again collected from the field, air dried, sieved and kept in the soil sample box. After the

full saturation, spectra measurements began. The spectra showed similar behavior as the first experiment. A total of 11 different spectra were used for the analysis of the second laboratory experiment.

Measuring Spectral Reflectance under Natural Light

On clear sunny days, the soil sample box was taken outside the Clifford building and measurements were taken following the same process as the laboratory experiment (Fig. 9). Soil moisture at the depths of 5 cm, 10 cm, and 15 cm were measured with ProCheck soil sensor.



Figure 9. The soil sample box with different instruments that were used in the outside measurement

To validate the laboratory experiments which used halogen lights as light source, and to determine whether natural sunlight might yield different results than halogen lights, outdoor experiment was conducted using natural sunlight as the light source. We observed significant disturbance in the spectra around three wavelengths, i.e. around

1400 nm, 1900 nm and 2400 nm due to water absorption in the atmosphere. Since these regions of the wavelengths are not included in all the bands of the Landsat 5 TM, we simply avoid these wavelengths during our study.

Field Measurement of Soil Moisture in the RRV of the North Basin

To verify the model built from the laboratory and outdoor experiments, field measurements of soil moisture were carried out in different parts of the RRV (Appendix D, Fig. 37-44) during the growing season of 2010. Several agricultural fields that were tilled but not planted (i. e. bare soil) were selected. As soil moisture can vary within a given area over a short interval of time, soil moisture measurements were conducted during the same day and time (noon) when the Landsat was passing over. Fields were selected with varying moisture condition in order to test the applicability of the model in a much diverse moisture condition. Several measurements were taken in each of these fields at different dates while some fields were only used once. Altogether, 65 different measurements were taken. Four different agricultural fields near Fairmount experimental field were used more than twice in order to take the measurements on a continuous basis and for the sake of convenience. Shapefiles were created based on the GPS location within each field where measurements were taken to correspond the location in the image. All the fields where measurements were carried out were subsetted from the Landsat image and were run according to our model.

Fig. 10 shows a detailed flowchart of the data collection procedure and the use of these data in the preparation and validation of the model, and Fig. 11 shows a detailed methodology used for Landsat 5 TM.

A Flow Chart for Data Collection

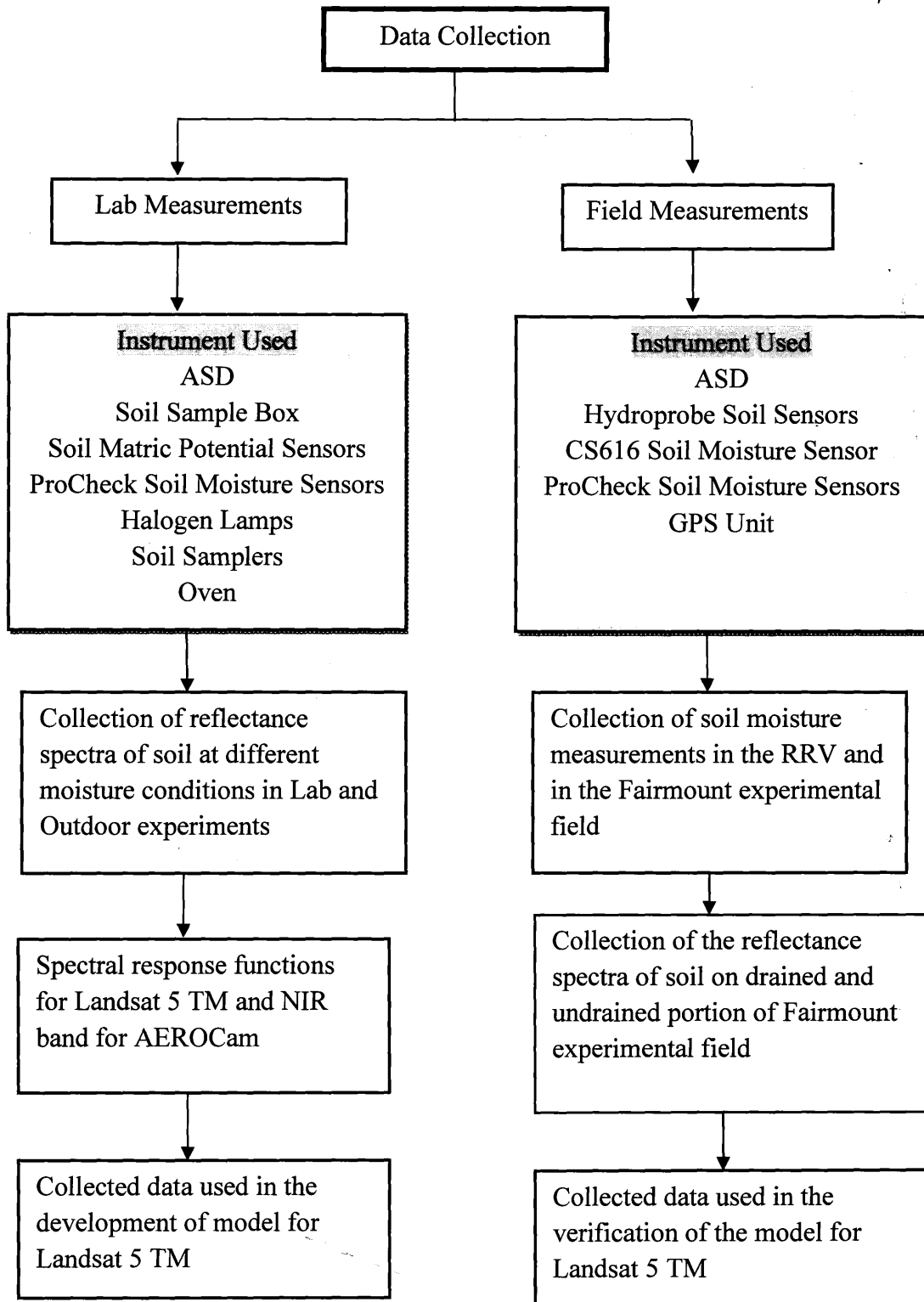


Figure 10. A Flowchart showing data collection in Lab and Field Experiment

A Flow Chart of Methodology Used for Landsat 5 TM

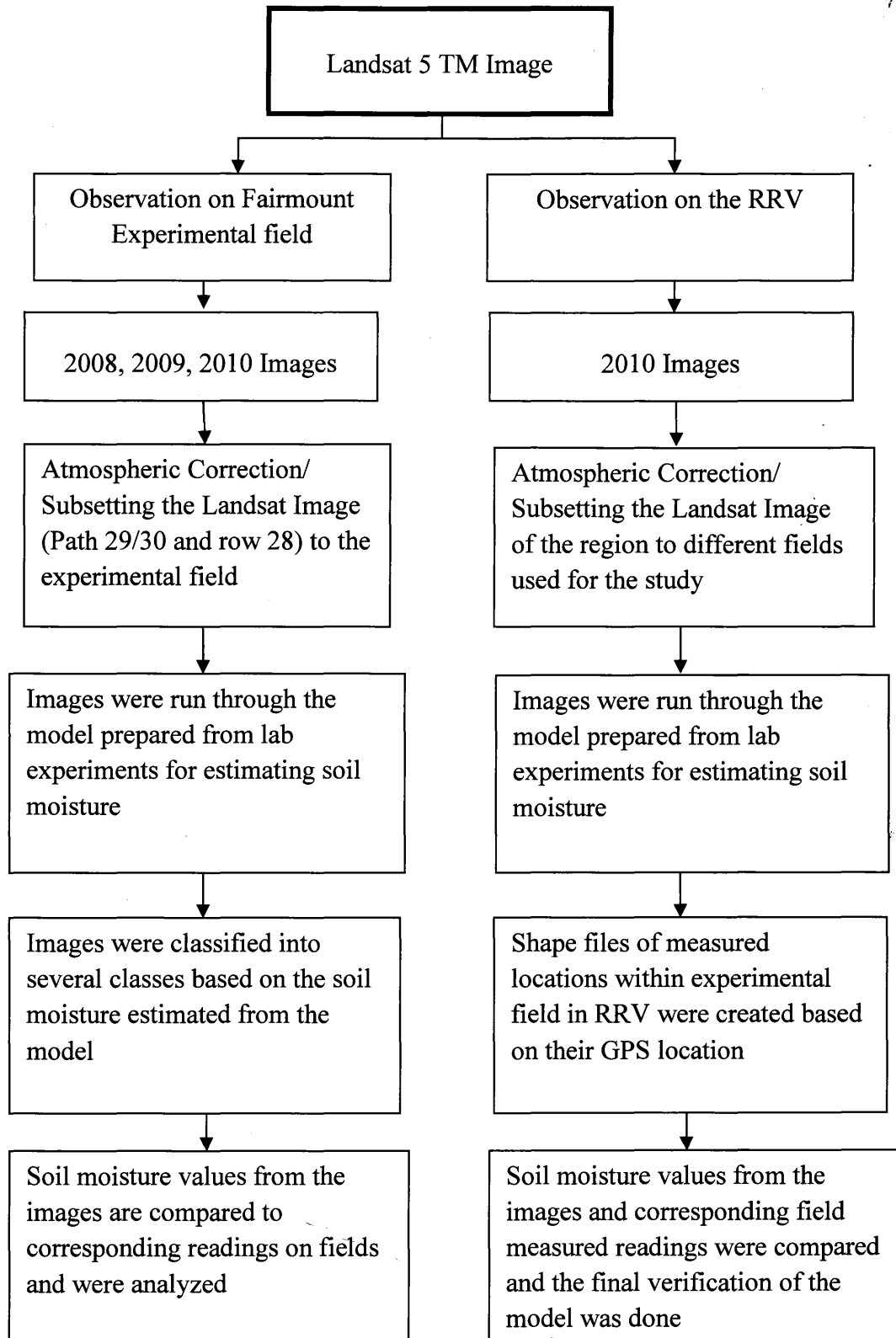


Figure 11. A Flowchart showing detailed methodology for developing the model for Landsat 5 TM

Variation of Spectral Reflectance with Moisture in the Experiments

Lab experiments were targeted to measure the spectral reflectance of soil under varying moisture condition at three different depths i.e. 5 cm, 10 cm and 15 cm. To begin with the experiment, the soil sample box was fully saturated. After obtaining the full saturation point by observation, measurement of both soil moisture and spectral reflectance began. Over the experimental time of about a week, we observed a distinct variation in the measurement of soil moisture at different depths. In a fully saturated condition and at 5 cm depth, soil moisture changed rapidly within a few hour of the beginning of the experiment. It remained almost constant with a subtle decrease in the midway through the experiment and slowly dropped and eventually remained constant in the final part of the experiment. Because of the nonlinear decrease in soil moisture, we did not select the spectral reflectance of soil based on soil moisture at 5cm depth. However, at 10 cm depth, we observed that soil moisture dropped slowly with an initial drop of 5 to 7 percent before stabilizing and remaining relatively constant until the end of the experiment. Since the spectral reflectance changed gradually throughout the experiment, the constant soil moisture reading at 10 cm depths were inappropriate to be used. This phenomenon is due to the movement of water from the 15 cm depth to the upper surface in the process of evaporation. At 15 cm depth, the soil moisture remained constant for a few hours in the beginning of the experiment and began to drop in a constant manner until the end of the experiment. As spectral reflectance also remained almost constant at the beginning of the experiment and started declining gradually, soil moisture reading at 15 cm depth and the corresponding spectral reflectance were chosen to derive the model for all the experiments.

Problems Encountered with the Reflectance Spectra while Continuously Using ASD

While using ASD to take the continuous reflectance spectra of soil in varying moisture condition, we encountered some problem in the spectral curve. We observed discontinuity in the reflectance spectra after about 25 hours of continuous operation of ASD.

The initial reflectance spectra appeared normal but as the experiment continued, the measured reflectance started to show noticeable discontinuity at two wavelengths of 975 nm and 1760 nm (Fig. 12), which correspond to the switch of detectors. First order derivative analysis were done to the measured spectra and we found that the normal spectra that do not exhibit noticeable jumps typically have changes of the reflectance per unit wavelength with absolute values less than 0.002 nm^{-1} . The jumps at the two wavelengths are significantly greater and the magnitudes increase with time almost linearly until at about 100 hours of continuous operation. After this time the jump are relatively stable. For example, the jump at 975 nm increased from 0.004 nm^{-1} at hour 25 to 0.029 nm^{-1} at hour 100 and remains almost stable after this time period. At 1760 nm, the jump increased from -0.010 at hour 25 to -0.026 at hour 100 to its maximum and remains relatively stable until the end of the experiment (Fig. 13).

The following figure shows the discontinuity at two wavelength and their first order derivatives:

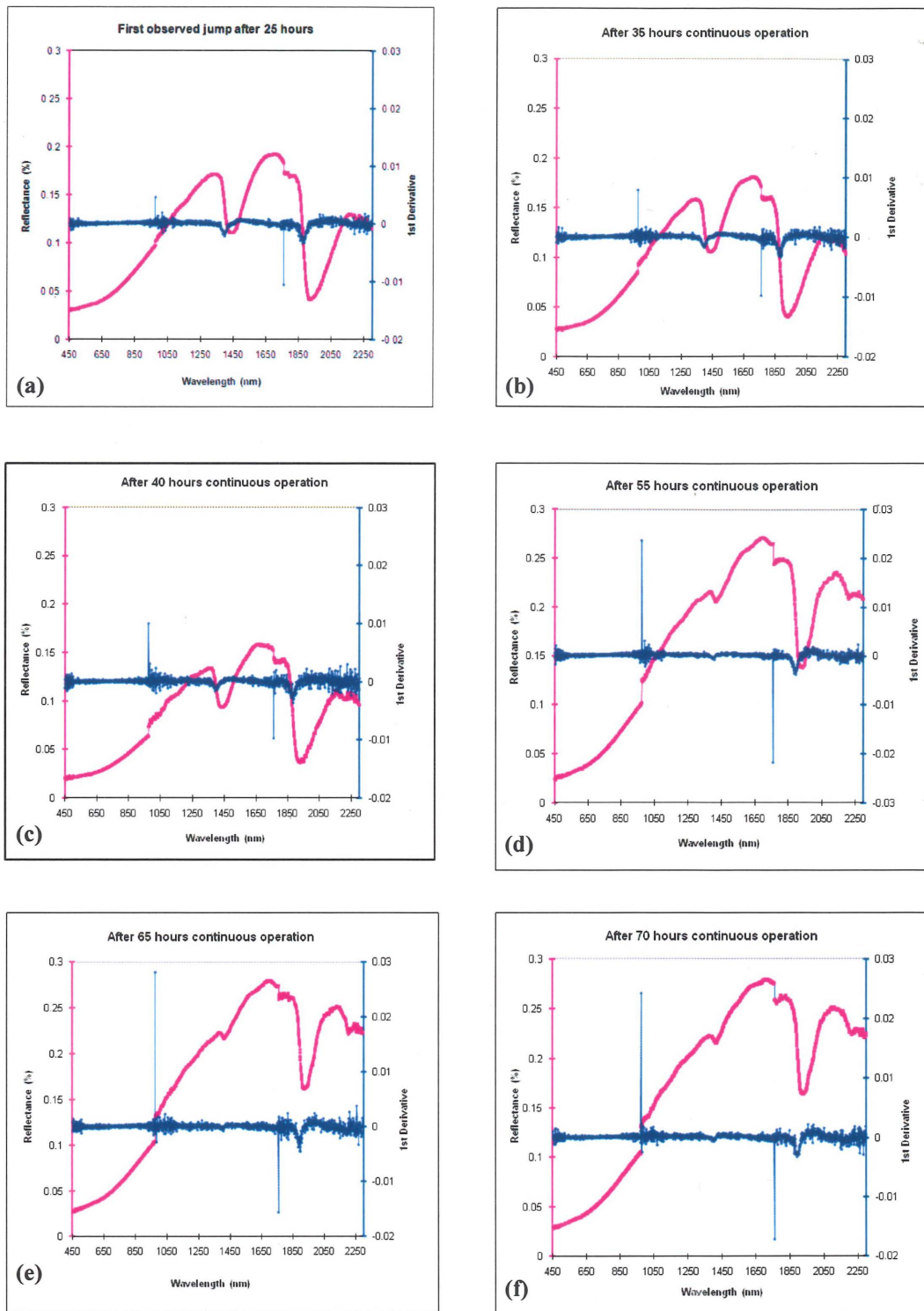


Figure 12. Measured reflectance spectrum (left y-axis) and its 1st derivative (right y-axis) with respect to wavelength (nm). (a) First observed jump at 25 hours of continuous operation, (b) after 35 hours of continuous operation, (c) after 40 hours of continuous operation, (d) after 55 hours of continuous operation, (e) after 65 hours of continuous operation and (f) after 70 hours of continuous operation

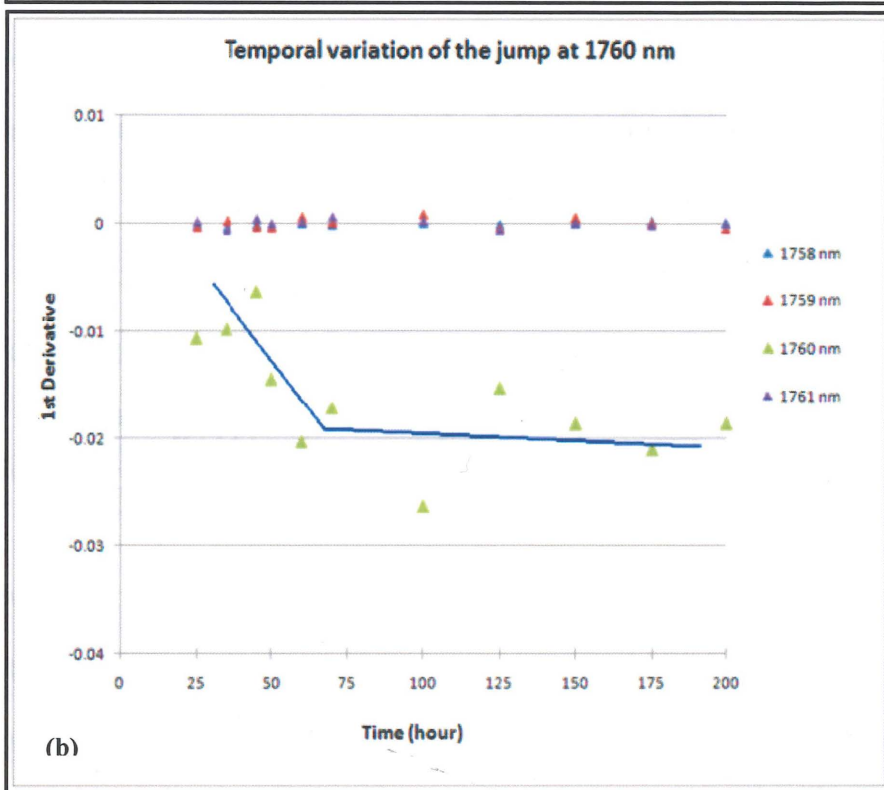
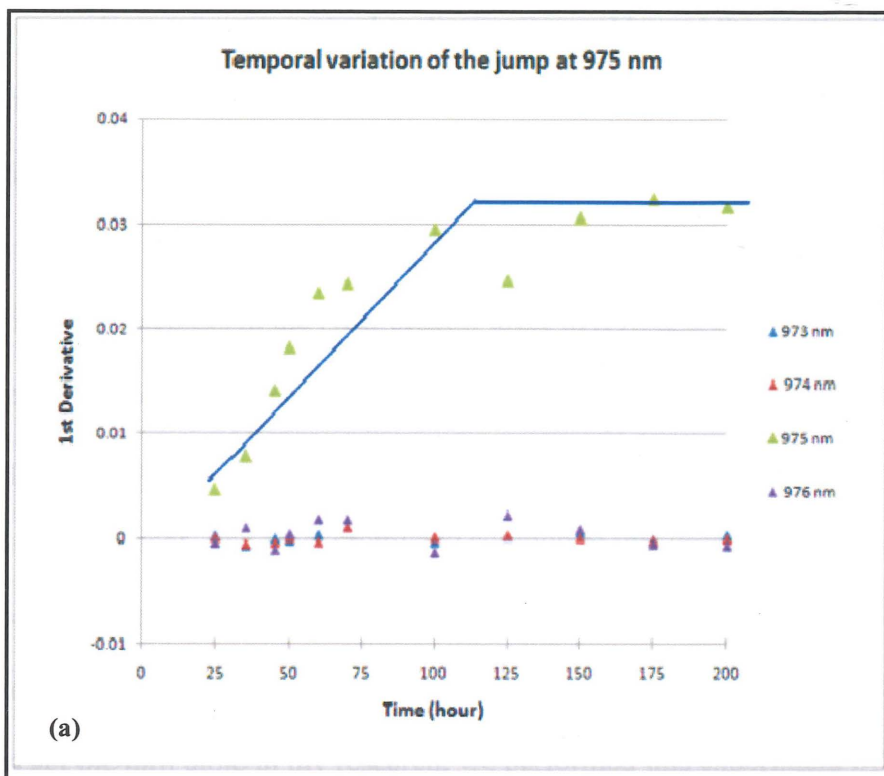


Figure 13. The temporal variation of the jump (a) at 975 nm and (b) at 1760 nm where they increased in a linear fashion at the beginning and remained relatively constant after about 100 hours of operation

A poster was prepared to discuss the problem of the spectral jumps at the ASD International Symposium which was held from Feb 24 to 26, 2010, in Boulder, Colorado. We found out that this problem is associated with the constant reading of the sensor at a fixed point in the soil box during the long period of the experiment. As there are three different detectors in the ASD sensor, these detectors are looking at three different points in the surface of the soil box when the sensors are fixed. This eventually will affect the spectral signature of the soil as surface moisture decreases randomly over the period of the experiment. The most promising solution to this problem is the use of the conveyor belt or the turn table (Goetz et al., 2009) over which the soil sample can be placed and accurate measurements can be obtained. However, due to the financial cost and time lag to get the turn table in my research, we performed this experiment by holding the sensor with hand everytime we took measurements. The shaking of the hand averaged the reading of the detectors and minimized the jump to a larger extent.

Model Preparation

To simulate the reflectance Landsat 5 TM and AEROCam would read, the following equation was used:

$$R_i = \frac{\sum_{j=A_i}^{B_i} W_{i,j} \cdot r_j}{\sum_{j=A_i}^{B_i} W_{i,j}} \quad \text{Eq. 6}$$

where,

R_i is the simulated reflectance for the Landsat band i ; j is the wavelength varying between A_i and B_i for the i th band; r_j is the spectral reflectance at the wavelength j ; and $W_{i,j}$ represents the spectral response for band i .

CHAPTER IV

RESULTS AND DISCUSSION

The spectra measured in all the experiment showed similar behavior. As soil moisture decreased, reflectance spectra increased distinctly. There was a subtle increase in the spectra at the beginning of the experiment, a significant increase in the middle of the experiment, and then they remained almost constant once the surface of the soil box had become completely dry.

Landsat and AEROCam

We can observe the widest dispersion of simulated reflectance values for band 5 (1550 nm-1750 nm) (Fig.14) among all the bands of Landsat 5 TM, which suggests the possibility of estimating surface soil moisture using this band. We can also observe that this dispersion gets wider as the wavelength increases. Both band 5 and band 7 (2080 nm-2350 nm) look better when choosing the right band for estimating surface soil moisture. However, further analysis was done to find out the optimal band or band combination. Similarly, among all bands of AEROCam, NIR band, with widest dispersion (Fig. 15), suggests the possibility of estimating soil moisture. All three experiment results were put together to find the best band or band combinations that can be used in our model. For this purpose, simple mathematical computation (addition, subtraction and division) among different bands for both Landsat 5 TM and AEROCam were done. An exponential regression line was used to best fit the data. Among many such combinations, a total of 15 different kinds are shown in Fig. 16 for Landsat 5 TM and in Fig. 17 for AEROCam.

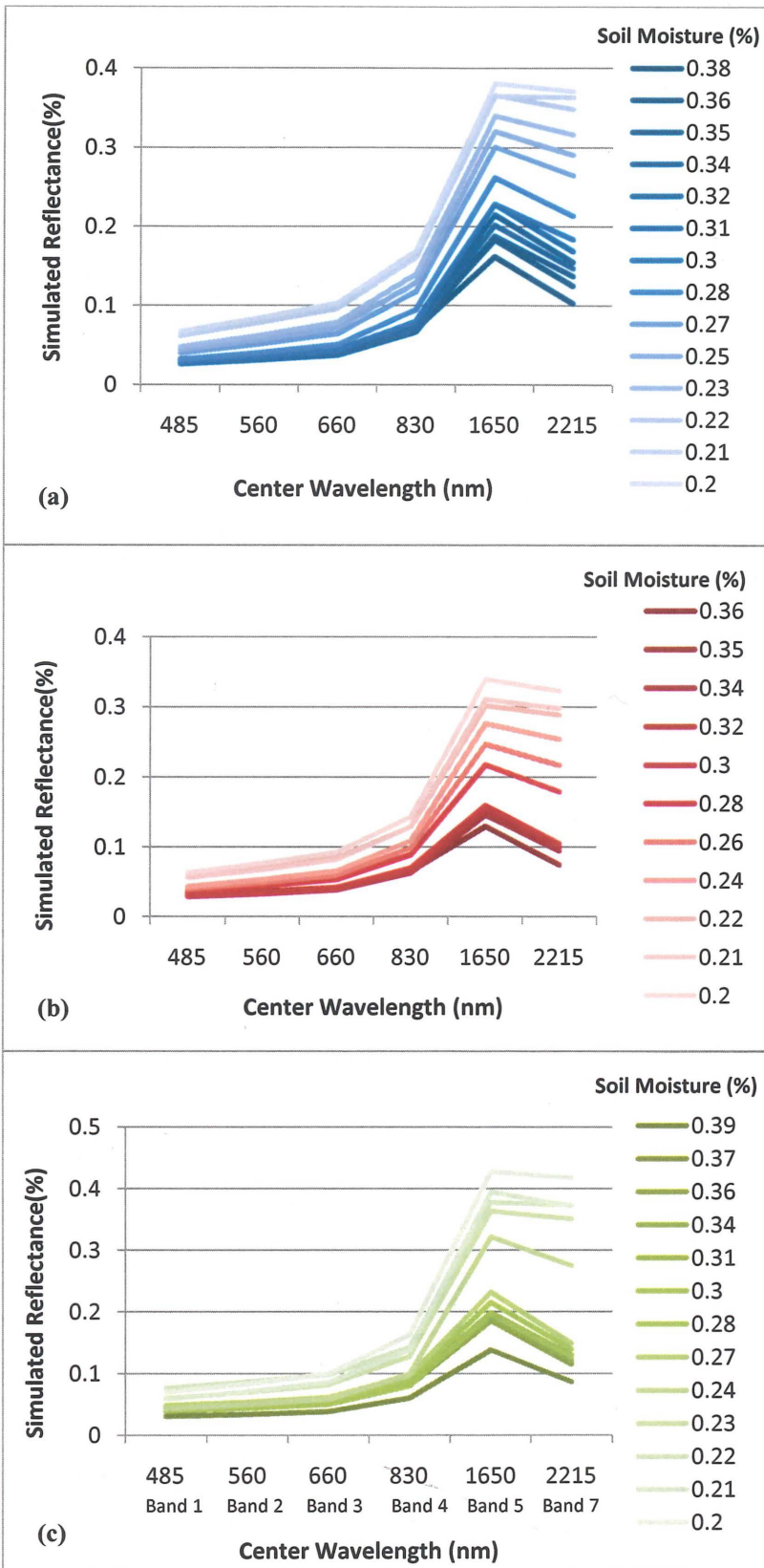


Figure 14. Simulated reflectance of soil collected at various moisture levels: (a) first lab experiment (b) second lab experiment (c) outdoor experiment with respect to the center wavelength for Landsat 5 TM

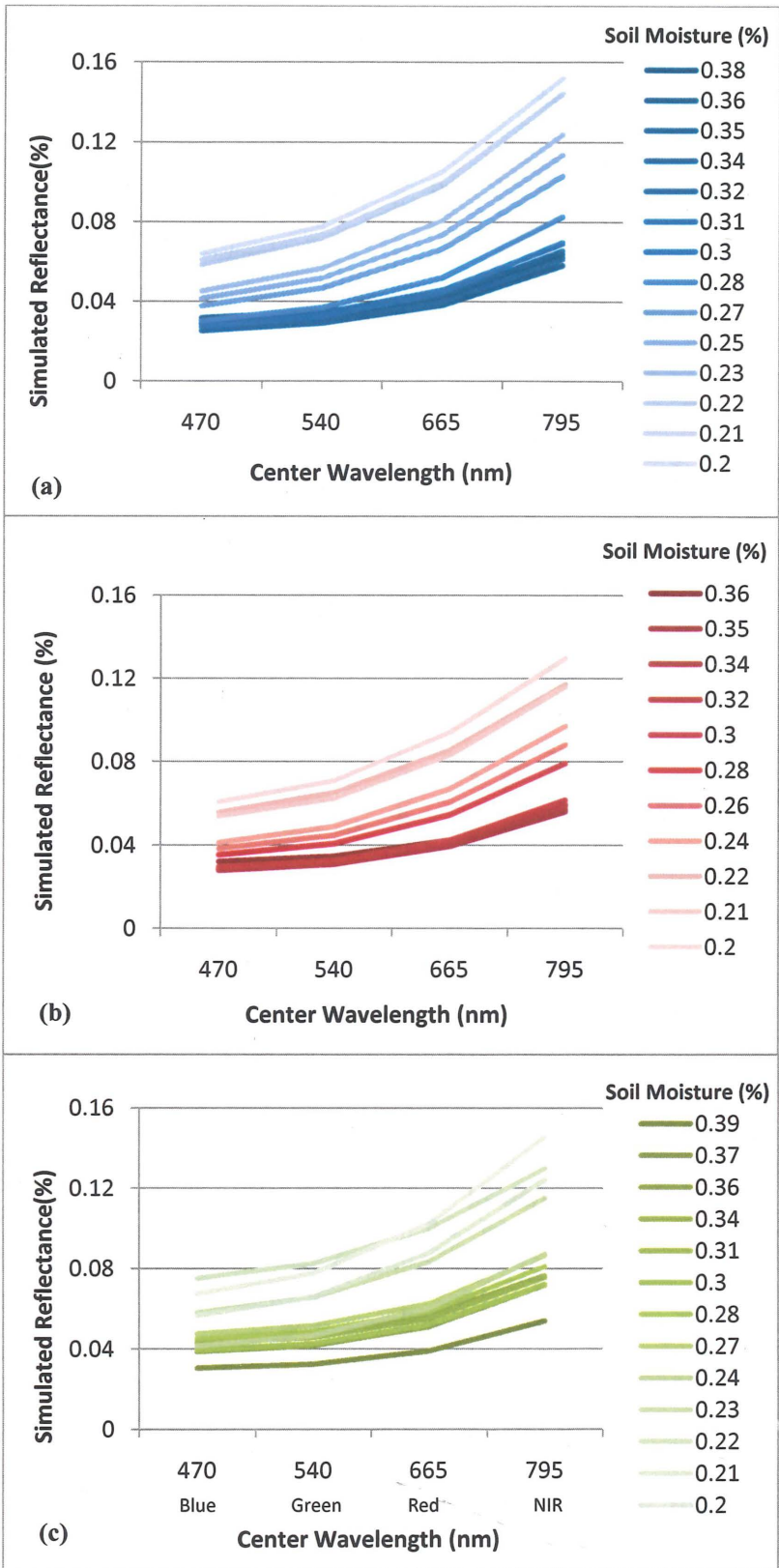


Figure 15: Simulated reflectance of soil collected at various moisture levels: (a) first lab experiment (b) second lab experiment (c) outdoor experiment with respect to the center wavelength for AEROCam

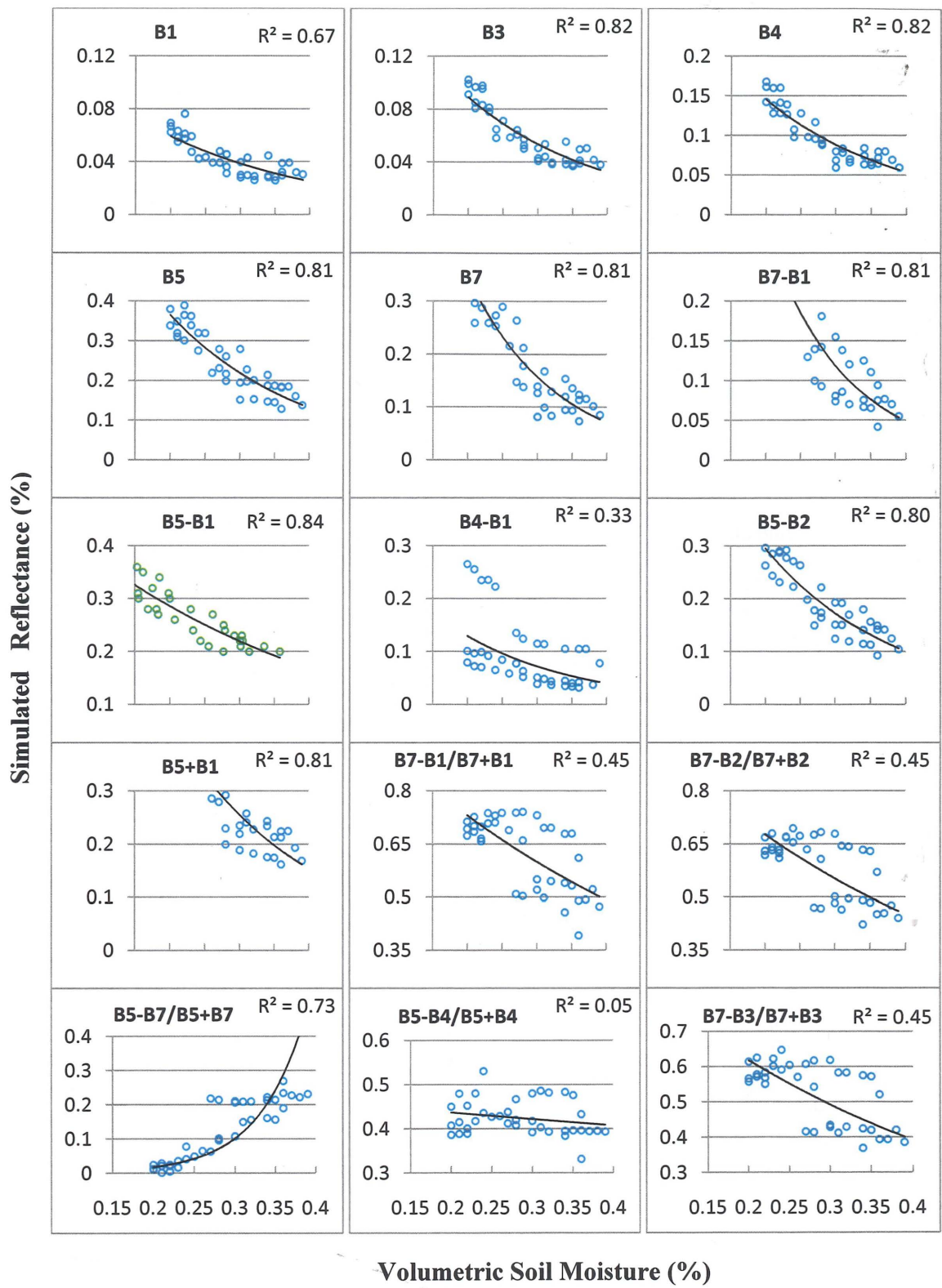


Figure 16. Different band and band combinations for the simulated reflectance value of Landsat 5 TM plotted with respect to soil moisture from all three experiments

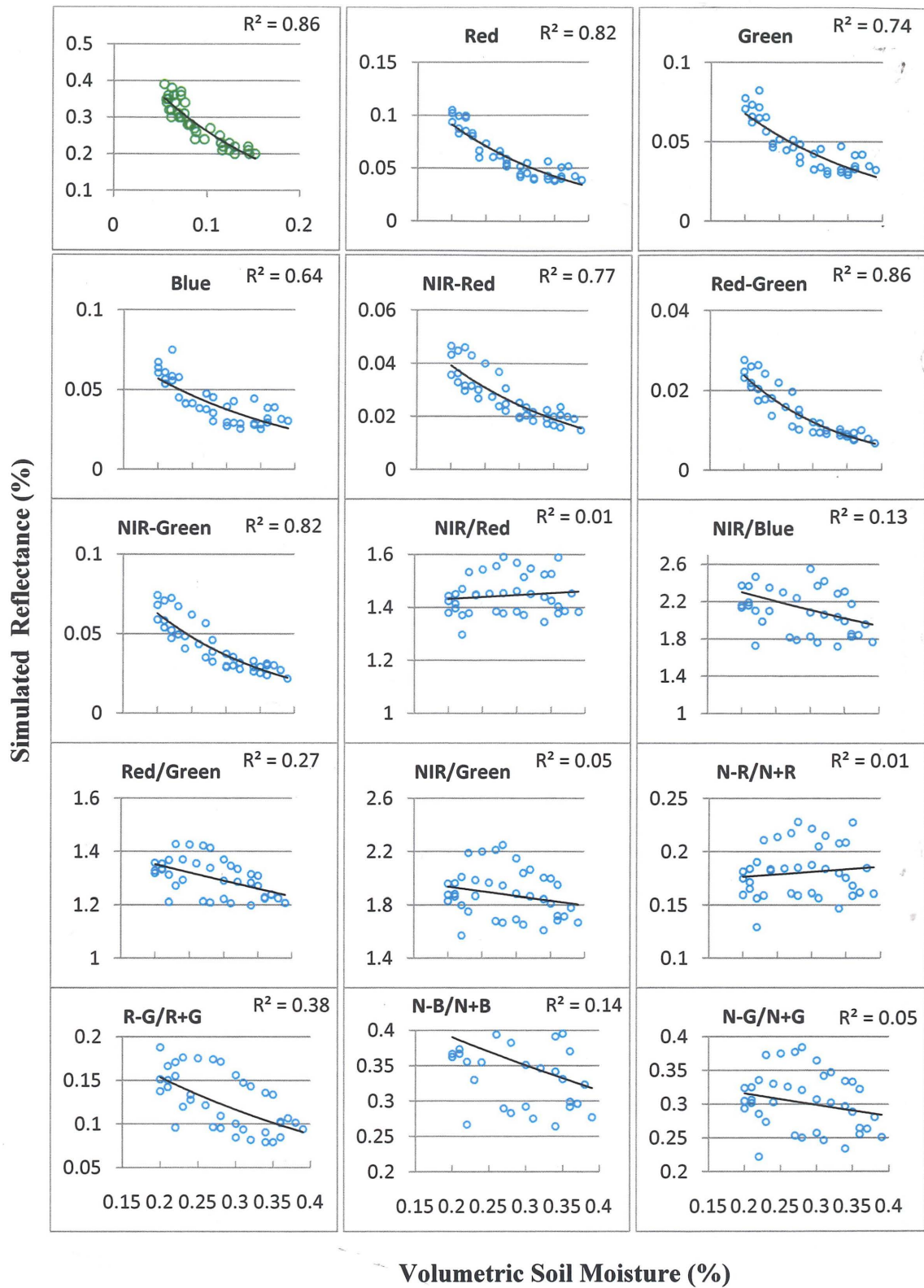


Figure 17. Different band and band combinations for the simulated reflectance value of AEROCam plotted with respect to soil moisture from all three experiments

With the results from the above mentioned combinations and judging from the correlation coefficient, subtracting band 1 (450 nm- 520 nm) from band 5 (1550 nm-1750 nm) (Fig. 16) gave the best results for Landsat 5 TM. For AEROCam, NIR band itself gave the best result (Fig. 17).

Volumetric soil moisture values were plotted with respect to the chosen band combinations (Band5-Band1) for Landsat 5 TM (Fig. 18) that was acquired during all the experiments and an exponential relationship was used. Repeatedly the results show that this band combination is the best with relatively higher R^2 values. R^2 values from the first, second and third experiments were 0.97, 0.97 and 0.90 respectively. Hence, this band combination was used for preparing the final model.

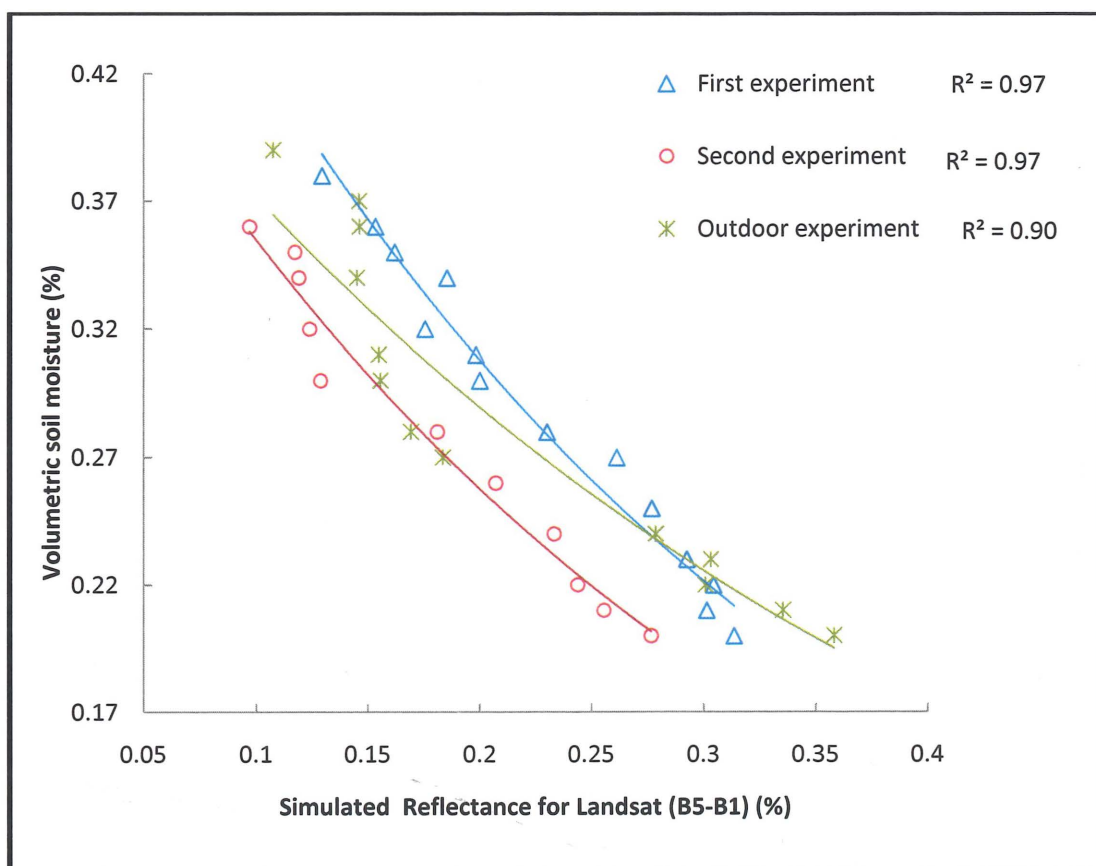


Figure 18. Relationship between volumetric soil moisture and simulated reflectance of Landsat band (B5-B1) collected during all three experiments

Volumetric soil moisture values were plotted with respect to the NIR band for AEROCam (Fig. 19). Repeatedly the result showed that NIR band is the best band with relatively higher R^2 values. The R^2 values for the first, second and third experiments were 0.93, 0.95 and 0.84 respectively. Hence, this band was used for preparing the final model.

With a trend in change in soil moisture values similar to the simulated reflectance value and their consistency in all the experiments (Fig. 18; Fig. 19), we finally decided to combine the results from all the experiment to get a single equation that could best represent the model.

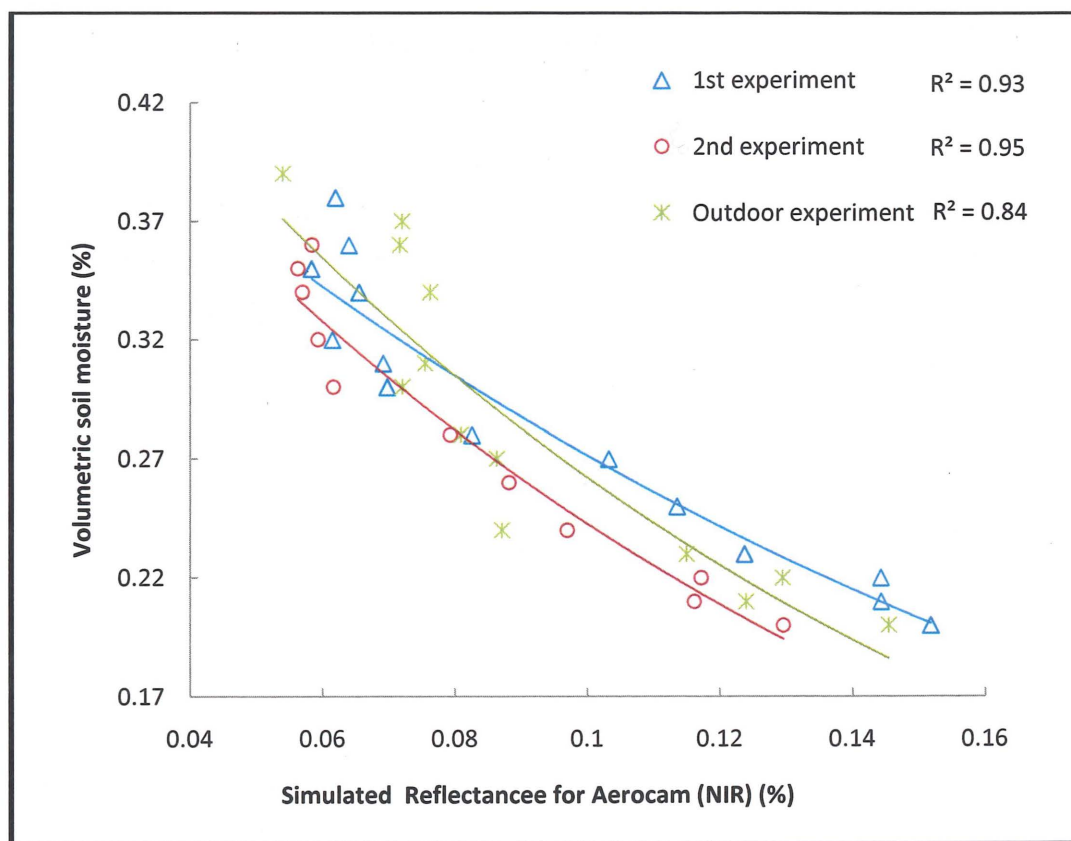


Figure 19. Relationship between volumetric soil moisture and simulated reflectance of AEROCam band (NIR) collected during all three experiments

Regression Analysis for Landsat 5 TM

Regression analysis was done for the selected band combination using Statistical Package for Social Sciences (SPSS). Table 3 shows an exponential regression results. Based on the table, soil moisture and the selected band difference (B5-B1) have a negative relationship which is indicated by the negative coefficient on the band combination.

Hence, the dependent variable, i.e. soil moisture, can be calculated by using the following formula:

$$y = 0.4842e^{-2.641 \times (B5-B1)} \quad \text{Eq. 7}$$

where y is the volumetric soil moisture content and $(B5-B1)$ is the selected band combination for Landsat 5 TM.

Table 3. Regression analysis for selected band combination (Band5-Band1) for Landsat 5 TM.

Dependent Variable: Soil Moisture			
Variables	Coefficient	(Standard Error)	Significant(P) <
Intercept	0.4842	0.02030	0.0001
(B5-B1)	-2.641	0.21342	0.0001

Number of Observations = 38

$R^2 = 0.84$

Root Mean Squared Error (RMSE) = 0.02495

Confidence Interval = 95%

The black solid line in Fig. 20 is the fitted values from the regression drawn from the relationship between the selected band combination and soil moisture. There were a total of 38 observations including two lab experiments and one outdoor experiment.

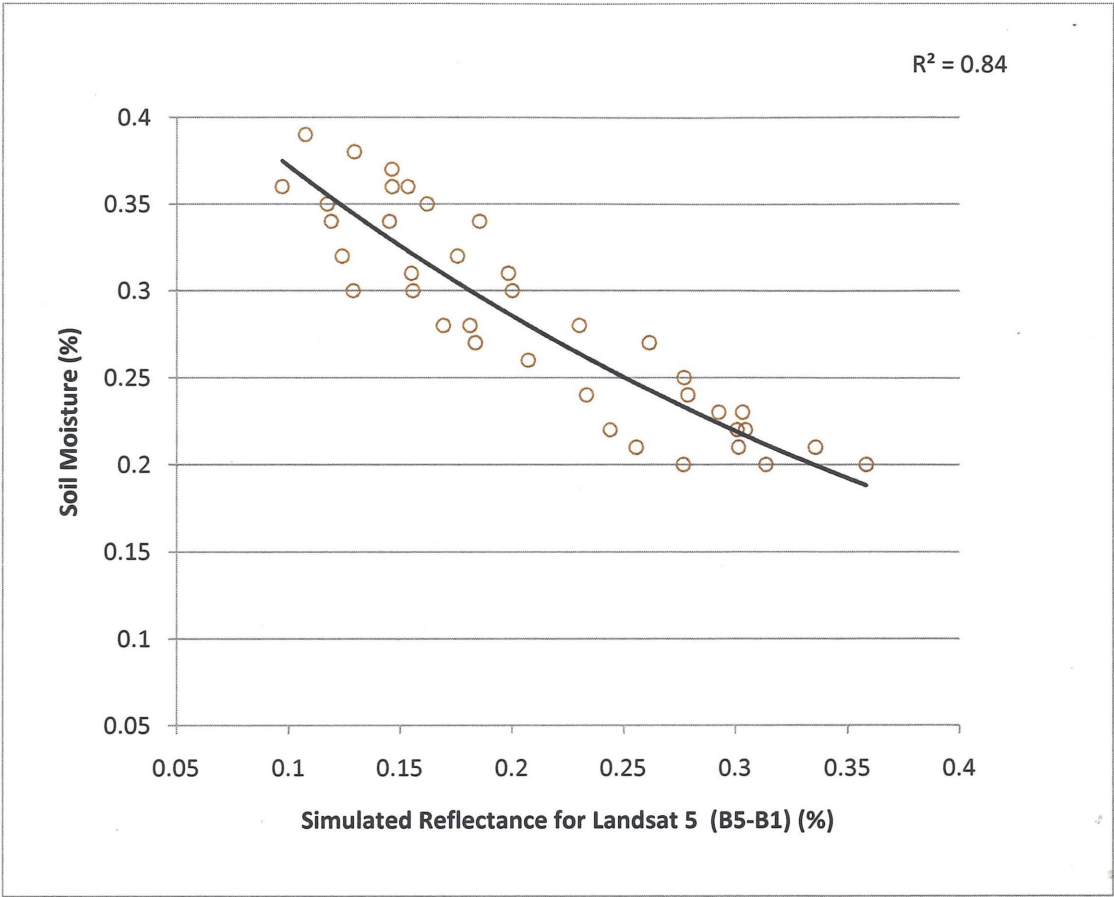


Figure 20. Graphical relationships between soil moisture and simulated reflectance of selected band combination (B5-B1) for Landsat 5 TM

Regression Analysis for AEROCam

Table 4 shows the exponential regression results. Based on the table, soil moisture and the selected band for AEROCam have a negative relationship, indicated by the negative coefficient on the NIR Band (Table 2).

Hence, dependent variable, i. e. soil moisture, can be calculated by using the following formula:

$$y = 0.5004e^{-6.5 \times (\text{NIR Band})} \quad \text{Eq. 8}$$

Where y is the volumetric soil moisture and NIR Band is the chosen band for AEROCam.

Table 4. Regression analysis for selected band (NIR) for AEROCam

Dependent Variable: Soil Moisture

Variables	Coefficient	(Standard Error)	Significant (P) <
Intercept	0.5004	0.023099	0.0001
NIR Band	-6.5	0.534572	0.0001

Number of Observations = 38
 $R^2 = 0.86$
 Root Mean Squared Error (RMSE) = 0.02384
 Confidence Interval = 95%

The black solid line in Fig. 21 is the fitted values from the exponential regression drawn from the relationship between the selected band and soil moisture. There were a total of 38 observations including two laboratory experiments and one outside experiment.

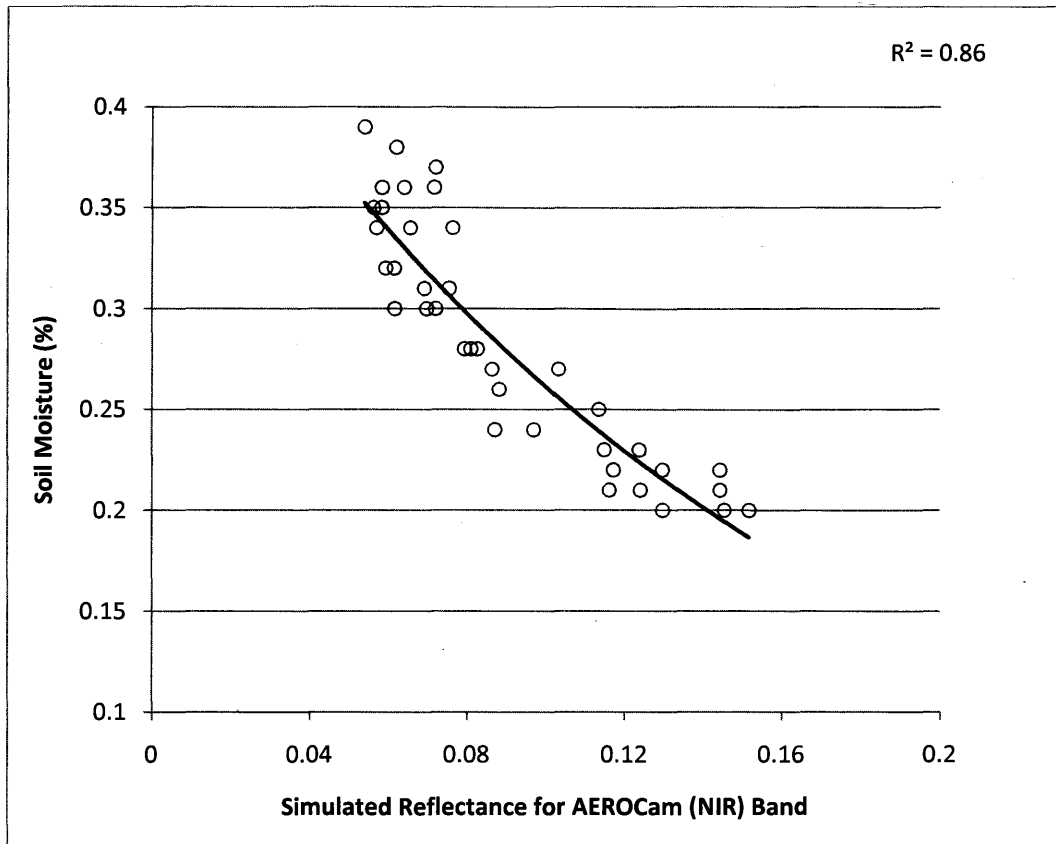


Figure 21. Graphical relationship between soil moisture and simulated reflectance of selected band (NIR) for AEROCam

From the results of the laboratory experiments, we can clearly observe that reflectance of soil increases as soil moisture decreases in a non-linear pattern (Fig. 22b). We observed that soil moisture, decreasing from high soil moisture percentage (approx. 38%), makes a subtle increase in the reflectance while it makes a bigger increase between 30 %-20 %. Again, this reflectance remains approximately constant when the soil becomes dry (approx. 20%). Therefore an exponential model best describes this relationship. Lobell and Asner (2002) studied the effect of moisture on soil reflectance over four different soil types of Mexico. They found that reflectance decreased with increasing moisture for all soils exhibiting a clearly nonlinear response that was well described by the exponential model. Kaleita et al. (2005), on their study to build a relationship between surface soil

moisture and spectral reflectance in the visible and near-infrared regions, found that an exponential model was appropriate to describe soil moisture from spectral reflectance data.

The use of Landsat 5 TM, band 5 for the study of surface soil moisture has been mentioned in the USGS web site (USGS, 2010). Table 3 shows the band designation for Landsat 5 TM and the scope of each of these bands in the study of different subjects. From table 3, we can see that Landsat band 5, reflected infrared, can be useful in discriminating moisture content of soil and vegetation (USGS, 2010).

Table 5. Band designation of Landsat 5 TM and the use of these bands

Band Designation	Spectral Bands	Use
1	blue-green	Useful for bathymetric mapping and distinguishing soil from vegetation and deciduous from coniferous vegetation.
2	green	Emphasizes peak vegetation, which is useful for assessing plant vigor.
3	red	Discriminates vegetation slopes.
4	Reflected IR	Emphasizes biomass content and shorelines.
5	Reflected IR	Discriminates moisture content of soil and vegetation; penetrates thin clouds.
6	Thermal IR	Useful for thermal mapping and estimated soil moisture.
7	Reflected IR	Useful for mapping hydrothermally altered rocks associated with mineral deposits.

Remote sensing techniques using the mid-infrared band to estimate soil surface moisture have been the focus of ongoing research (Shih and Jordan, 1992; Everitt et al., 1989). Landsat MIR data can provide useful information for monitoring regional surface soil moisture conditions (Shih and Jordan, 1992). With the use of Landsat TM to assess

regional soil moisture condition over the Lee and Collier County in Florida, Shih and Jordan (1992) found that high-resolution assessment of regional soil moisture conditions can be accomplished with Landsat TM, MIR imagery. On the basis of their qualitative ground observations, they also concluded that MIR reflectance is inversely related to the surface soil moisture conditions.

Fig. 22a illustrates the variation of soil-surface MIR reflectance at different wavelengths with changing soil moisture (Bowers and Hanks, 1965). As in Fig. 22a, we also observed the variation in soil-surface reflectance at MIR band with changing soil moisture in all of our experiments. (Fig.22b) is an example of spectral reflectance obtained under the first laboratory experiment.

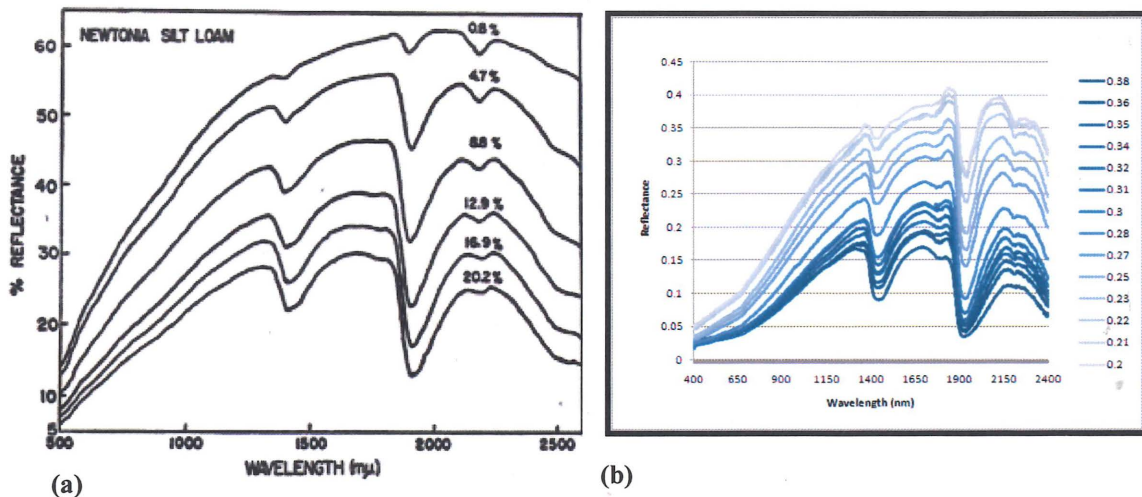


Figure 22. Variation of surface soil reflectance with changing soil moisture (a) for Newtonia Silt Loam (Bowers and Hanks, 1965) and (b) from first laboratory experiment (Roliss-Lindas Hamerly Doran)

In order to develop methods to estimate soil moisture from TM images, numerous authors have investigated the factors influencing the spectral reflectance curves of soils especially in the visible and infrared bands (Peterson et al., 1979; Stoner et al., 1979). According to Profeti and Macintosh (1997), the best regions for mapping water content of

soil are those adjacent to 1.50-1.73 μm and 2.08-2.32 μm , corresponding respectively to band 5 and band 7 of Landsat TM. In these bands, the spectral reflectance of the surface is strongly influenced by water content. Frazier and Page (2000) conducted a study to quantify the classification accuracy of single band density slicing of Landsat 5 TM data to delineate water bodies of the Murrumbidgee River near the city of Wagga Wagga, Australia, and found that mid-infrared (band 5) can be very helpful in detecting water bodies with highest accuracy. They also conclude that band 4 (760 nm-900 nm) and band 7 (2080 nm-2350 nm) of Landsat 5 TM are also useful for locating water bodies, however, band 5 proved to be the best among all of these bands. Frazier et al. (2003) used Landsat TM band 5 for inundation analysis over the same area for relating wetland inundation to river flow.

According to Miller and Yool (2002), in a study conducted for mapping forest post fire canopy consumption, MIR bands of Landsat 5 TM, (band 5 and band 7) are sensitive to moisture content of soil and vegetation and these bands further contribute new information for classifying burn severity. Hall and Ormsby (1987) conducted a research on characterizing snow and ice reflectance zones on Glaciers using Landsat TM data and found that the ratio of TM band 4 (0.76-.90 μm) to TM band 5 (1.55-1.75 μm) was useful for enhancing reflectivity differences on the glaciers.

To observe the relation of the reflectance spectra of soil with the water absorption coefficient in respective wavelengths, water absorption coefficients in the VIS-NIR-SWIR (400 nm-2500 nm) region of the electromagnetic spectrum was plotted with the ASD measured spectra taken during the first laboratory experiment (Fig. 23). One can

notice water absorption coefficient peaks in the water absorption bands around 735 nm, 840 nm of the NIR region and around 1400 nm and 1900 nm in the SWIR region.

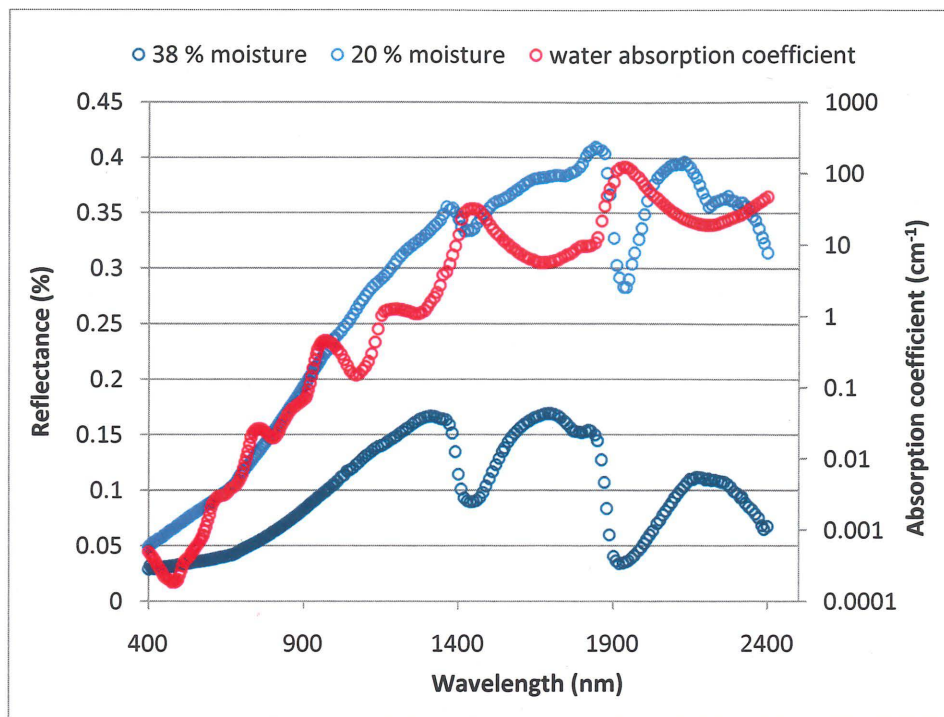


Figure. 23 Absorption coefficient of water (Segelstein, 1981) with the ASD measured spectra obtained in first lab experiment

Simulated reflectance band of Landsat 5 TM is plotted with the average water absorption coefficient at corresponding wavelengths (Fig. 24). Higher absorption coefficient of water in certain wavelength suggests that more light (irradiance) is observed, as soil moisture increases, and consequently reflectance would decrease. Based on this statement, water content has higher impact in band 5 of Landsat. Water absorption coefficient in band 1 is very low suggesting that change in soil moisture does not significantly change soil reflectance at this band, however, this region is influenced by other soil properties such as soil color. Hence, the combination of band 5 and band 1 of Landsat 5 TM can provide strong basis for the estimation of soil moisture. Simulated

reflectance band of AEROCam is plotted with average absorption coefficient of water at corresponding wavelengths (Fig. 25). Higher absorption coefficient of water in the NIR suggests that this band can be useful to estimate soil moisture. Spectral reflectance of plant canopy in the NIR provides important information of health of plant which can be related to the contribution of properties of soil including soil moisture. According to Rondeaux (1996), the spectral reflectance of plant canopy in the NIR region is the combination of spectral reflectance of plant and soil components governed by the optical properties of these elements.

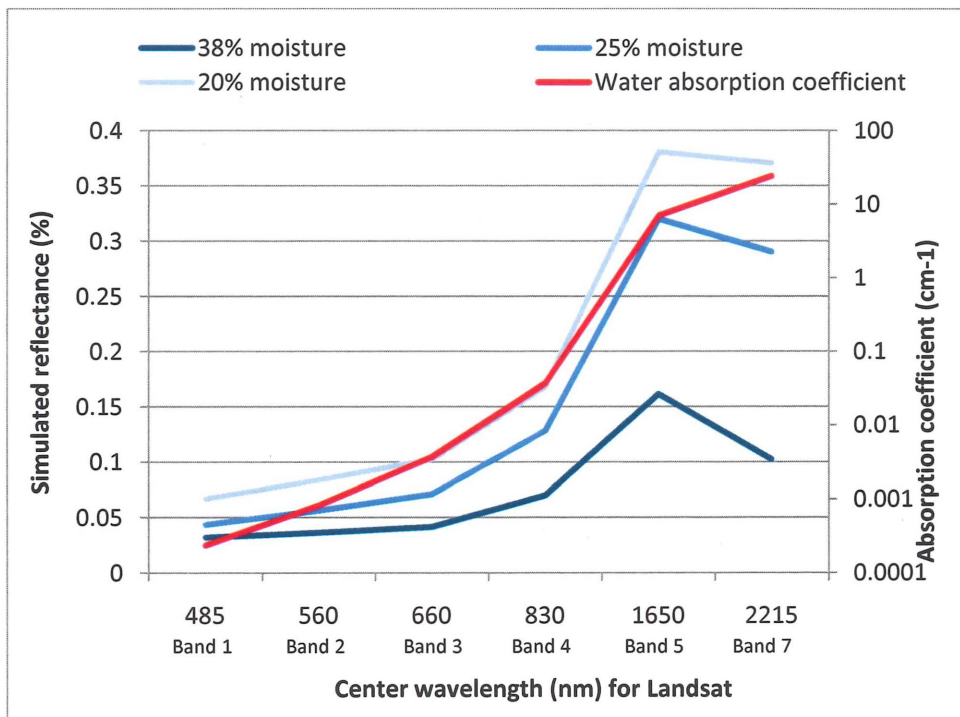


Figure 24. Absorption coefficient of water (Segelstein, 1981) with the simulated reflectance of Landsat in first lab experiment

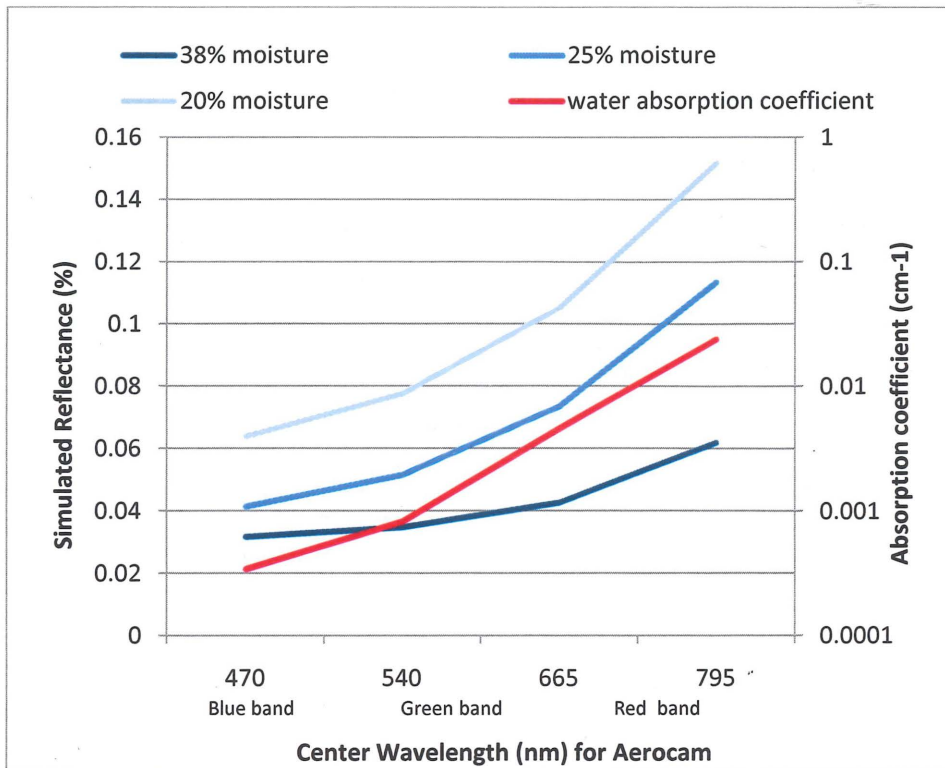


Figure 25. Absorption coefficient of water (Segelstein, 1981) with the simulated reflectance of AEROCam in first lab experiment

Observations in the Red River Valley

The model was tested over eight agricultural fields (Appendix D, Fig 37-44) in the RRV. Soil moisture values in the images showed a very close correlation with soil moisture values measured in every location in each of these fields (Fig. 26).

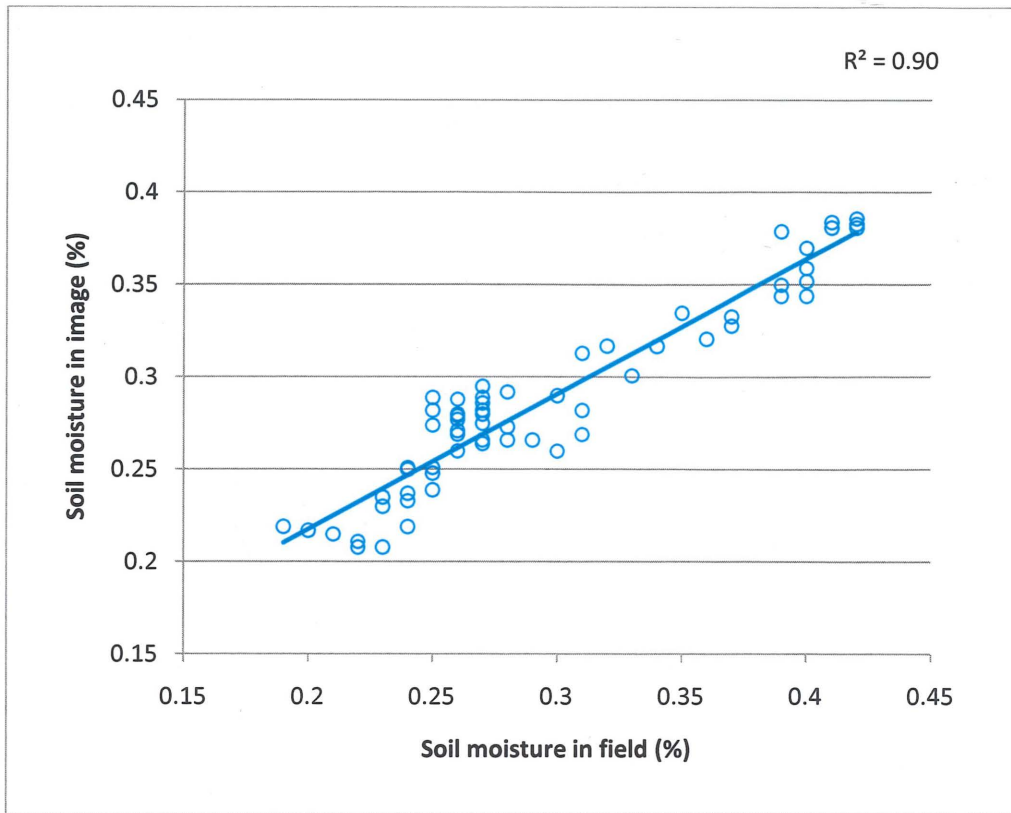


Figure 26. A comparison of surface soil moisture content measured in different experimental fields in the RRV compared to the soil moisture content estimated from Landsat 5 TM based model

Pearson correlation coefficient was calculated using Statistical Package for Social Sciences (SPSS) to see how closely estimated soil moisture from the image and measured soil moisture in field are related. The result shows a significant positive correlation between estimated soil moisture and field observations (Table 6, $P < 0.0001$). However, there is more variation in observations for field soil moisture than for estimated soil moisture, which is normally expected and this result could be attributed to experimental uncertainty in the field.

Table 6. Correlation analysis between estimated soil moisture and soil moisture measured in field

Variables (P)<	Pearson Correlation	df	Standard Error	Significant
Estimated Soil Moisture vs. Field	0.949	1	0.0205	0.001

Number of Observation = 65

$R^2 = 0.90$

Confidence Interval = 95%

Mean Estimated Soil Moisture = 0.286 Standard deviation = 0.049

Mean Field Soil Moisture = 0.294 Standard deviation = 0.646

Fitted regression line showed relatively higher R^2 ($R^2=0.90$). These results showed that the model is very good and can reliably be used to estimate surface soil moisture in the RRV area. The model works well in dry and average soil moisture conditions. But it underestimates the soil moisture value by about 3 to 4 percent when surface soil moisture is greater than 40 percent.

Observation in the Fairmount Experimental Field

Soil moisture readings in the Fairmount experimental field were taken in three different years, 2008, 2009 and 2010. Different soil moisture measuring instruments such as a CS616 Soil Moisture Sensor probe and a Hydroprobe were used to collect soil moisture readings at a depth of 15 cm. Soil moisture readings acquired from these sensors were matched with estimated soil moisture readings as an important step for the analysis and the validation of the model. Fig. 27 shows the location of the sensors that were

installed in three different years and the approximate division of the drained and undrained portion in the field.

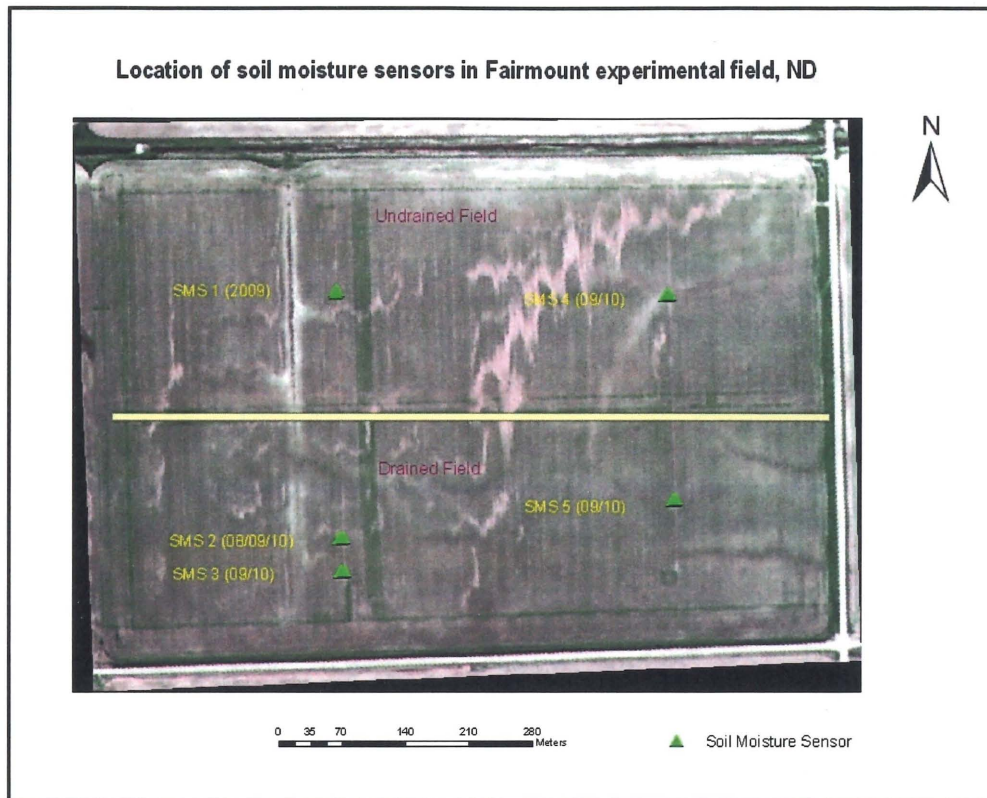


Figure 27. Location of soil moisture sensors (SMS) overlaid in a false color AEROCam image of the Fairmount experimental field

Observation of soil moisture at the Fairmount experimental field was made from April to May. The results demonstrated two major trends: Soil moisture varies significantly from year to year, and regardless of overall moisture levels, the drained portions of the field consistently have lower moisture level than the undrained portion.

Soil moisture estimated from images acquired over the Fairmount experimental field in all three years were separated in different classes, with 2% soil moisture increment, for the ease of observation and analysis. In 2008, we see slight differences in soil moisture between the drained and undrained portion of the field, as is evident in the

images acquired on 11th of May. Soil moisture content range from 28.1 to 34 percent in the entire field (Fig. 28a), with soil moisture being significantly higher in the undrained portion of the field compared to the drained portion. The mean soil moisture in the undrained portion remained about 31 percent while in the drained field it remained about 30 percent. After seven days of sunny weather and no rainfall, surface soil moisture in the field dropped, as shown in classification of May 18th image (Fig. 28b). However, surface soil moisture values on the undrained portion remained slightly higher, with mean 20 percent, than those on the drained portion of the field with mean of 19 percent. Soil moisture content on May 21st, 2009, image ranges from 36.1 to 40 percent (Fig. 29a) suggesting much wetter conditions than in 2008. Mean soil moisture in the drained field remains about 37 percent for both the drained and undrained field. Soil moisture content dropped down to about 20 percent on the image of 30th of May (Fig. 29b) due to continuous sunshine. However, we see that soil moisture in the undrained portion remains higher with a mean of 22 percent than that of the drained portion of the field with a mean of 20 percent, regardless of overall moisture levels.

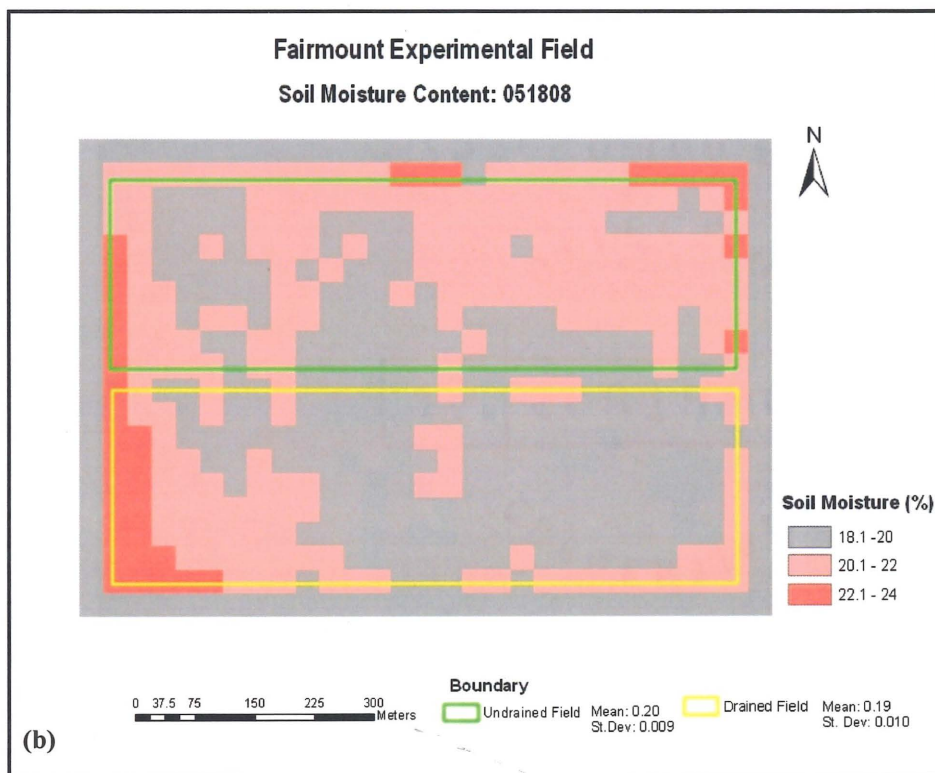
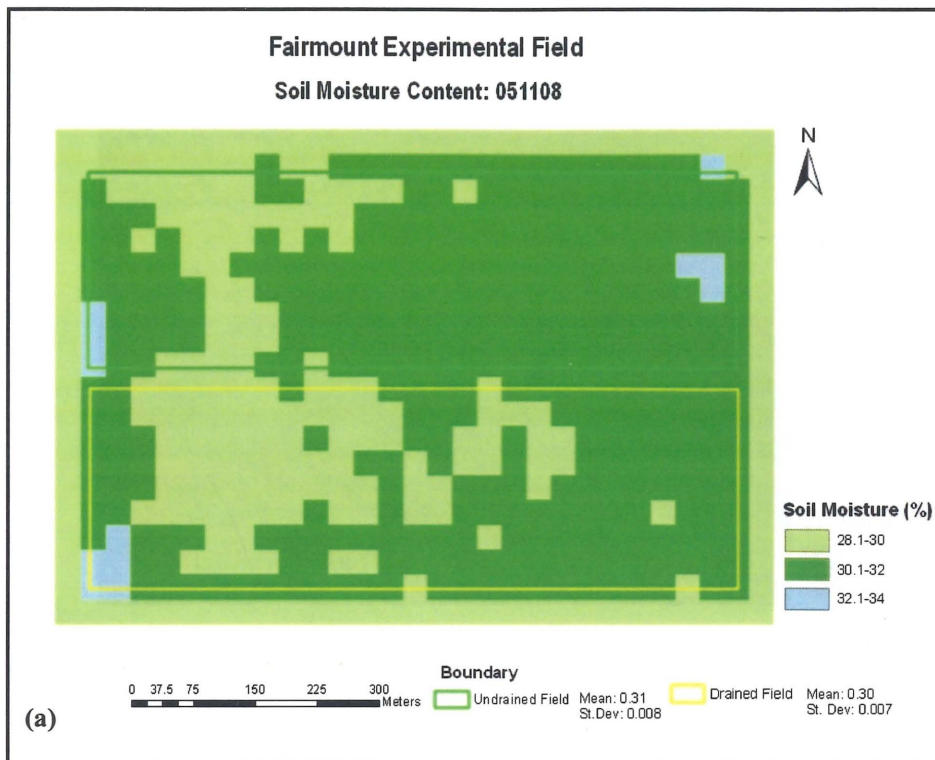


Figure 28. The difference in estimated soil moisture on drained and undrained portion of the Fairmount experimental field (a) on May 11, 2008 and (b) May 18, 2008

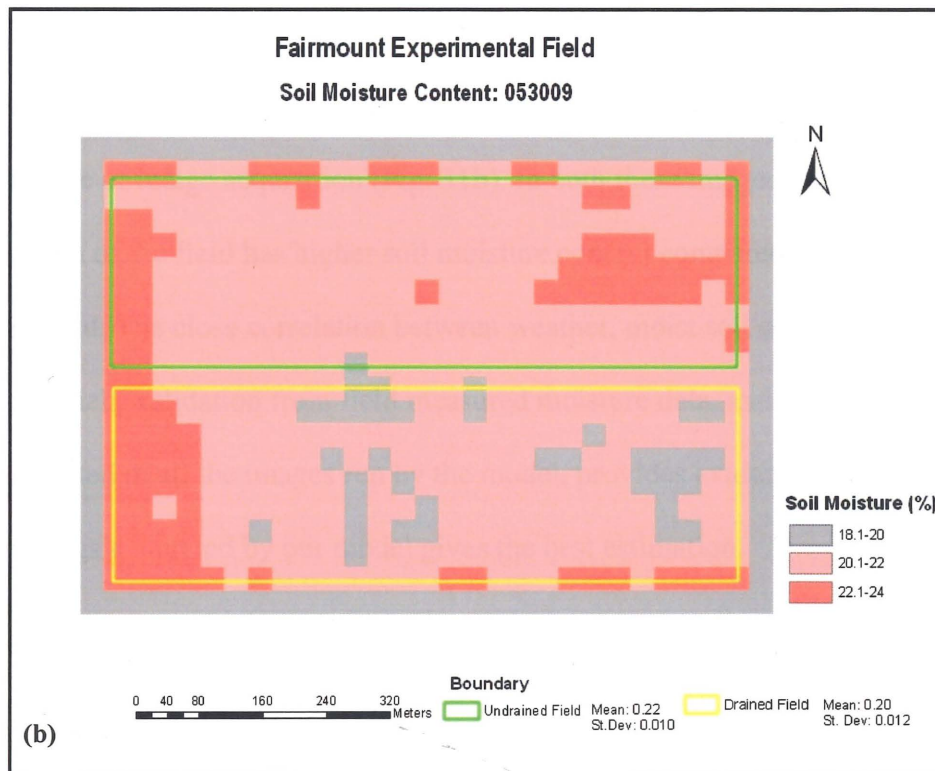
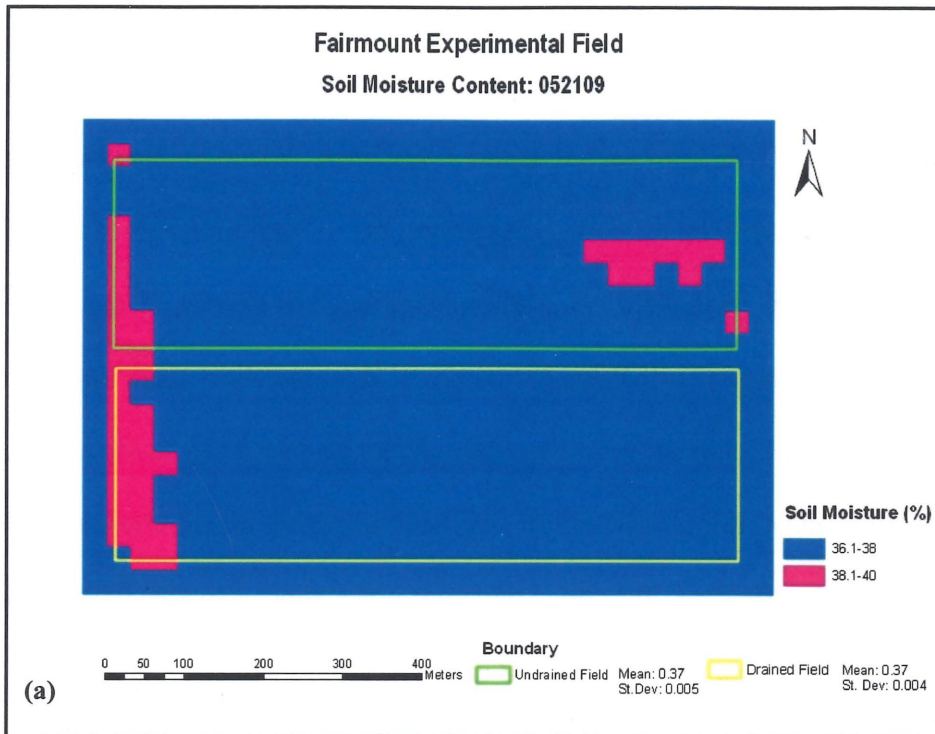


Figure 29. The difference in estimated soil moisture on drained and undrained portion of the Fairmount experimental field (a) on May 21, 2009 and (b) May 30, 2009

For the April 2010 images, we see the same trend regarding the soil moisture difference between the drained and undrained portions of the field. The estimated soil moisture content on 15th April 2009, image ranges from 20.1 to 30 percent (Fig. 30a). The mean moisture level in the undrained portion remains about 25 percent while it remains at 22 percent in the drained portion. For 22nd April 2010 image (Fig. 30b), the estimated mean moisture level in the undrained portion remains about 26 percent while it remains about 24 percent in the drained portion of the field. Field-measured data were also available for the first time provided by Dr. Xinhua Jia (NDSU) for the month of May, 2010. We can see that soil moisture content is significantly lower in the April 22, 2010 image. Soil moisture rises for the 8th May 2010 image. This increase in the moisture level is due to rainfall in the days prior to the image acquisition (Fig. 31a) (Weather Underground, 2010). The soil moisture value at the Fairmount experimental field for the date of May 17, 2010, is even higher due to continuous rainfall for about 4 days prior to the date of image acquisition (Fig. 31b). In both these images, we see that the undrained portion of the field has higher soil moisture content compared to the drained portion of the field. The close correlation between weather, moist soil conditions immediately after snowmelt, validation from field measured moisture data, and the corresponding moisture estimated in all the images run by the model, provides evidence that soil moisture readings generated by our model gives the best estimation.

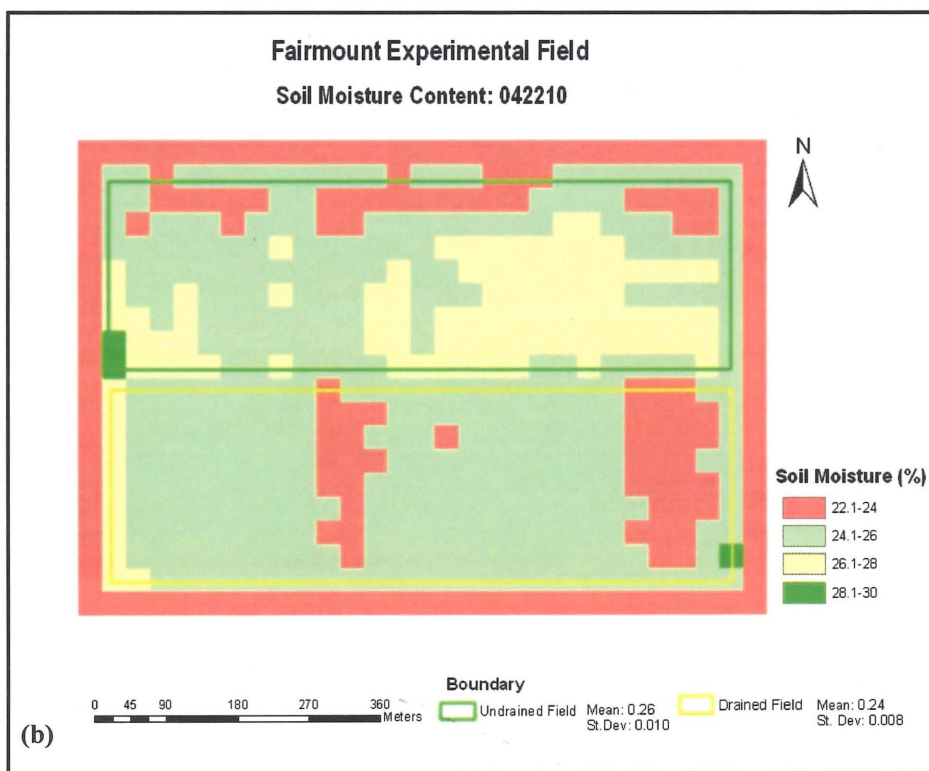
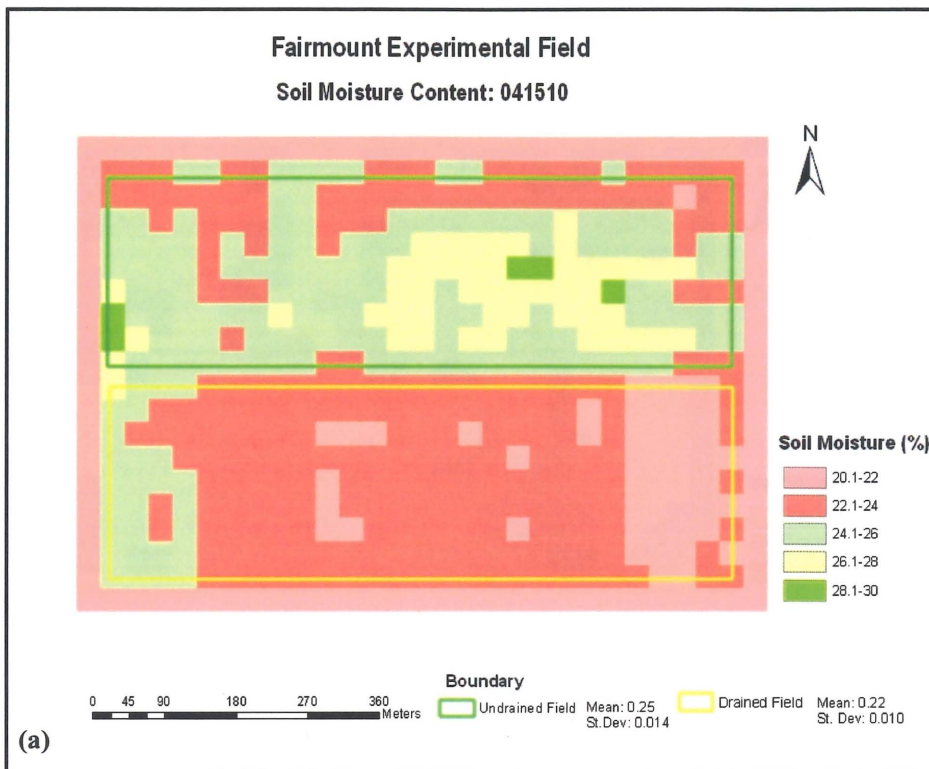


Figure 30. The difference in estimated soil moisture on drained and undrained portion of the Fairmount experimental field (a) on April 15, 2010 and (b) April 22, 2010

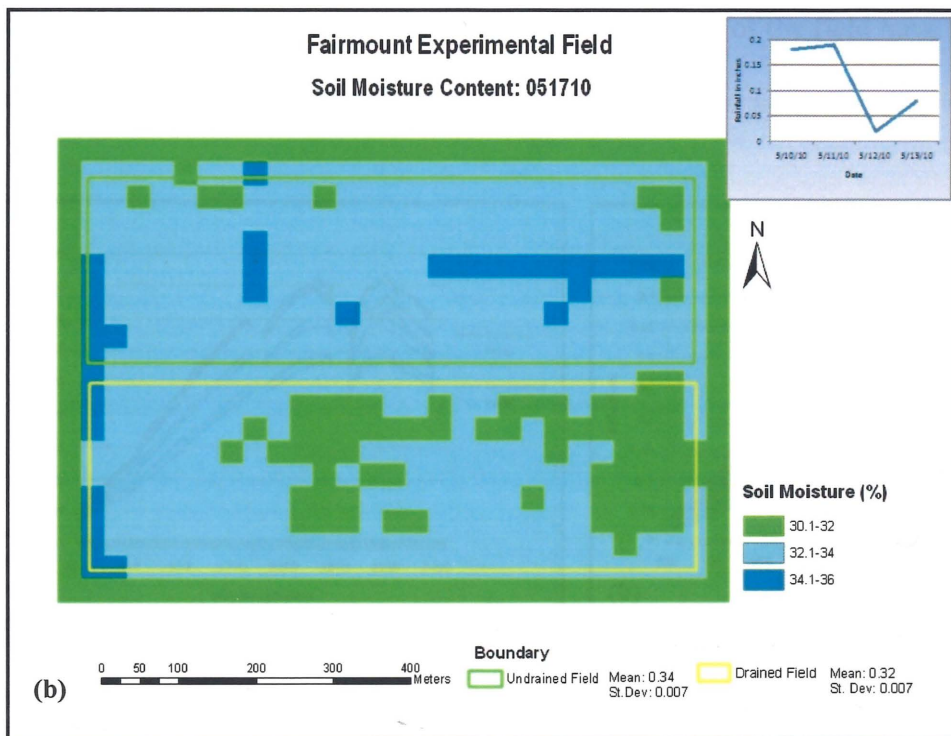
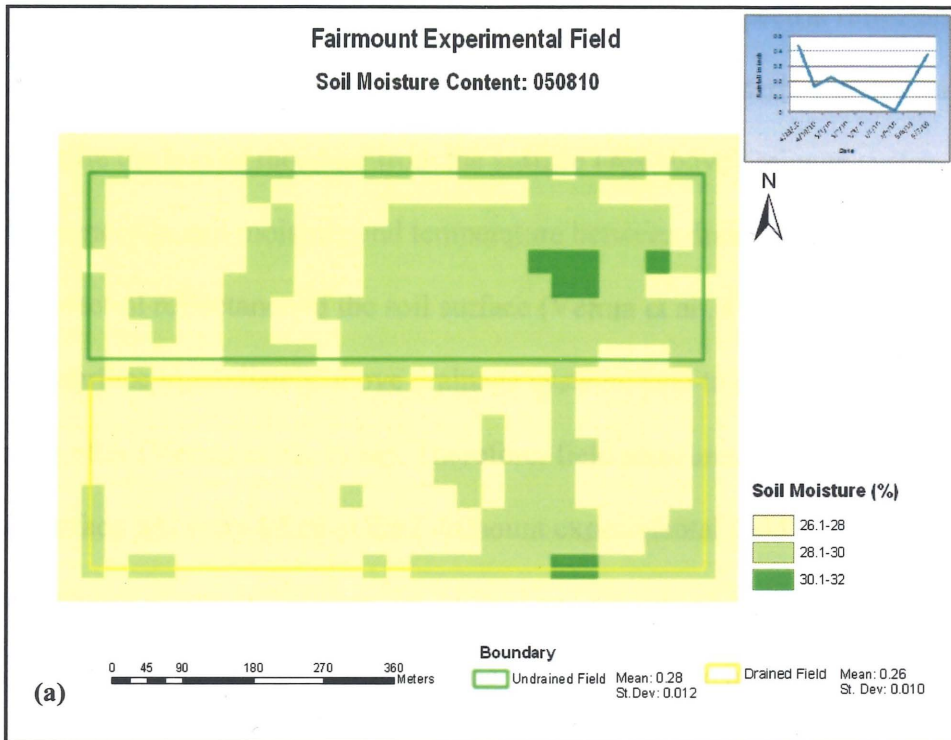


Figure 31. The difference in estimated soil moisture on drained and undrained portion of the Fairmount experimental field (a) on May 7, 2010 and (b) May 17, 2010

Drained and undrained fields exhibit variation in spectral reflectance as the surface of the soil is highly influenced by the drainage system, which eventually will expedite the loss of moisture from the surface area above drainage systems. In the spring, differences in soil moisture and temperature between drained and undrained field affect the spectral reflectance of the soil surface (Verma et al., 1996; Choi and Jacobs, 2007). Soil surface immediately above drainage systems tend to dry faster than surrounding areas after (Verma et al., 1996). Therefore, field measurements of the spectral reflectance of surface soil were taken at the Fairmount experimental field to observe differences in reflectance spectrum between the drained and undrained portion of the field, and consequently, to provide a basis for the validation of the model. Systematic random sampling method was used to collect the spectral reflectance of soil at different locations. Results showed that surface soil over the drained portion of the field have higher reflectance compared to the undrained portion (Fig. 32)

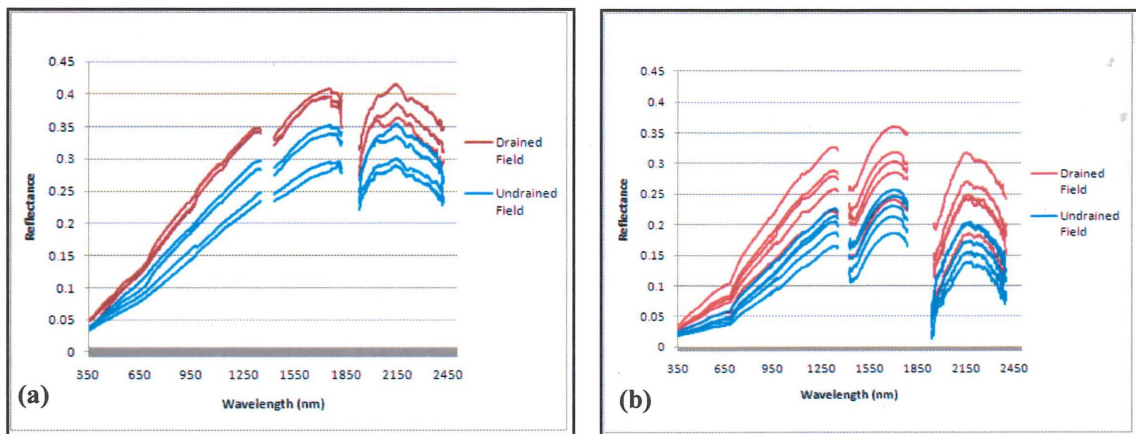


Figure 32. Comparison of reflectance spectra of soil on drained/undrained portion of Fairmount experimental field collected (a) on June 5, 2009 (b) on September 10, 2009

Deriving soil moisture from remote sensing data remains rather difficult, as the reflectance of a soil is not just a function of moisture but is also influenced by soil-specific chemical and physical properties like presence of organic matter, mineralogy, crusts or grain size and color of soil elements (Goldshleger et al., 2001; Goldshleger et al., 2004). As such, in the context of remote sensing applications these natural conditions are present and therefore are being investigated. Recent tillage changes soil surface moisture, roughness, and the amount of residue left after cultivation. These factors can affect the soil reflectance differently at different wavelengths and thus can lead to large spatial variation in surface reflectance patterns (Naz and Bowling, 2008). There are several other factors that play an important role in the surface reflectance of soil that can be significant in calculating surface soil moisture from remote sensing. Surface soil color is a very significant parameter for determining the spectral reflectance pattern.

Developing relationships for surface soil color in terms of reflectance would help to identify and quickly estimate physical and hydraulic properties of soils using remotely sensed information (Mattikalli, 1997). Soil surface reflectance is also determined by the inherent scattering and absorption properties of its components and by the way they are arranged within the soil. Therefore, soil moisture has greater influence on reflectance followed by several other characteristics such as observation conditions like illumination and observation directions (Weidong et al., 2002).

CHAPTER V:

CONCLUSION, LIMITATIONS AND FUTURE WORK OF THE STUDY

Conclusion

Laboratory and outdoor experiments were successfully carried out as a first step to develop a model to estimate the surface soil moisture of the RRV. Test applications of the model were done at different locations of the RRV for Landsat 5 TM imagery.

Results showed that the model reliably estimates surface soil moisture in many regions of the RRV. These results were based on field measurements that were carried out in several agricultural fields ranging from the Devil's lake area to Wahpeton and Fairmount, all conducted on days of Landsat overpass. Soil moisture estimated from images and soil moisture collected from field based measurements were compared, demonstrating a significantly high correlation ($R^2=0.90$). Results also showed that the model works best at lower or medium soil moisture condition. However, when the field is excessively wet, the model slightly underestimates soil moisture readings, by about 3 to 4 percent. This underestimation of soil moisture value in the image was observed in the 'Walcott experimental field' and 'Fairmount Field A' image on 13th of September, 2010.

The model was run using Landsat images of the Fairmount experimental field acquired before the growing season. Results showed that there is comparatively higher soil moisture in the undrained portion than the drained portion of the experimental field irrespective of the overall moisture condition. The resultant higher moisture level in the undrained portion compared to the drained portion, over the period of growing season,

has been verified by continuous soil moisture measurement made in the Fairmount experimental field. Along with this, the overall weather condition in the field and the results in the image suggest that the model works perfectly.

From both of the lab and outdoor experiments, we can conclude that soil spectral reflectance changes very narrowly at higher soil moisture levels, but between 30 and 20 percent volumetric water content, we can see a wide dispersion in the spectral reflectance pattern. The spectral reflectance curve remains almost stable when it reached about 20% volumetric soil moisture content.

Limitation of the Study

Remote sensing of soil moisture is limited by errors introduced by the type of soil, roughness of the landscape and vegetation cover, and the inadequate ground coverage both in space and time (Houser et al., 1998). Besides, regular acquisition of clear images over the same field from multispectral sensors like Landsat 5 TM in the limited duration of the study of soil moisture is often very hard. While planning for field measurements, it was very important to find a clear day of Landsat overpass within the RRV. Furthermore, field without vegetation and without crop residues was hard to find in the middle of growing season. There were numerous circumstances that limited the validation of the model in some images of the Fairmount experimental field, such as, soil moisture sensors were installed in a late hour as a precaution to the possible damage to the sensors due to ploughing the field. After the beginning of the growing season, vegetation began to appear in the field, which restricted the study on the field. For AEROCam imagery, test application could not be done due to lack of irradiance value for AEROCam.

The limitation of the study primarily includes types of soils used in the experiments and their properties. In nature, we find diverse type of soil inherent to its parent material and modified over the course of time. This large variety of soil in various regions of the world has distinct properties and is often changing. Even within a small region, soil color and properties can vary in which case the model may not be applicable. The texture of the soil used for the experiment is another limitation of the study. The model is prepared from the soil of Fairmount experimental field that has specific texture and may not be applicable to soils of different texture. Another limitation is the structure of the soil. The individual soil granules used to take the spectra in the laboratory experiment varies with the soil granules found in the field which can have impact in the spectra. Other limitation of the study includes the surface roughness. For multispectral sensors like Landsat 5, the impact of soil roughness on reflectivity cannot be neglected.

Future Work

The remote sensing algorithm has been developed primarily to detect surface soil moisture in the RRV. Therefore, two laboratory experiments under different illumination including the outside experiment have been carried out using soil of this region which has specific properties. Consequently, this model is only applicable to the RRV or any other region with similar soil properties. Due to the presence of a large variety of soil types in nature, it becomes important to look at the spectral reflectance patterns of these different types of soil under different moisture conditions. By combining this spectral reflectance pattern with the spectral response function of Landsat 5 TM, one can easily develop a Landsat 5 TM algorithm for detecting soil moisture that can be applicable to regions having similar soil properties.

Further researchers in similar topics are encouraged to be able to prepare a model or verify the existing model for detecting the surface soil moisture in the RRV using the AEROCam Imagery. Using the lab experiment and calculating through the band response function, I found that NIR band is helpful to detect the surface soil moisture for AEROCam. Nevertheless, lack of irradiance value for the AEROCam, I was unable to validate the model as an important part of my research. However, in a certain period of the day, irradiance value can be calculated which can finally be used to develop or test the existing model.

APPENDICES

APPENDIX A

LIST OF ACRONYMS AND SYMBOLS

AEROCam	Airborne Environmental Research Observational Camera
AIRSAR	Airborne Synthetic Aperture Radar
AMSR-E	Advanced Microwave Scanning Radiometer
ASAR	Advance Synthetic Aperture Radar
ENVISAT	Environmental Satellite
EROS	Earth Resource Observation and Science
ERS	European Remote Sensing
ESTAR	Electronically Scanned Thin Array Radiometer
IFOV	Instantaneous Field of view
JERS	Japanese Earth Resource Satellite
NASA	National Aeronautics and Space Administration
NASDA	National Space Development Agency
NIR	Near-infrared
nm	Nanometer
PMBR	Pushbroom Microwave Radiometer
RADARSAT	Radar Satellite
RRV	Red River Valley of the North Basin
SAR	Synthetic Aperture Radar

SSM/I	Special Sensor Microwave/Imager
SWIR	Shortwave Infrared
TM	Thematic Mapper
UMAC	Upper Midwest Aerospace Consortium
USGS	United States Geological Survey
VIS	Visible region of electromagnetic spectrum
μm	Micrometer

LIST OF SYMBOLS

j	The wavelength varying between A_i and B_i for the i th band
L	Attenuation caused by vegetation canopy
M_v	Volumetric soil moisture
r	Smooth surface reflectivity
R_i	The simulated reflectance for the Landsat band i
r_j	The spectral reflectance at the wavelength j and
R_s	Surface roughness
$T(H)$	Atmospheric transmissivity for a radiometer at height H
T_{atm}	Average thermometer Aperture
T_{soil}	Thermometric temperature of the soil
$W_{i,j}$	The spectral response for band i
σ°	Radar backscatter coefficient
σ_v	Backscatter from vegetation
σ_s	Backscatter from soil

APPENDIX B

TYPE OF SOIL USED IN THE EXPERIMENT

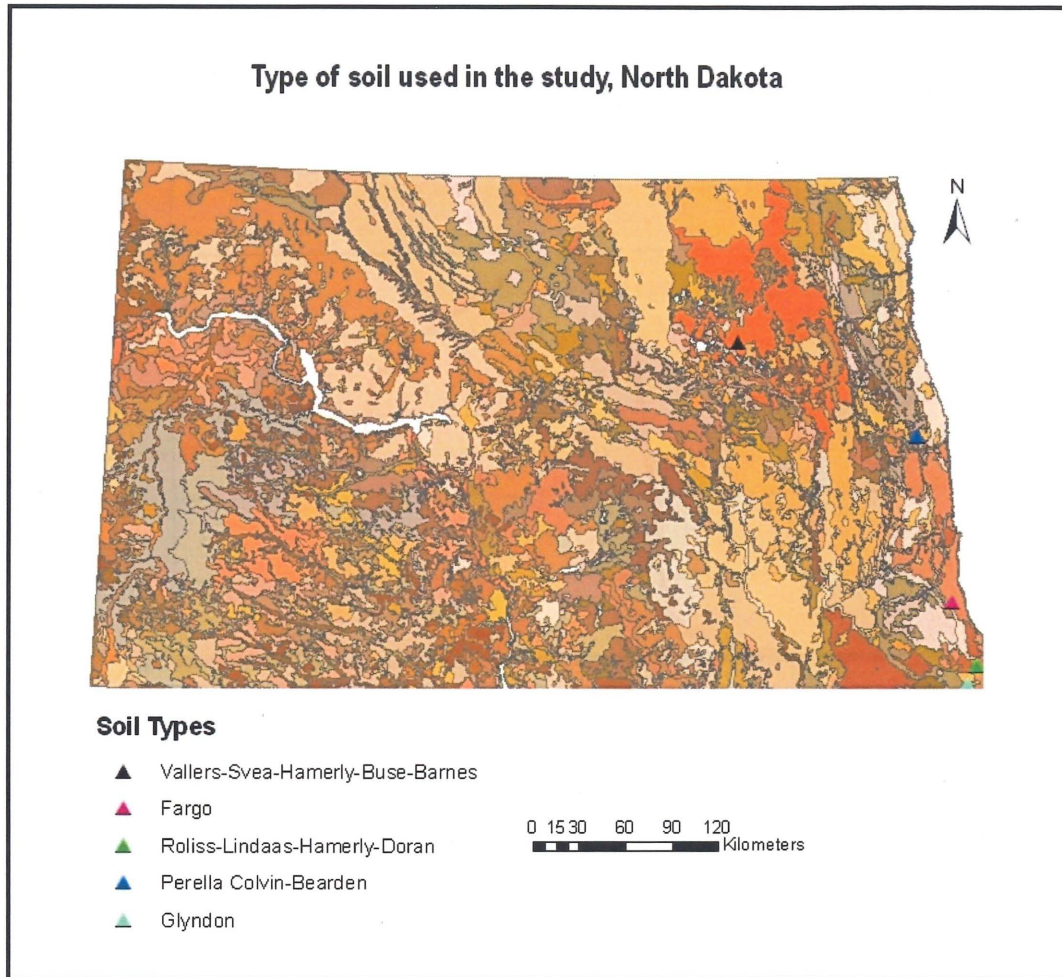


Figure 33. Soil map of North Dakota with the location of field measurement indicated by the triangles

APPENDIX C
SPECTRAL RESPONSES

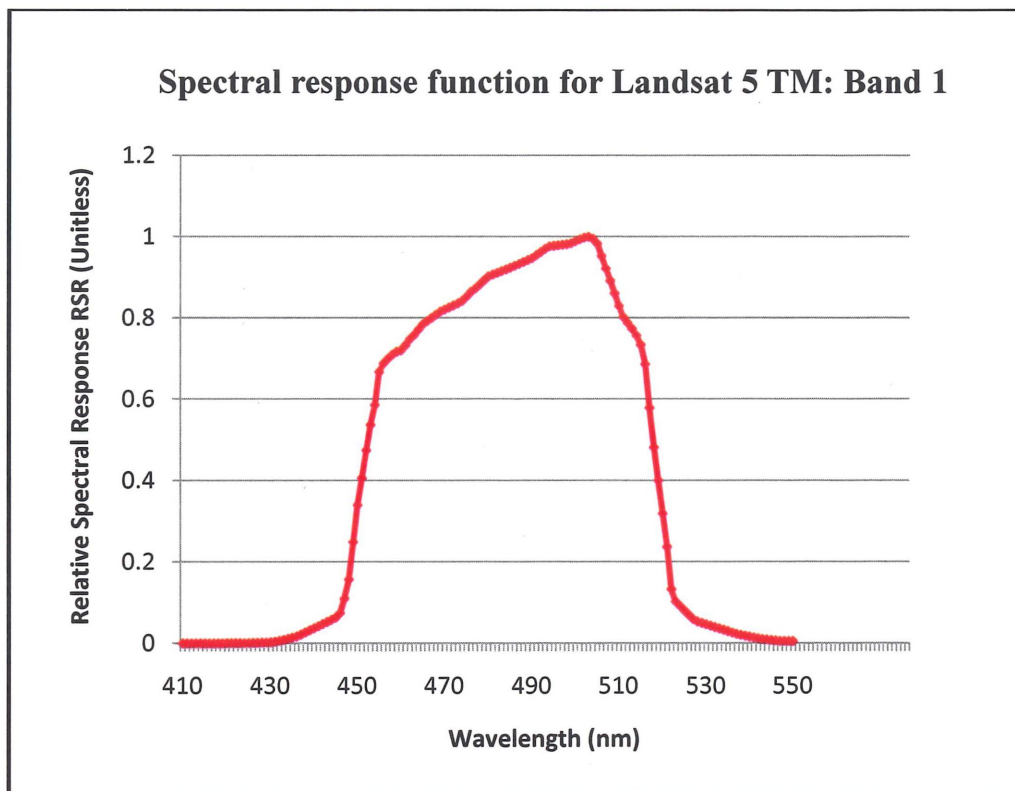


Figure 34. The spectral response function for Landsat 5 TM, Band 1 (CEOS, 2010)

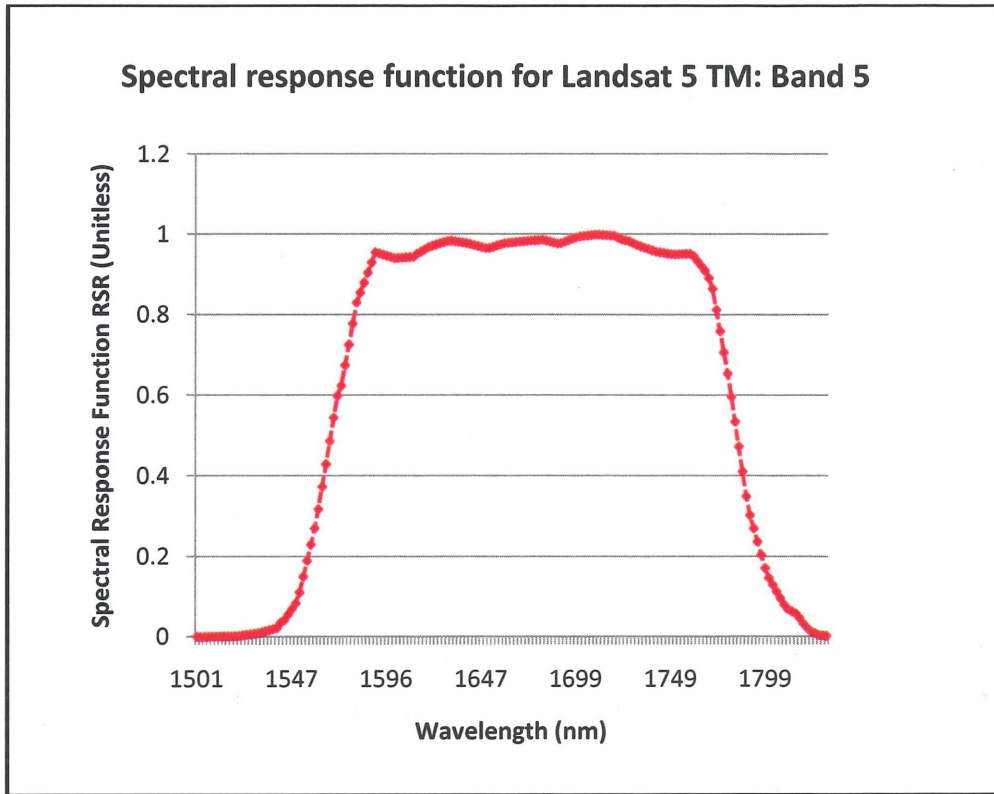


Figure 35. The spectral response function for Landsat 5 TM, Band 5 (CEOS, 2010)

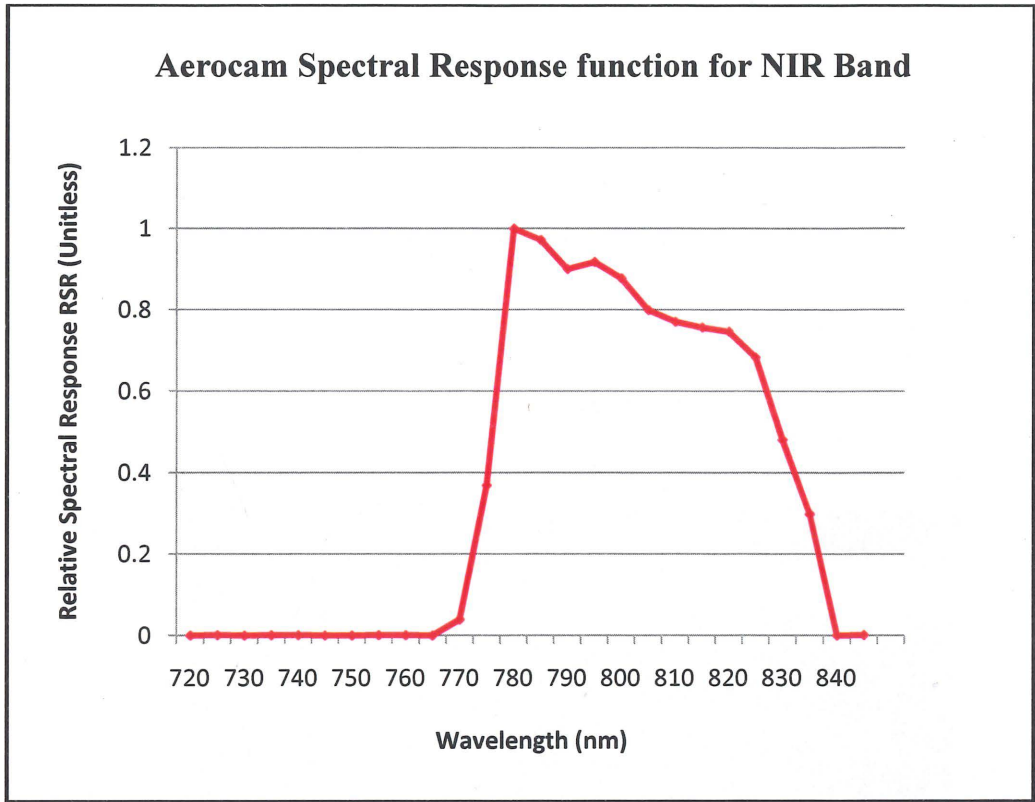


Figure 36. The spectral response function for NIR Band of AEROCam

APPENDIX D
FIELDS USED IN THE STUDY

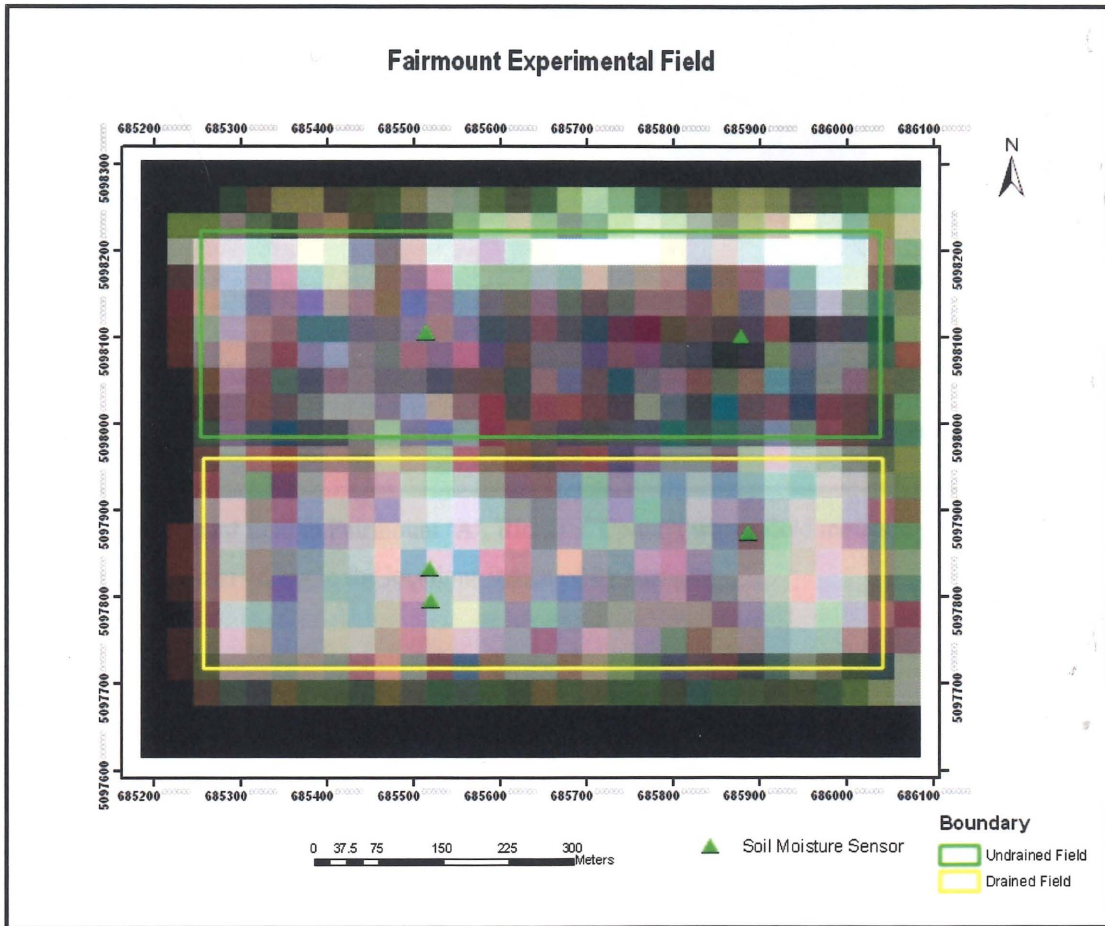


Figure 37. Fairmount experimental field, Richland County, where field moisture measurements were carried out in the locations indicated by triangles

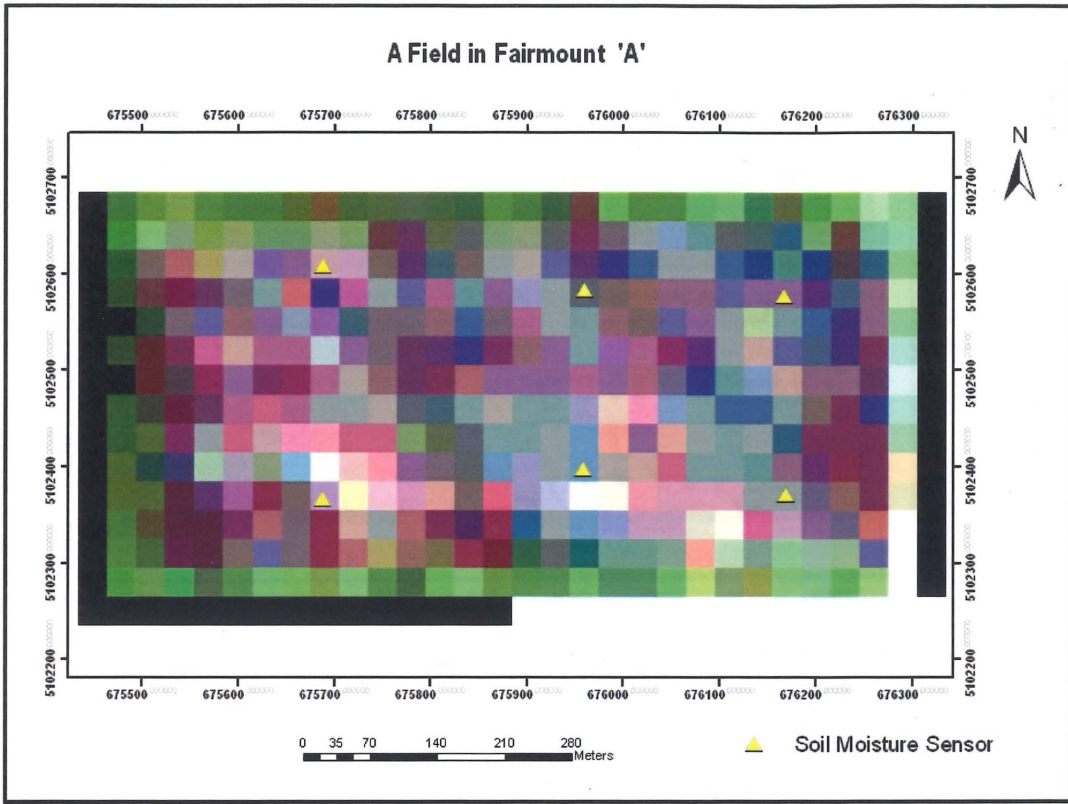


Figure 38. Experimental field in Fairmount 'A', Richland County, where field moisture measurements were carried out in the locations indicated by triangles

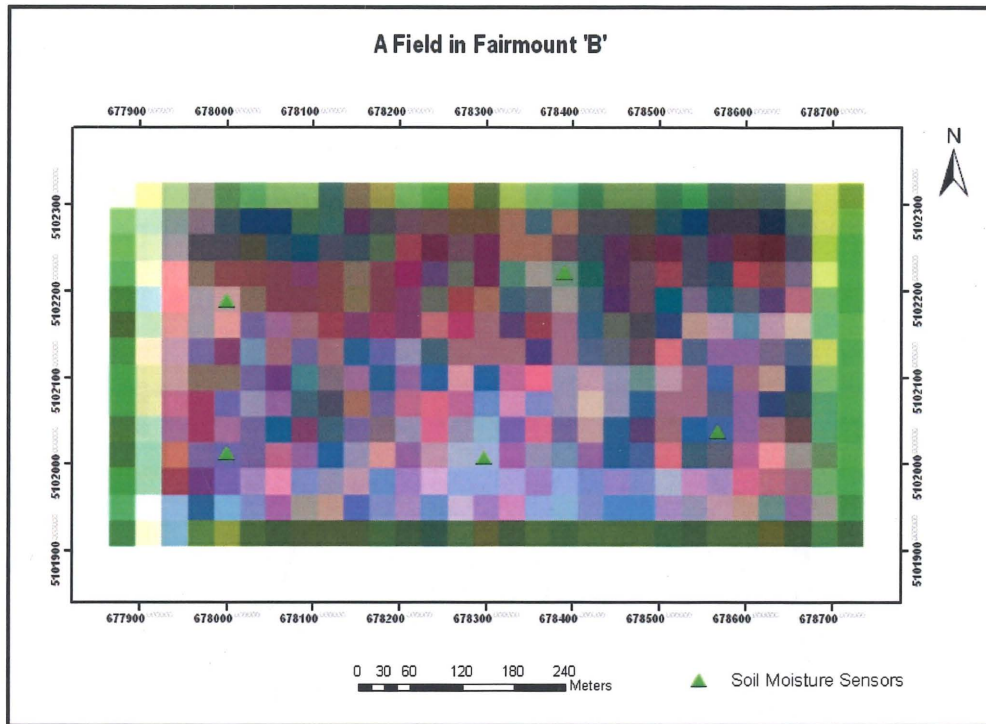


Figure 39. Experimental field in Fairmount 'B', Richland County, where field moisture measurements were carried out in the locations indicated by triangles

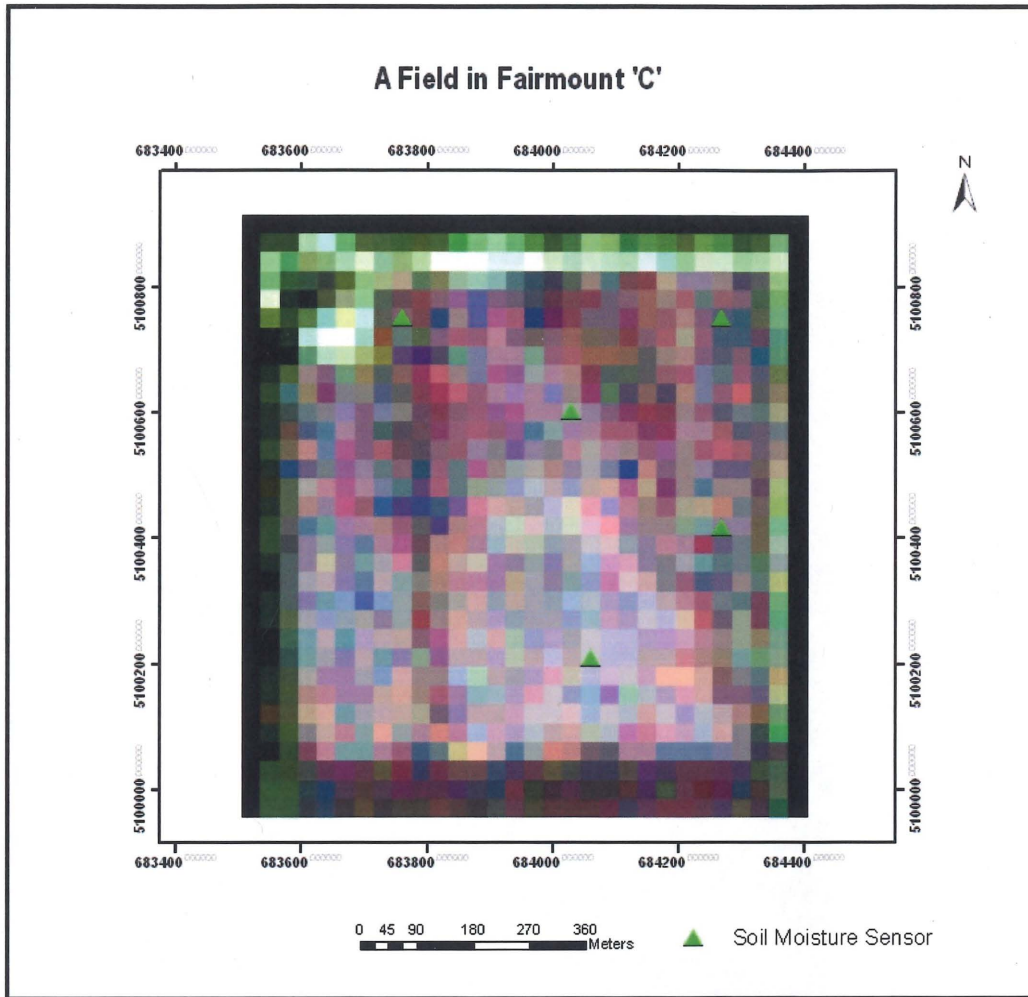


Figure 40. Experimental field in Fairmount 'C', Richland County, where field moisture measurements were carried out in the locations indicated by triangles

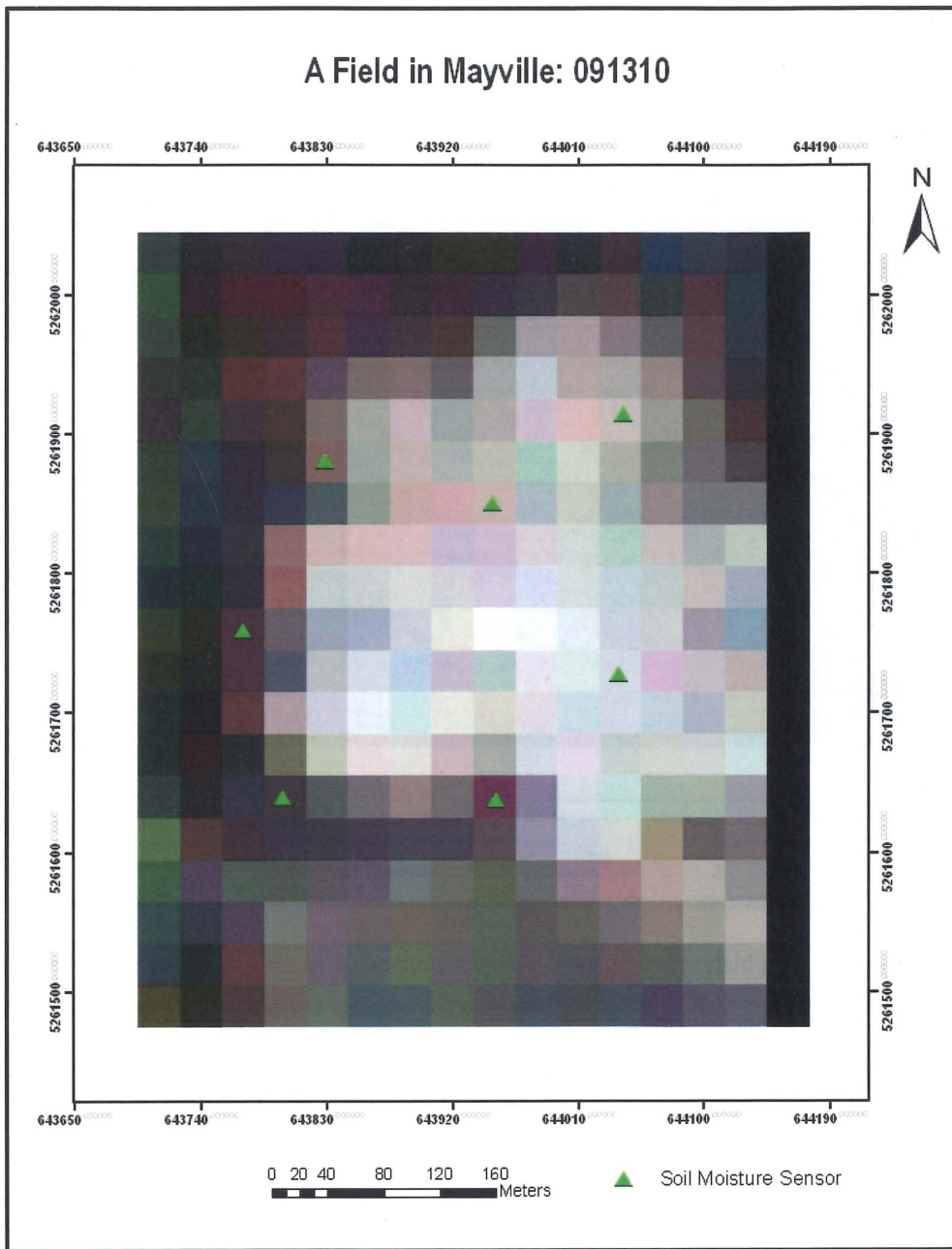


Figure 41. Experimental field in Mayville, Trail County, where field moisture measurements were carried out in the locations indicated by triangles

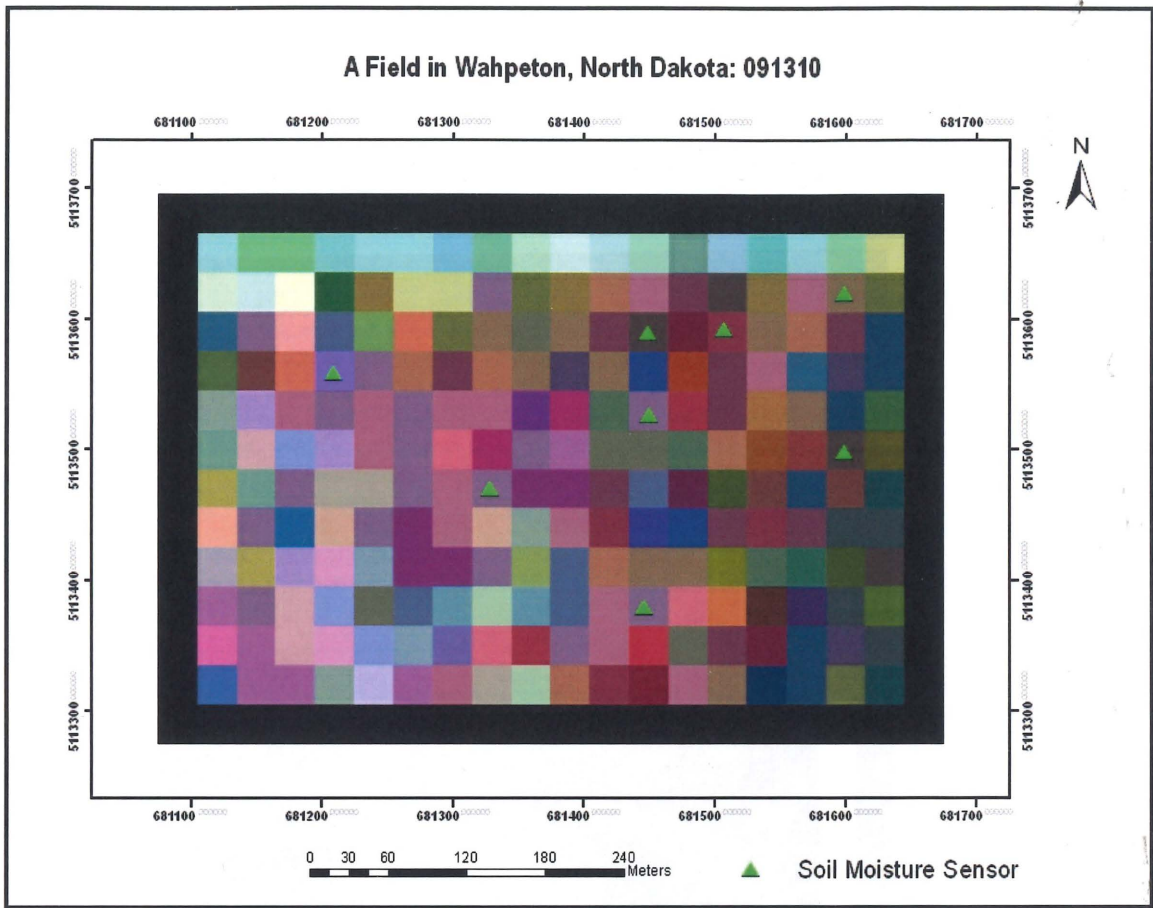


Figure 42. Experimental field in Wahpeton, Richland County, where field moisture measurements were carried out in the locations indicated by triangles

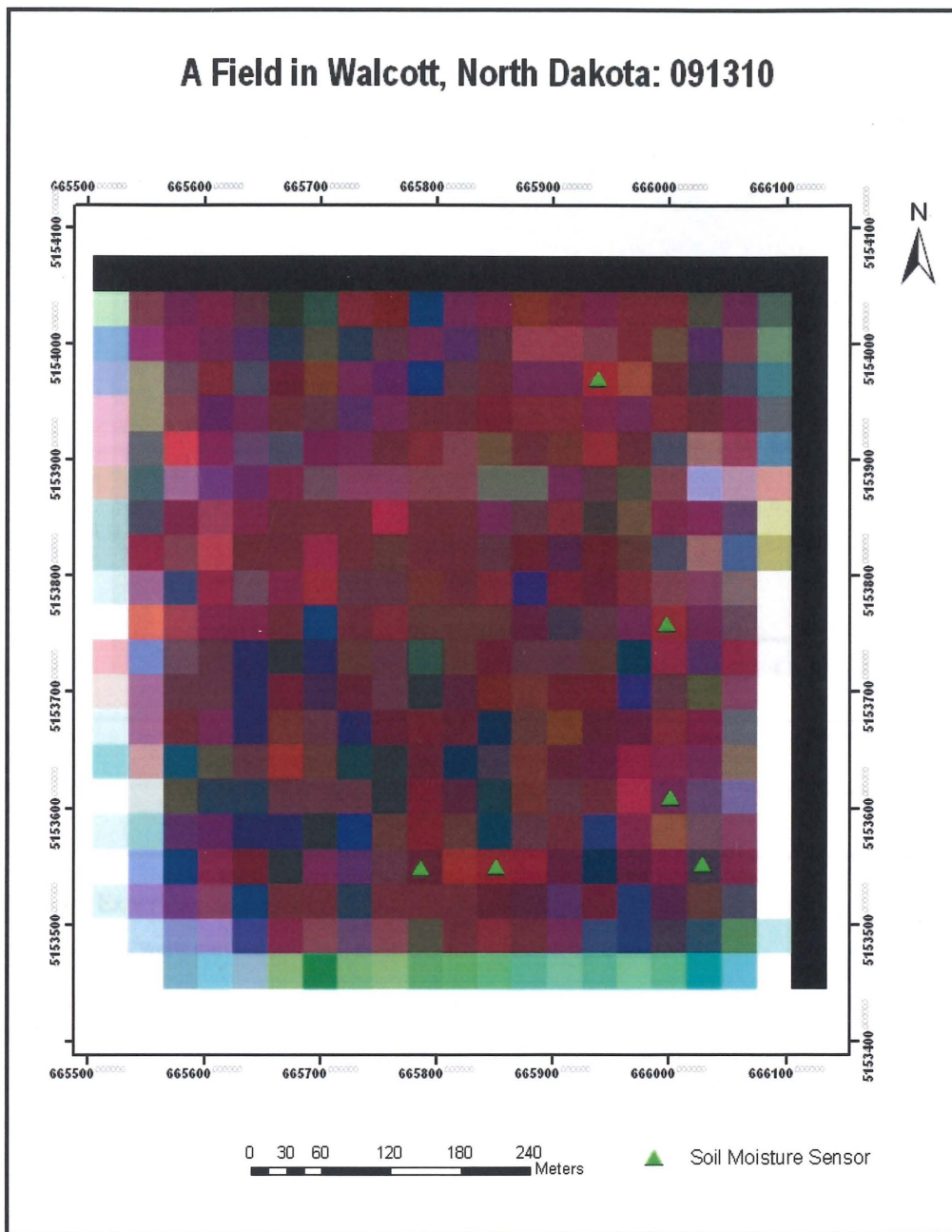


Figure 43. Experimental field in Walcott, Richland County, where field moisture measurements were carried out in the locations indicated by triangles

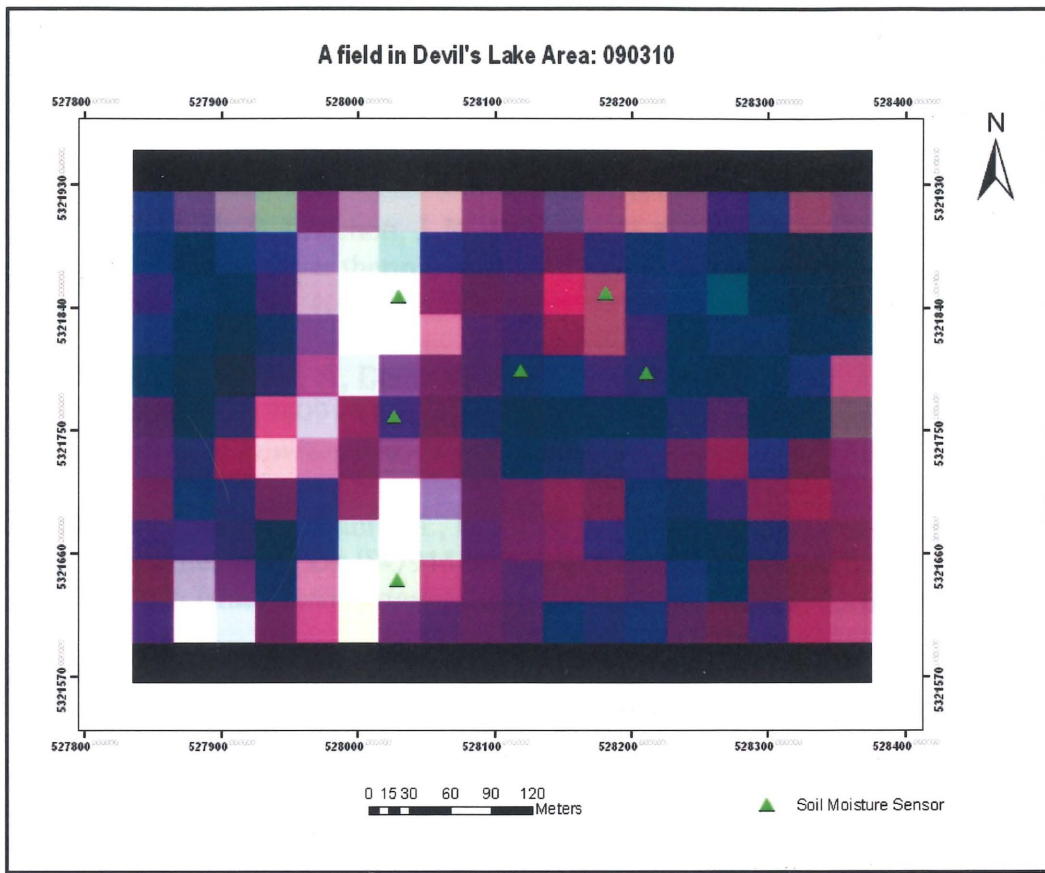


Figure 44. Experimental field in Devils Lake, Ramsey County, where field moisture measurements were carried out in the locations indicated by triangles

REFERENCES

- Barsi, J. A., Hook, S. J., Schott, J. R., Raqueno, N. G., Markham, B. L. (2007). Landsat-5 thematic mapper thermal band calibration update. *IEE Geoscience and Remote Sensing Letters*, 4(4), 552-555.
- Ben-Dor, E., Chabrillat, S., Dematte, J. A. M., Taylor, G. R., Hill, J., Whiting, M. L., Sommer, S. (2009). Using imaging spectroscopy to study soil properties. *Remote Sensing of Environment*, 113, S38-S55.
- Ben-Dor, E., Patkin, K., Banin, A., Karnieli, A. (2002). Mapping of several soil properties using DAIS-7915 hyperspectral scanner data- a case study over clayey soils in Israel. *International Journal of Remote Sensing*, 23(6), 1043-1062.
- Bogrekci, I., Lee, W. S. (2004). The effects of soil moisture content on reflectance spectra of soils using UV-VIS-NIR spectroscopy. 7th International Conference on Precision Agriculture.
- Bowers, S. A., Hanks, R. J. (1965). Reflection of radiant energy from soils. *Soil Science*, 2, 130-138.
- Bowers, S. A., Smith, S. J. (1972). Spectrophotometric determination of soil water content. *Soil Science Society of America Proceedings*, 36, 972-980.
- Bryant, R., Thoma, D., Moran, S., Holifield, C., Goodrich, D., Keefer, T., Paige, G., Williams, D., Skirvin, S. (2003). Evaluation of hyperspectral, infrared temperature and radar measurements for monitoring surface soil moisture. 1st Interagency Conference on Research in the Watersheds, pp. 528-533.
- Campbell, J. C. (2009). Remote sensing of soil. In Timothy A. Warner, M Duane Nellis and Gilles M. Foody (Eds.), (pp 341).
- CEOS. (2010). Spectral response function information. Online material retrieved on 15th January, 2010. URL: <http://calvalportal.ceos.org/cvp/web/guest/landsat-5-tm>
- Chander, G., Helder, D. L., Markham, B. L., Dewald, J. D., Kaita, E., Thome, K. J., Micijevic, E., Ruggles, T. A. (2004). Landsat 5-TM reflective-band absolute radiometric calibration. *Geoscience and Remote Sensing*, 42(12), 2747-2760.

- Chander, G., Markham, B. (2003). Revised landsat-5 TM radiometric calibration procedures and postcalibration dynamic ranges. *Geoscience and Remote Sensing*, 41, 2674-2677.
- Chebouni, A., Nouvellon, Y., Kerr, Y. H., Moran, M. S., Watts, C., Prevot, L., Goodrich, D. C., Rambal, S. (2001). Directional effect on radiative surface temperature measurements over a semiarid grassland site. *Remote Sensing of Environment*, 76, 360-372.
- Choi, M., Jacobs, J. M. (2007). Soil moisture variability of root zone profiles within SMEX02 remote sensing footprints. *Advances in Water Resources*, 30, 883-896.
- Davidson, M. W. J., Toan, T. L., Mattia, F. (2000). On the characterization of agricultural soil roughness for radar remote sensing studies. *Transactions on Geoscience and Remote Sensing*, 38(2), 630-640.
- de Rosnay, P., Co authors. (2006). SMOSREX: A long term field campaign experiments for soil moisture and land surface processes remote sensing. *Remote sensing of Environment*, 102, 377-389.
- de Troch F. P., Troch, P. A, Su, Z., Lin, D. S. (1996). Chapter 9: Application of remote sensing for hydrological modeling. In: Abbott M B, Refsgaard J C, eds. Distributed Hydrological Modeling. Dordrecht: Kluwer Academic Publishers.
- Dubois, P. C., van Zyl, J., Engman, T. (1995). Measuring soil moisture with imaging radars. *Geoscience Remote Sensing*, 33, 915-926.
- Engman, E. T., Chauhan, N. (1995). Status of microwave soil moisture measurements with remote sensing. *Remote sensing of the Environment*, 51, 189-198.
- Everitt, J. H., Escobar, D. E., Alaniz, M. A., Davis, M. R. (1989). Using multispectral video imagery for detecting soil surface condition. *Photogrammetric Engineering and Remote Sensing*, 55(4), 467-471.
- Famiglietti, J. S., Devereaux, J. A., Laymon, C. A., Tsegaye, T., Houser, P. R., Jackson, T. J., Graham, S. T., Rodell, M., van Oevelen, P. J. (1999). Ground-based investigation of soil moisture variability within remote sensing footprints during the southern Great Plains 1997 (SGP97) hydrology experiment. *Water resources research*, 35, 1839-1851.
- Frazier, P. S., Page, K. J. (2000). Water body detection and delineation with Landsat 5 TM data. *Photogrammetric Engineering and Remote Sensing*, 66(12), 1461-1467.
- Frazier, P. S., Page, K., Louis, J., Briggs, S., Robertson, A. I. (2003). Relating wetland inundation to river flow using Landsat TM data. *International Journal of Remote Sensing*, 24(19), 3755-3770.

- Friedl, M. A., Davis, F. W. (1994). Sources of variation in radiometric surface temperature over a tallgrass prairie. *Remote Sensing of the Environment*, 48, 1-17.
- Goetz, A. F. H., Curtiss, B., Shiley, D. A. (2009). Rapid gangue mineral concentration measurement over conveyors by NIR reflectance spectroscopy. *Minerals Engineering*, 22, 490-499.
- Goldshleger, N., Ben-Dor, E., Benyamini, Y., Agassi, M. (2004). Soil reflectance as a tool for assessing physical crust arrangement of four typical soils in Israel. *Soil Science*, 169, 677-687.
- Goldshleger, N., Ben-Dor, E., Benyamini, Y., Agassil, M., Blumberg, D. G. (2001). Characterization of soil's structural crust by spectral reflectance in the SWIR region (1.2 ± 2.5 μm). *Terra Nova*, 13(1), 12-17.
- Haider, S. S., Said, S., Kothyari, U. C., Arora, M. K. (2004). Soil moisture estimation using ERS 2 SAR data: a case study in the Solani River Catchment. *Hydrological Sciences*, 49(2), 323-334.
- Hall, D. K., Ormsby, J. P., Bindschadler, R. A., Siddalingaiah, H. (1987). Characterization of snow and ice reflectance zones on glaciers using landsat thematic mapper data. *Annals of Glaciology*, 9, 104-108.
- Haubrock, S. N., Chabrillat, S., Lemnitz, C., Kaufmann, H. (2008). Surface soil moisture quantification models from reflectance data under field conditions. *International Journal of Remote Sensing*, 29, 3-29.
- Heusinkveld, B. G., Berkowicz, S. M., Jacobs, A. F. G., Hillen, W., Holtslag, A. A. M. (2008). A new remote optical wetness sensor and its applications. *Agricultural and Forest Meteorology*, 148, 580 - 591.
- Houser, P. R., Shuttleworth, W. J., Famiglietti, J. S., Gupta, H. V., Syed, K. H., Goodrich, D. C. (1998). Integration of soil moisture remote sensing and hydrologic modeling using data assimilation. *Water Resources Research*, 34(12), 3405-3420.
- Huan-Jun, L., Zhang, Y. Z., Zhang, X. L., Zhang, B., Song, K. S., Wang, Z. M., Tang, N. (2009). Quantitative analysis of moisture effect on black soil reflectance. *Pedosphere*, 19(4), 532-540.
- Jackson, T. J., Schmugge, J., Engman, E. T. (1996). Remote sensing applications to hydrology: soil moisture. *Hydrological Sciences Journal*, 41(4), 517-530.

- Jia, X., Scherer, T. F., DeSutter, T. M., Steele, D. D. (2008). Change of soil hardness and soil properties due to tile drainage in the Red River Valley of the North. Written for presentation at the 2008 ASABE Annual International Meeting Sponsored by ASABE Rhode Island Convention Center Providence, Rhode Island June 29 – July 2, 2008. Paper number: 084369
- Kaleita, A. L., Tian, L. F., Hirschi, M. C. (2005). Relationship between soil moisture content and soil surface reflectance. *American Society of Agricultural Engineers*, 48, 1979–1986.
- Kustas, W. P., Moran, M. S., Norman, J. M. (2003). Evaluating the spatial distribution of evaporation. Chapter 26. In *Handbook of weather, Climate and Water: Atmospheric Chemistry, Hydrology and Societal Impacts*. Edited by T. D. Potter and B. R. Colman. John Wiley and Sons Inc., Hoboken, N. J. pp. 461-492.
- Lindsey, S. D., Gunderson, F. W., Riley, J. P. (1992). Spatial distribution of point soil moisture estimates using landsat TM data and Fuzzy-C classification. *Water Resources Bulletin*, 28(5), 865-875.
- Lobell, D. B., Asner, G. P. (2002). Moisture effects on soil reflectance. *Soil Science Society of America*, 66, 722–727.
- Mattikalli, N. M. (1997). Soil color modeling for the visible and near infrared bands of Landsat sensors using laboratory spectral measurements. *Remote Sensing of the Environment*, 59, 14-28.
- Miller, J. D., Yool, S. R. (2002). Mapping forest post-fire canopy consumption in several overstory types using multi-temporal Landsat TM and ETM data. *Remote Sensing of Environment*, 82, 481-496.
- Moran, M. S., Hymer, D. C., Qi, J., Sano, E. E. (2000). Soil moisture evaluation using multi-temporal synthetic aperture radar (SAR) in semi arid rangeland. *Agriculture and Forest Meteorology*, 105, 69-80.
- Moran, M. S., Inoue, Y., Barnes, E. M. (1997). Opportunities and limitations for image-based remote sensing in precision crop management. *Remote Sensing of the Environment*, 61, 319-346.
- Moran, M. S., Peters-Lidard, C. D., Watts, J. M., McElroy, S. (2004). Estimating soil moisture at the watershed scale with satellite-based radar and land surface models. *Canadian Journal of Remote Sensing*, 30(5), 805-826.
- Muller, E., Decamps, H. (2000). Modeling soil moisture-reflectance. *Remote sensing of Environment*, 76, 173-180.

- Naz, B. S., Bowling, L. C. (2008). Automated identification of tile lines from remotely sensed data. *American Society of Agricultural and Biological Engineers*, 51(6), 1937-1950.
- Nemani, R., Pierce, L., Running, S. (1993). Developing satellite-derived estimates of surface moisture status. *Journal of Applied Meteorology*, 31, 548-557.
- Njoku, E. G., Entekhabi, D. (1996). Passive microwave remote sensing of soil moisture. *Journal of Hydrology*, 184, 101-129.
- Njoku, E. G., Jackson, T. J., Lakshmi, V., Chan, T. K., Ngheim, S. V. (2003). Soil moisture retrieval from AMSR-E. *Geoscience and Remote sensing*, 41(2), 215-229.
- Peterson, J. B., Robinson, B. F., Beck, R. H. (1979). Predictability of change in soil reflectance on wetting. LARS Technical Reports. Paper 73.
- Price, J. C. (1982). One the use of satellite data to infer surface fluxes at meteorological scales. *Journal of Applied Meteorology*, 21(8), 1111-1122.
- Profeti, G., Macintosh, H. (1997). Flood management through Landsat TM and ERS SAR data: A case study. *Hydrological Processes*, 11, 1397-1408.
- Rondeaux, G., Steven, M., Baret, F. (1996). Optimization of soil-adjusted vegetation indices. *Remote Sensing of Environment*, 55, 95-107.
- Rossel, R. A. V., McBratney, A. B. (1998). Laboratory evaluation of a proximal sensing technique for simultaneous measurement of soil clay and water content. *Geoderma*, 85, 19-39.
- Rossel, R. A. V., Walvoort, D. J. J., McBratney, A. B., Janik, L. J., Skjemstad, J. O. (2006). Visible, near infrared, mid infrared or combined diffuse reflectance spectroscopy for simultaneous assessment of various soil properties. *Geoderma*, 131, 59-75.
- Schmugge, T. (1978). Remote sensing of surface soil moisture. *Journal of Applied Meteorology*, 17, 1549-1557.
- Scott, C. A., Bastiaanssen, W. G. M., Ahmad, M. D. (2003). Mapping root zone soil moisture using remotely sensed optical imagery. *Journal of Irrigation and Drainage Engineering*, 129, 326-335.
- Segelstein, D. (1981). The complex refractive index of water. Masters thesis, University of Missouri, Kansas City.

- Shih, S. F., Jordan, J. D. (1992). Landsat Mid-infrared data and GIS in regional surface soil-moisture assessment. *Water Resources Bulletin*, 28(4), 713-719.
- Stoner, E. R., Baumgardner, M. F., Weismiller, R. A., Biehl, L. L., Robinson, B. F. (1979). Extension of laboratory-measured soil spectra to field conditions. LARS Technical Reports. Paper 278.
- Stoner, J. D., Lorenz, D. L., Wiche, G. J., Goldstein, R. M. (1993). Red River of the North basin, Minnesota, North Dakota and South Dakota. *JAWRA Journal of the American Water Resources Association*, 29(4), 575-615.
- UMAC. (2010). Airborne Environmental Research Observational Camera (AEROCam) Overview. Online material retrieved on 10 October, 2010. URL: <http://www.umac.org/sensors/AEROCam/bkgd.html>
- USGS. (2010). Landsat: A global land-observing program. Online material retrieved on 10 October 2010. URL: <http://egsc.usgs.gov/isb/pubs/factsheets/fs02303.html>
- Verma, A. K., Cooke, R. A., Wendte, L. (1996). Mapping sub surface drainage systems with color infrared aerial photographs. American Water Resource Association's 32nd Annual Conference and Symposium "GIS and Water Resource". September 22-26, Ft. Lauderdale, Florida.
- Wang, L., Qu, J. J. (2009). Satellite remote sensing applications for surface soil moisture monitoring: A review. *Frontiers of Earth Science in China*, 3(2), 237-247.
- Weather Underground. (2010). Weather history of Wahpeton, North Dakota. Online material retrieved on 15 August, 2010. URL: <http://www.wunderground.com/cgi-bin/findweather/getForecast?query=58030>
- Web soil survey. (2010). USDA Natural Resource Conservation Service. Online material retrieved on 20 August, 2010. URL: <http://websoilsurvey.nrcs.usda.gov/app/WebSoilSurvey.aspx>
- Weidong, L., Baret, F., Xingfa, G., Bing, Z., Qingxi, T., Lanfen, Z. (2003). Evaluation of methods for soil surface moisture estimation from reflectance data. *International Journal of Remote sensing*, 24 (10), 2069-2083.
- Weidong, L., Baret, F., Xingfa, G., Qingxi, T., Lanfen, Z., Bing, Z. (2002). Relating soil surface moisture to reflectance. *Remote Sensing of Environment*, 81, 238- 246.
- Zhang, X., Seelan, S., Seielstad, G. (2010b). Digital Northern Great Plains: A web-based system delivering near real time remote sensing data for precision agriculture. *Remote Sensing*, 2, 861-873.

Zhang, X., Streeter, C., Kim, H., Olsen, D. (2010a). Article in review. Near real time meter resolution airborne imagery for precision agriculture. *Journal of precision agriculture*. Retrieved on 10 October, 2010. URL: http://www.icpaonline.org/finalpdf/abstract_135.pdf